

## **ES322 Geomorphology Fall 2023**

### **Oregon Coast Field Trip Reading Supplement**

Peters et al., 2007, Sedimentology of Tsunami Deposits, Cascadia Subduction Zone

Briggs, 1994, Tsunami Sand-Peat Deposits, Central Oregon Coast, PSU M.S. Thesis  
(Excerpts)

Peterson et al., 2002, Field Guide to Dunal Landscapes of Central Oregon Coast

Bretz Club Field Guide, 2012, Battendorf Beach-Sunset Bay Coast Processes

Bretz Club Field Guide, 2023, Oregon Coast Range Geomorphology, Lower Siuslaw Basin

Whetherell et al., 2022, FOP Field Guide, Lower Umpqua River to Coast (Excerpts)

# Distribution and sedimentary characteristics of tsunami deposits along the Cascadia margin of western North America

Robert Peters<sup>a,\*</sup>, Bruce Jaffe<sup>a</sup>, Guy Gelfenbaum<sup>b</sup>

<sup>a</sup> USGS Pacific Science Center, 400 Natural Bridges Drive, Santa Cruz, CA 95060, United States

<sup>b</sup> USGS 345 Middlefield Road, Menlo Park, CA 94025, United States

## Abstract

Tsunami deposits have been found at more than 60 sites along the Cascadia margin of Western North America, and here we review and synthesize their distribution and sedimentary characteristics based on the published record. Cascadia tsunami deposits are best preserved, and most easily identified, in low-energy coastal environments such as tidal marshes, back-barrier marshes and coastal lakes where they occur as anomalous layers of sand within peat and mud. They extend up to a kilometer inland in open coastal settings and several kilometers up river valleys. They are distinguished from other sediments by a combination of sedimentary character and stratigraphic context. Recurrence intervals range from 300–1000 years with an average of 500–600 years. The tsunami deposits have been used to help evaluate and mitigate tsunami hazards in Cascadia. They show that the Cascadia subduction zone is prone to great earthquakes that generate large tsunamis. The inclusion of tsunami deposits on inundation maps, used in conjunction with results from inundation models, allows a more accurate assessment of areas subject to tsunami inundation. The application of sediment transport models can help estimate tsunami flow velocity and wave height, parameters which are necessary to help establish evacuation routes and plan development in tsunami prone areas.

© 2007 Published by Elsevier B.V.

*Keywords:* Tsunami deposits; Cascadia tsunami; Cascadia earthquake; Sedimentary structures; Grain size

## 1. Introduction

Sedimentary deposits from tsunamis are a valuable source of information for geologists and emergency planners. They provide evidence of past tsunami inundation and provide estimates of tsunami recurrence and magnitude which can be used to improve our understanding of tsunamis and help mitigate the hazards from future tsunamis. They also help evaluate earthquake hazard by providing evidence for past subduction

zone earthquakes and may help estimate the magnitude of these earthquakes.

Tsunami deposits are particularly important for reconstructing the history of tsunamis in the Cascadia region of the Pacific Northwest. Cascadia is the region of the Pacific Northwest from Northern California, U.S.A. to northern Vancouver Island, B.C., Canada and is located onshore of the Cascadia Subduction Zone (CSZ)(Fig. 1). There have been no records of a great earthquake (moment magnitude > 8) and associated tsunami occurring during the historical period in Cascadia. However, the absence of recorded great earthquakes on the CSZ in the recent past does not necessarily imply that the CSZ is not capable of

\* Corresponding author.

E-mail address: [rpeters\\_geol@skyhighway.com](mailto:rpeters_geol@skyhighway.com) (R. Peters).

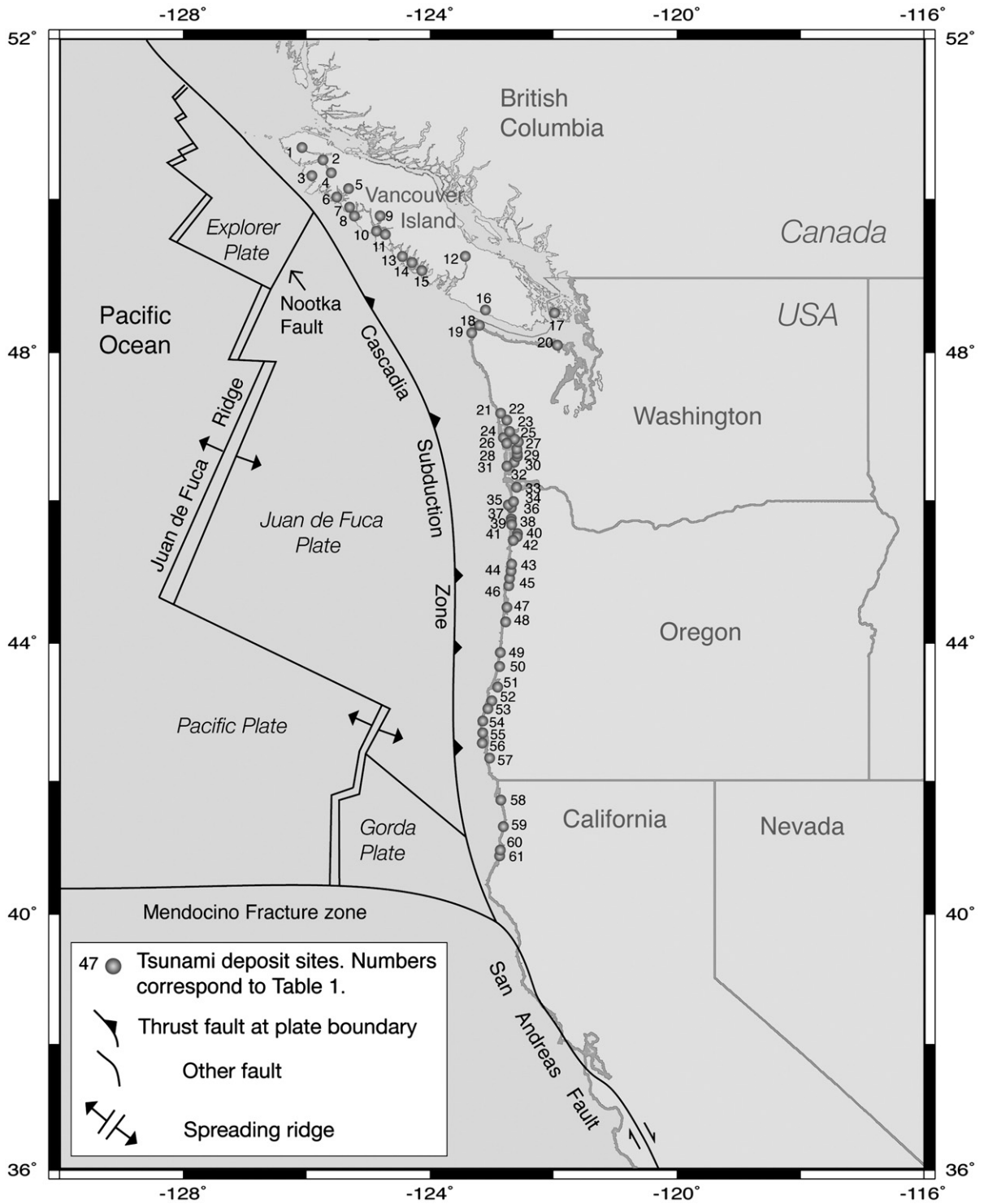


Fig. 1. Map of the Cascadia region of North America, showing the tectonic setting and location of sites where tsunami deposits have been identified.

producing them. The CSZ shares many features with other subduction zones around the world that have produced great earthquakes and tsunamis (Heaton

and Kanimori, 1984; McAdoo et al., 2004). Native American oral tradition from the Pacific Northwest describes catastrophic ground shaking and associated

coastal flooding occurring in the past (Heaton and Snively, 1985; Woodward, 1990; Clague, 1995; Hutchinson and McMillan, 1997; Ludwin, 2002). Heaton and Snively (1985) recognized there was a possible connection between the Native American oral tradition and CSZ earthquakes and tsunamis.

Over the past two decades, abundant geologic evidence has emerged to support the past occurrence of tsunamis and great earthquakes on the CSZ. Evidence that the CSZ produces large earthquakes can be seen in the turbidite record off of the Cascadia Margin (Adams, 1990; Goldfinger et al., 2003), but the evidence that these earthquakes can produce large tsunamis is most easily seen in the stratigraphy of coastal marshes and lakes. Atwater (1987) first published evidence for tsunami deposits in Cascadia in coastal marshes in Washington. Sand layers overlying buried peat were interpreted to be sediments deposited by a tsunami accompanying a great earthquake (Atwater, 1987). Since Atwater's paper was published in 1987, there has been a period of growth in the documentation and interpretation of tsunami deposits in the Pacific Northwest. Numerous studies document tsunami deposits in California, Oregon, Washington, and British Columbia (Peters et al., 2003a,b) (Fig. 2, Table 1). These studies help to increase the awareness of the tsunami hazard along the Cascadia margin.

In this paper, we summarize previously published literature on Cascadia tsunami deposits to characterize their distribution patterns and sedimentary characteristic. We examine how tsunami deposits have been used to

assess the recurrence and magnitude of tsunamis in Cascadia. Then we explore the role of tsunami deposits in further mitigating the tsunami hazard for the Cascadia region.

## 2. Tectonic setting

The Cascadia Subduction Zone extends for about 1000 km from northern California to northern Vancouver Island, British Columbia (Fig. 1). The Juan de Fuca plate, and the smaller Gorda Plate to the south, subduct beneath the North American Plate. To the north, the Nootka fault separates the Explorer plate from the Juan de Fuca plate. The Explorer plate constitutes a broad deformational zone where convergence changes into strike-slip motion between the Pacific plate and the North American plate (Rohr and Furlong, 1995). The Juan de Fuca plate is converging with respect to the North American plate at velocities of 35–45 mm/yr (Wang et al., 1995). Subduction along the CSZ is currently locked (Hyndman and Wang, 1995) and the coast is experiencing interseismic uplift at a rate of 1–4 mm/yr (Wilson, 1993; Hyndman and Wang, 1995).

## 3. Cascadia tsunami deposit distribution

For this study, we consider Cascadia tsunami deposits to be those formed by a tsunami generated by a CSZ earthquake. Tsunami deposits from other sources are found in the Cascadia region, particularly in the Puget Sound area. These deposits were formed by

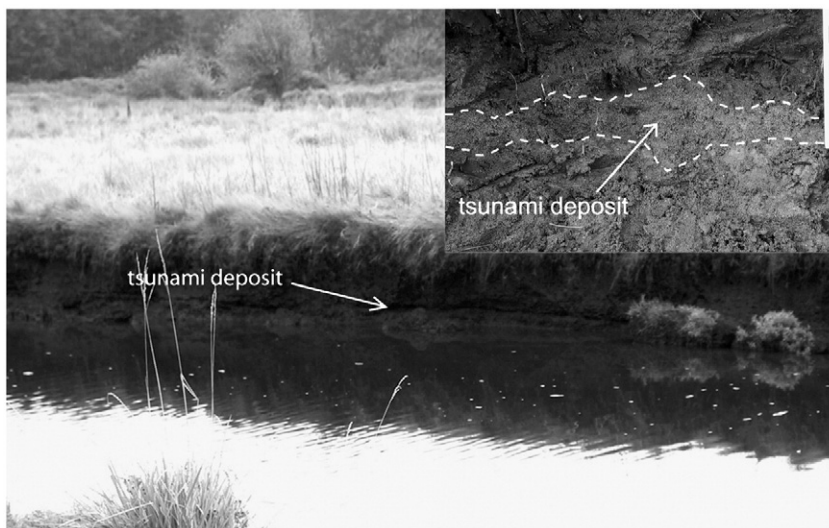


Fig. 2. Tidal marsh at low tide, Neawanna Creek, Oregon. A deposit from the 1700 AD tsunami is exposed in the cutbank as a sand layer that is more deeply eroded than the surrounding mud and peat. Inset shows a detail of the deposit. Scale bar at right of inset is in 1 cm intervals.

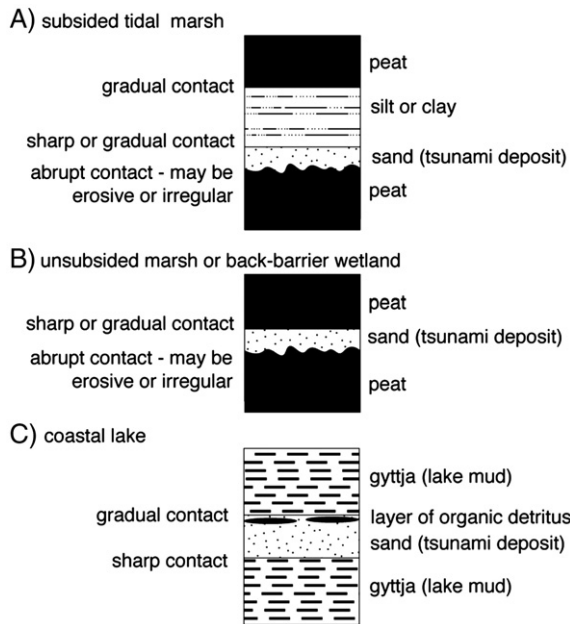


Fig. 3. Idealized stratigraphic relationships of Cascadia tsunami deposits in (A) a tidal marsh that has undergone coseismic subsidence, (B) a back-barrier wetland or tidal marsh that has not undergone coseismic subsidence, and (C) a coastal lake.

distant earthquake source or a tsunami of non-seismic origin (Darienzo et al., 1994) (Fig. 3B).

Tsunami deposits in lakes usually consist of a bed of sand layered above and below by gytija (Hutchinson et al., 1997; Clague et al., 1999; Hutchinson et al., 2000) (Fig. 3C). A layer of organic debris and/or a massive mud may overlie the sand layer. Tsunami deposits in back barrier wetlands are characterized by tsunami-deposited sand sandwiched between layers of peat or mud, resembling the stratigraphy of a tidal marsh that has not undergone coseismic subsidence (Fig. 3B). Coastal lakes and back-barrier marshes are protected from tidal influences, resulting in little or no evidence for coseismic subsidence. In these settings, determining the source of the tsunami may be difficult (Clague, 1997).

#### 4. Characteristics of Cascadia tsunami deposits

Sedimentary characteristics of tsunami deposits are important, both to determine a sedimentary origin for the deposits and to provide information about the tsunami that deposited them. Tsunami deposits reflect the high-energy conditions of the tsunami and often provide a sharp contrast to the low-energy deposits that characterize tidal marsh deposition. Considerable variation may be seen laterally within a single deposit,

between correlated deposits at different sites and between deposits from separate events at a single site.

##### 4.1. Grain size

The range of grain sizes found in Cascadia tsunami deposits is dependent on the available source material. Cascadia tsunami deposits are typically composed of medium to fine sand, silt, and clay. The source material for the sand is usually the beach and near shore. In deposits along stream banks, a portion of the sand fraction may be made up of sand entrained from stream banks and channels. Sediment eroded from hill slopes may also make up some of the coarse fraction of the deposit. The primary source for silt and clay in the deposits is mud from the tidal channels and tidal flats. Mud is often present between layers in the deposits (e.g. Benson et al., 1997; Atwater and Hemphill-Haley, 1997). Mud may also be present at the base of the deposit. Some Cascadia tsunami deposits fine landward, indicating decreasing flow velocity as the tsunami approaches the limit of inundation (Abramson, 1998; Williams and Hutchinson, 2000).

Cascadia tsunamis are also capable of transporting very large clast sizes, up to cobble size (e.g. Nelson et al., 1998b; Hutchinson et al., 2000). Coarse clasts have been found at the base of the deposit (e.g. Clague and Bobrowsky, 1994a) or at the base of layers within the deposit (e.g. Witter and Kelsey, 1996). Gravel is found adjacent to tidal channels in deposits at Fair Harbour, B.C. (Hutchinson et al., 1997).

##### 4.2. Grading

Deposits from Cascadia tsunamis tend to be normally graded when grading is apparent. Normal grading is consistent with deposition by sediment settling out of suspension. One model for tsunami sediment transport involves a tsunami entraining sediment near the coast and carrying it inland. When the tsunami nears the limit of inundation, flow velocities become low enough that the entrained sand grains fall out of suspension, creating a tsunami deposit (Jaffe and Gelfenbaum, 2002). Normal grading is sometimes observed within the individual layers of the deposit (Witter and Kelsey, 1996; Hutchinson et al., 1997; Witter, 1999; Williams and Hutchinson, 2000; Kelsey et al., 2002). Often, however, no grading is apparent in Cascadia tsunami deposits. This may reflect uniformity in the sediment source, large flow velocities relative to the grain size of the transported sediment, or indicate other sediment transport processes are responsible for the deposit.

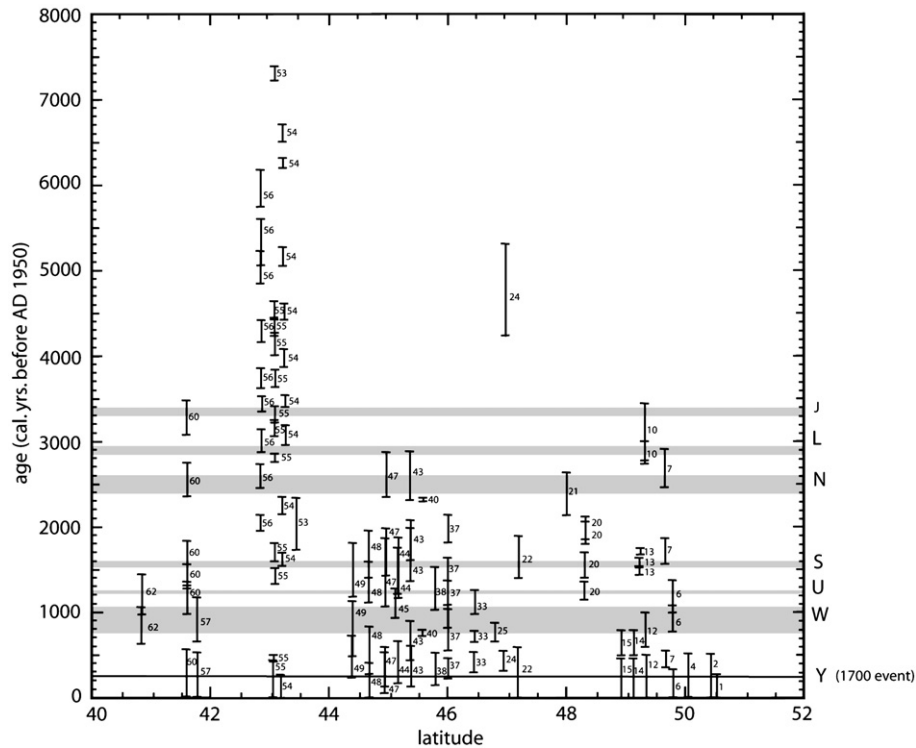


Fig. 4. Calibrated age ranges, in calendar years before 1950, reported for Cascadia tsunami deposits. Letters on the right correspond to age ranges for Cascadia Subduction Zone earthquakes based on the paleoseismic and tsunami records of SW Washington (Atwater and Hemphill-Haley, 1997). The age ranges (gray bars) correspond to the revised chronology for these events reported in Atwater et al. (2003).

7300 years (Kelsey et al., 1998a). Kakawis Lake, British Columbia has a 14,000 year-long record, yet deposits from only 3–4 tsunamis were identified there, suggesting tsunamis from other events may not have penetrated inland far enough to reach the lake (Lopez and Bobrowsky, 2001). While it is often possible to correlate deposits between cores and outcrops at a single site using radiocarbon ages and deposit depth, ambiguities in stratigraphic relationships and error in radiocarbon age make it difficult to correlate tsunami deposits with any certainty across the entire Cascadia margin.

The tsunami record preserved in coastal sediments varies throughout Cascadia (Fig. 4). At some sites there are tsunami deposits that don't correlate in time with other Cascadia tsunami deposits or with Cascadia Subduction Zone earthquake chronologies, while at other sites, more tsunami deposits are found in a given time interval (Atwater et al., 2003; Goldfinger et al., 2003). McAdoo and Watts (2004) suggest that landslide tsunamis may account for anomalous tsunami deposits found locally that are not present throughout Cascadia. Cascadia earthquakes may differ in the length and location of the rupture or in the amount of slip and this

could account for differences in tsunamis and, therefore, in the deposit record. Segmentation of the CSZ may produce differing records on either side of the segment boundary (Darienzo and Peterson, 1995; Kelsey et al., 2005). Differences in the record may also be a function of tide level, sediment supply or coastal configuration at the time of the tsunamis. The tsunami deposit record suggests that each tsunami affects the region uniquely and that it may be difficult to characterize a typical Cascadia tsunami.

Several attempts have been made to establish tsunami and CSZ earthquake recurrence intervals based on a combination of tsunami and subsidence events. Darienzo and Peterson (1990) calculated an average recurrence interval of 600 years based on tsunami deposits and subsidence events at Netarts Marsh, Oregon. Darienzo and Peterson (1995) calculated an average recurrence interval for CSZ earthquakes and tsunamis of 200–600 years, based on seven estuaries along 175 km of the northern Oregon coast. Atwater and Hemphill-Haley (1997) calculated an average recurrence interval for CSZ earthquakes of 500–540 years based on subsidence events along the Niawiakum River

COASTAL CROSSING OF THE ELASTIC STRAIN ZERO-ISOBASE,  
CASCADIA MARGIN, SOUTH CENTRAL OREGON COAST.

by

GREGORY GEORGE BRIGGS

A thesis submitted in partial fulfillment of the  
requirements for the degree of

MASTERS OF SCIENCE  
in  
GEOLOGY

Portland State University  
1994

## ABSTRACT

An abstract of the thesis of Gregory George Briggs for the Masters of Science in Geology presented August 3, 1994.

Title: Coastal Crossing of the Elastic Strain Zero-Isobase, Cascadia Margin, South Central Oregon Coast.

The analysis of marsh cores from the tidal zones of the Siuslaw, Umpqua, and Coos River systems on the south-central Oregon coast provides supporting evidence of coseismic subsidence resulting from megathrust earthquakes and reveals the landward extent of the zero-isobase. The analysis is based on lithostratigraphy, paleotidal indicators, microfossil paleotidal indicators, and radiocarbon age. Coseismic activity is further supported by the presence of anomalous thin sand layers present in certain cores. The analysis of diatom assemblages provides evidence of relative sea-level displacement on the order of 1 to 2 m. The historic quiescence of local synclinal structures in the Coos Bay area together with the evidence of prehistoric episodic burial of wetland sequences suggests that the activity of these structures is linked to megathrust releases. The distribution of cores containing non-episodically buried marshes and cores that show episodically buried wetlands within this area suggests that the landward extent of the zero-isobase is between 100 km and 120 km from the trench.

The zero-isobase has a minimum width of 10 to 15 km.

2

Radiocarbon dating of selected buried peat sequences yields an estimated recurrence interval on the order of 400 years.

The apparent overlapping of the landward margin of both the upperplate deformation zone (fold and/or thrust fault belt)

and the landward extent of the zero-isobase is interpreted to represent the landward limit of the locked zone. The

earthquake magnitude is estimated to be 8.5 based on an

arbitrary rupture length of 200 km and a locked zone width of 105 km. The identification of the zero-isobase on the south-

central Oregon coast is crucial to the prediction of regional coseismic subsidence and tsunami hazards, the testing of

megathrust dislocation models, and the estimation of

megathrust rupture areas and corresponding earthquake

magnitudes in the Cascadia Margin.

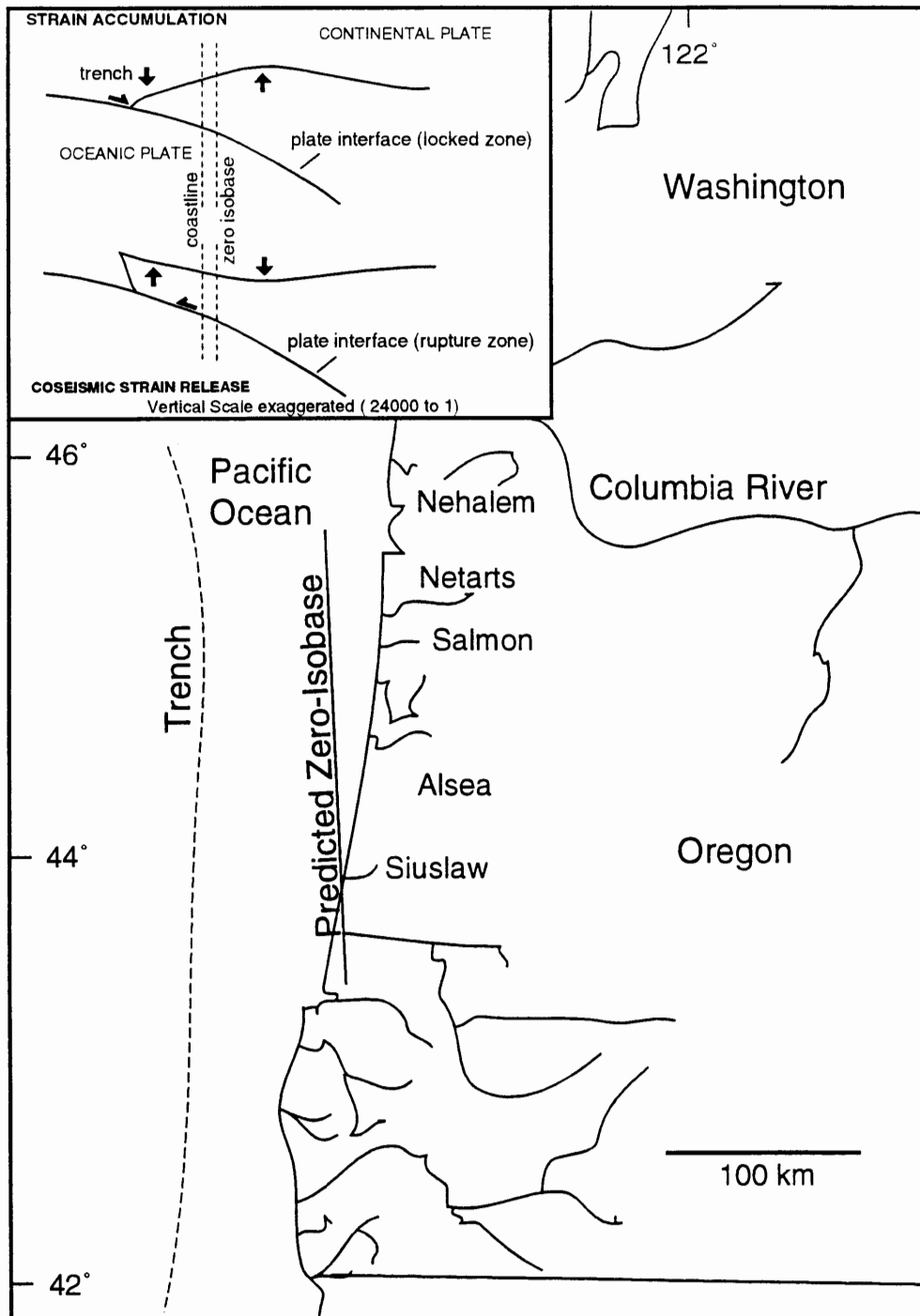


**Figure 2.** Hypothetical location of zero-isobase in which predicted areas of subsidence would lie east of the zero-isobase. Inset shows cross-sectional view of continental plate response to interseismic strain accumulation followed by coseismic strain release (after Peterson and Darienzo, 1990).

## RESULTS

### SIUSLAW BAY

#### Core Locations:

Siuslaw Bay is located in the northern part (approximately UTM4872000 mN) of the study area on the south-central Oregon coast (figure 5). Twenty-five cores were taken in this locality. Of these, 5 cores (213, 216, 220, 222, and 225) were vibra/pound cores, the remaining 20 cores were gouge cores. The sites cored include tidal marshes on Siuslaw Bay, Siuslaw River, and tidally influenced tributary streamlets of the Siuslaw River up to a distance of 23 km due east of the ocean, i.e. to Hadsell Creek at Mapleton. Four cores were taken at Lily Lake, a perched back dune pond, located approximately 13 km (8 mi) north of Florence.

Of the twenty-five cores taken from this area, four cores were subsampled for radiocarbon dating (figure 6). These were core 225 from Lily Lake, core 222 from Deming Creek, core 213 from Bernhardt Creek, and core 216 from Karnowsky Creek (figure 7 - Siuslaw C-14 core site map).

Elevations for core sites were corrected to mean sea level and are recorded in Appendix B for future use in correlations. Field core logs which document core site marsh stratigraphic records are shown in Appendix A.

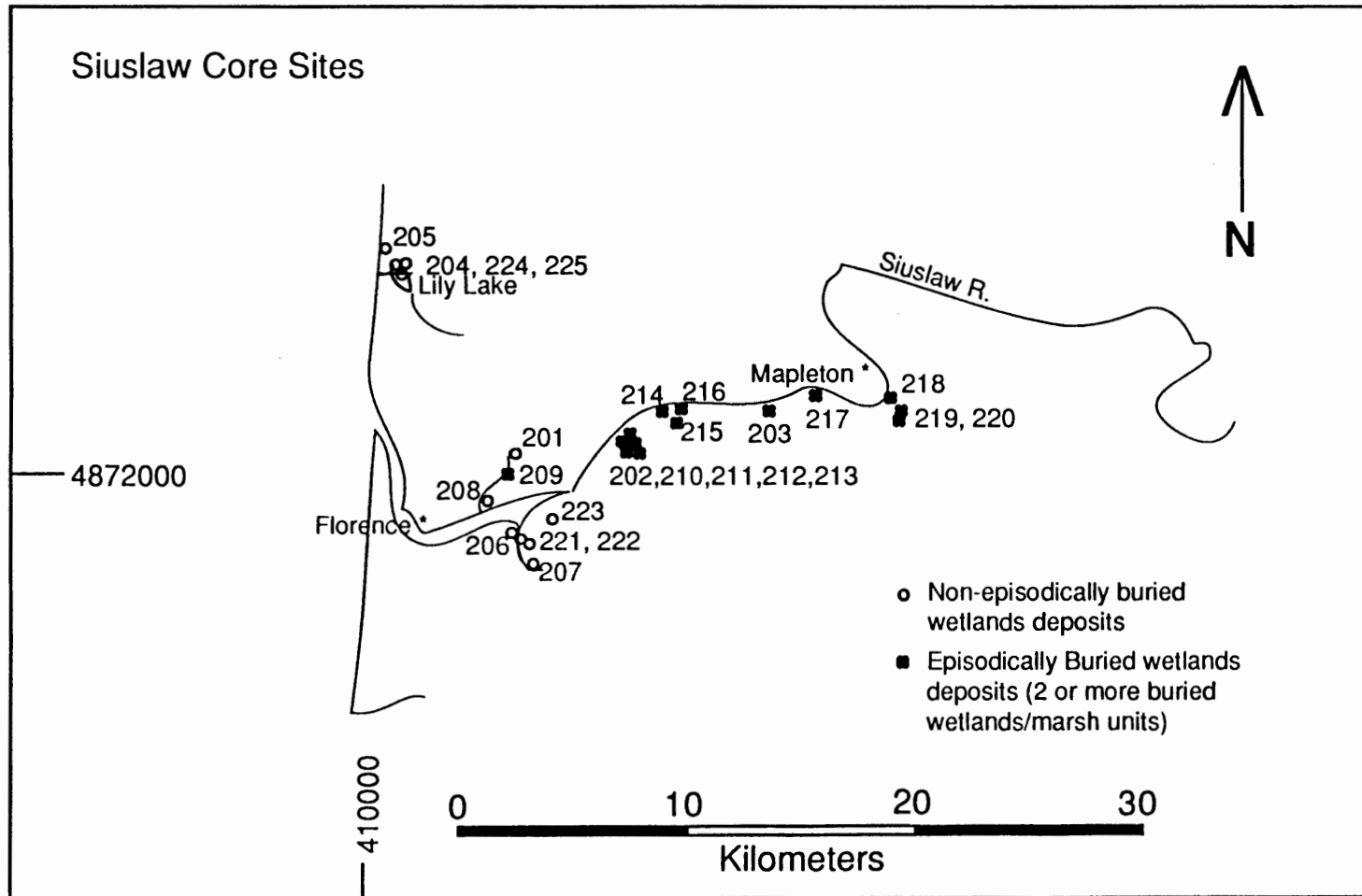


**Figure 5.** Siuslaw core location map. Sites included tidal marshes and tidally influenced tributary streamlets of the Siuslaw River.

# SIUSLAW CORES

Radiocarbon dates (C-14 AGE YRS B.P.  $\pm 1\sigma$ )

West

East

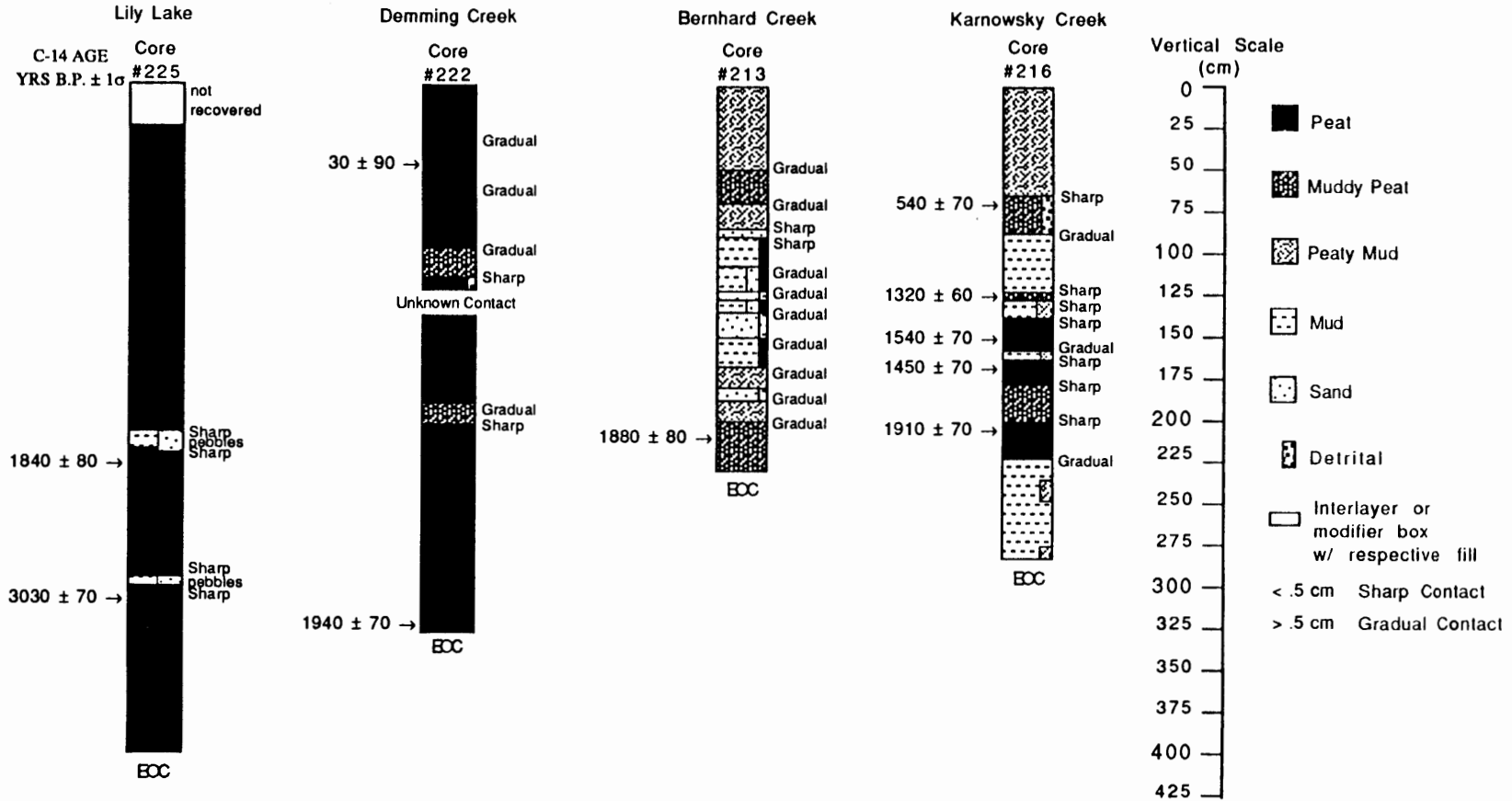


Figure 6. Siuslaw area radiocarbon dated cores. Elevation corrections for the tops of these cores were +0.72 m to +1.10 m above MSL (high marsh, upper intertidal level). Core 225 was not surveyed into mean sea level (MSL).

**Sweet Creek Cores - 217**

This small meandering creek flows through a relatively wide valley. It is an inlet on the south side of the Siuslaw River, and it is approximately 19 km (11.6 mi) due east of the ocean (figure 5).

Core 217- This core is 300 cm long. Muddy peat is evident from the top surface of the core to a depth of 50 cm. Very slightly rooted mud is found at 50 cm to 90 cm and it overlays a peaty mud at 90 cm to 110 cm. From 110 cm to 170 cm mud with some sand and a few rootlets is evident. A peat is found at 170 cm to 190 cm. Below the peat a mud layer is evident from 190 cm to 300 cm (end of core). This core records two buried events, one at 90 cm and the other at 170 cm.

**Hadsall Creek Cores - 218, 219, 220**

This is an inlet on the south side of the Siuslaw River approximately 24 km (14.6 mi) due east of the ocean (figure 5).

Core 218- Of the cores taken near Hadsall Creek, this core was taken at a location closest to the Siuslaw River. It records 4 burial events, Mu 1 at 170 cm, Mu 2 at 268 cm,

Mu 3 at 280 cm, and Mu 4 at 290 cm. The marsh units at 268 cm and 280 cm are each 5 cm thick with a slightly rooted mud layer in between them. They may represent one marsh unit rather than two.

Core 219- This core was taken from a location adjacent to and upstream of core 218. It is 400 cm long. The portion of the core from the top to a depth of 65 cm is muddy peat. From 65 to 75 cm it is mud which tops muddy peat (sharp contact) at 75 cm to 100 cm. Slightly rooted mud is found at 100 cm to 125 cm and a muddy peat grading downward into a peat, containing four mud laminates, which extends from 125 cm to 315 cm. Mud is found at 315 cm to 375 cm and it tops a layer of sand at 375 cm to 400 cm.

Core 220- The top 13 cm of this core flowed out of the core barrel. From 13 cm to 50 cm there is muddy peat and at 50 cm to 190 cm there are mud and peat laminates (multiple thin peat layers topped with mud). Peat is found below this at 190 cm to 240 cm. The bottom of the core from 240 cm to 250 cm consists of slightly rooted mud.

It is noted that progressing west to east in the Siuslaw River Basin the cores change in nature from continuous peats to episodically buried peats and the incidence of sharp contacts increases. This suggests sudden, rather than gradual subsidence.

TABLE IV

## SUMMARY OF SIUSLAW C-14 DATES

<u>CORE#</u>	<u>DEPTH</u>	<u>AGE</u>
225	218 cm	1840 ± 80 yrs
	310 cm	3030 ± 70 yrs
222	322 cm	1910 ± 70 yrs
213	210 cm	1880 ± 80 yrs
216	68 cm	540 ± 70 yrs
	127 cm	1320 ± 60 yrs
	153 cm	1540 ± 70 yrs
	167 cm	1450 ± 70 yrs
	210 cm	1910 ± 70 yrs

## DIATOMS

There is a limit to the value that analysis of diatom assemblages can provide in explaining depositional environments. Seasonal and other environmental variables which can impact accurate interpretation of diatom data will be addressed in the discussion and conclusion section. It can be said at this point that studies have shown that fresh water diatoms dominate in areas where water salinity is 5 ‰ or less. Below this level of salinity the incidence of marine/brackish diatoms drops off dramatically. Therefore,

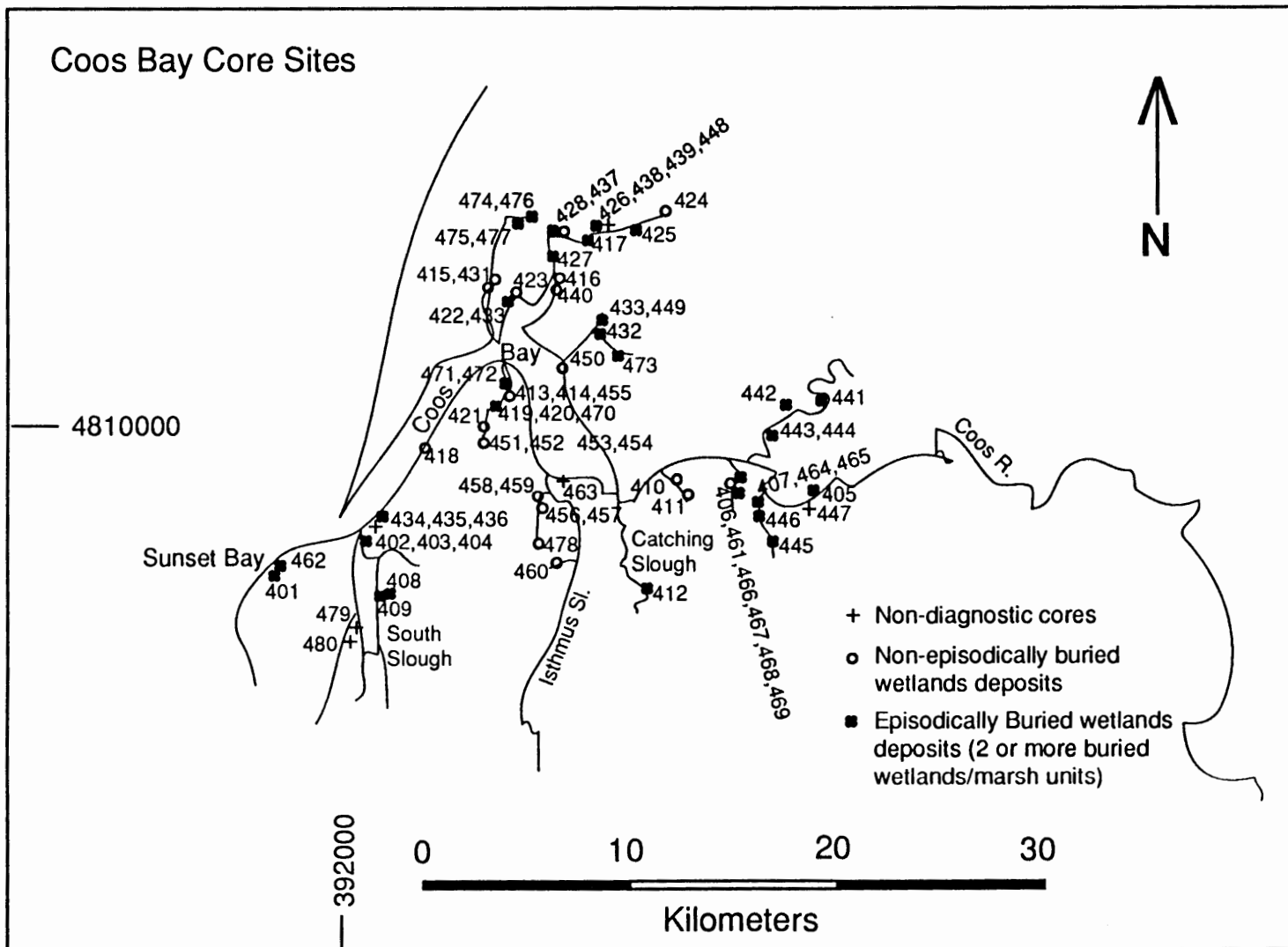


Figure 12. Coos Bay area core location map. Sites included tidal marshes, low lying pastures, and tidally influenced tributary streams of the Coos River, Coos Bay area.

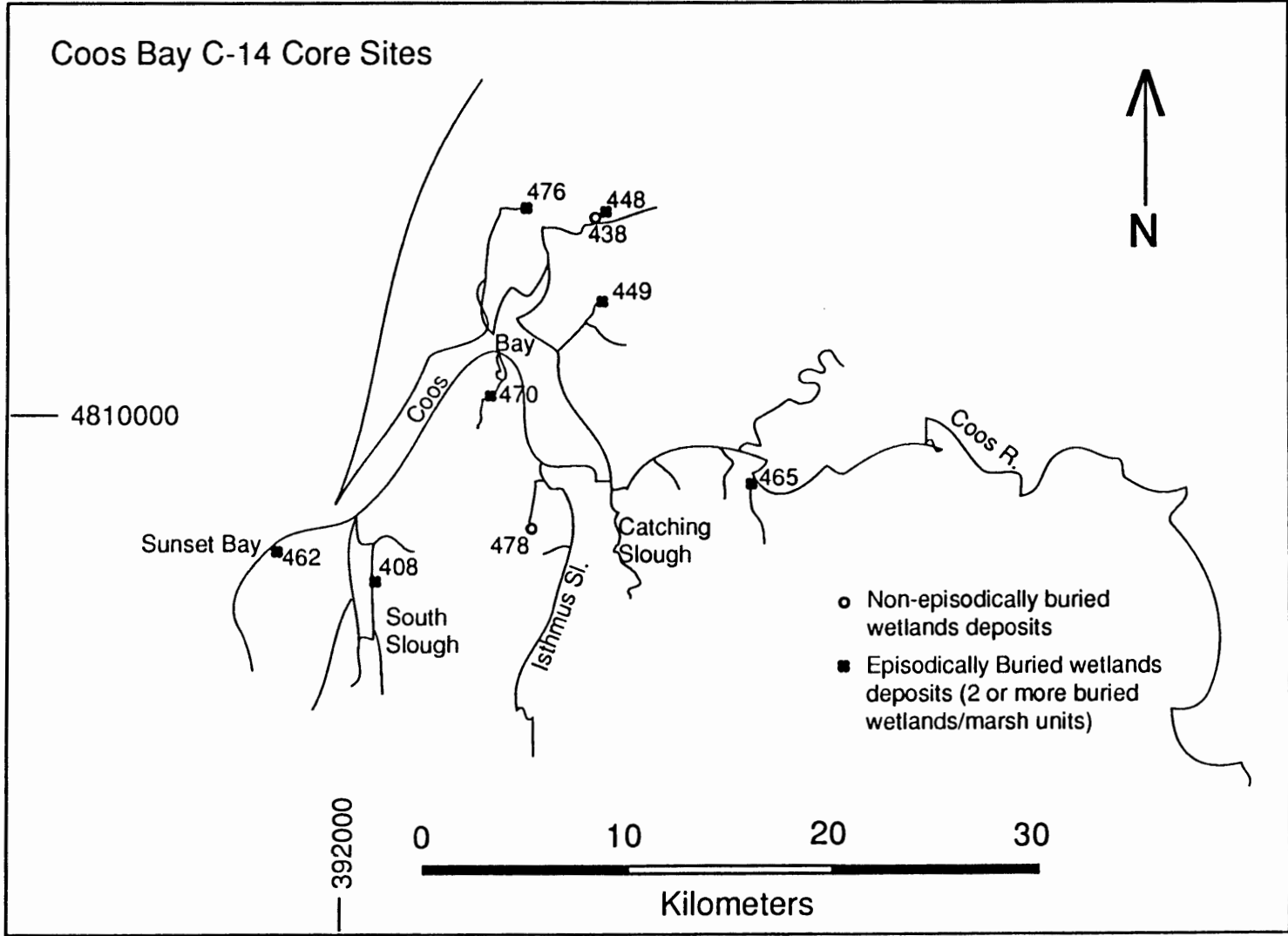


Figure 13. Coos Bay study area C-14 dated cores - Site Map.

**Sunset Bay Cores - 401, 462**

These cores were taken from a low lying wooded area in Sunset Bay State Park just off of Big Creek 0.2 km (0.12 mi) southeast of Sunset Bay. These core sites are presently above the reach of high tides. Nevertheless, an abundance of peaty sections downcore suggests the river valley has back-filled in response to rising sea level in late Holocene time. The episodic development of wetlands (peat) might reflect local changes in relative sea level in Sunset Bay. However, this small embayment is also directly exposed to storm surges from the open ocean. The response of wetlands to open ocean storm surges, river floods and/or tectonic vertical displacements in embayments such as Sunset Bay have not previously been investigated.

Core 401- This 400 cm long core consists of peat from the surface down to 20 cm. At 20 cm it grades down into sandy mud which extends to 60 cm where there is a gradual lower contact. From 60 cm to 83 cm there is sandy muddy peat which has a gradual lower contact. At 83 cm the sandy muddy peat grades down into sandy peaty mud to a depth of 150 cm. At this point the sandy peaty mud grades into sandy peat which has a sharp lower contact at 163 cm. From 163 cm to 215 cm there is mud which contains small amounts of detrital

material and has a gradual lower contact. It grades down into peaty mud which has a gradual lower contact at 230 cm. From 230 cm the peaty mud grades down into muddy peat which contains small amounts of sand and detrital material. At 258 cm there is a gradual lower contact. From 258 cm to the end of the core at 400 cm the muddy peat grades into peat which contains detrital material throughout.

Core 462 (figure 15)- This core is 585 cm long. From the surface to a depth of 23 cm there is peat with a gradual lower contact. The peat grades into sandy mud which extends down to 75 cm. At 75 cm there is slightly sandy muddy peat which has a sharp upper contact and a gradual lower contact at 95 cm where it grades into slightly peaty mud below. The slightly peaty mud continues to a depth of 141 cm. At this point it grades into muddy peat which has a sharp lower contact at 150 cm. From 150 cm to 157 cm there is slightly peaty mud. Peat is evident from 157 cm to 169 cm. The peat has sharp upper and lower contacts. From 169 cm to 195 cm there is mud which has a gradual lower contact. The mud grades into muddy peat which extends to 200 cm. From 200 cm to 225 the muddy peat grades into mud. At 225 cm peat with a sharp upper contact and sharp lower contact at 259 cm is found. Mud is seen from 259 cm to 263 cm. At 263 cm there is peat with a sharp upper contact and a gradual lower contact. At 285 cm the peat grades into slightly peaty mud

COOS BAY CORES (Southern area)

Radiocarbon dates (C-14 AGE YRS B.P.  $\pm 1\sigma$ )

West

East

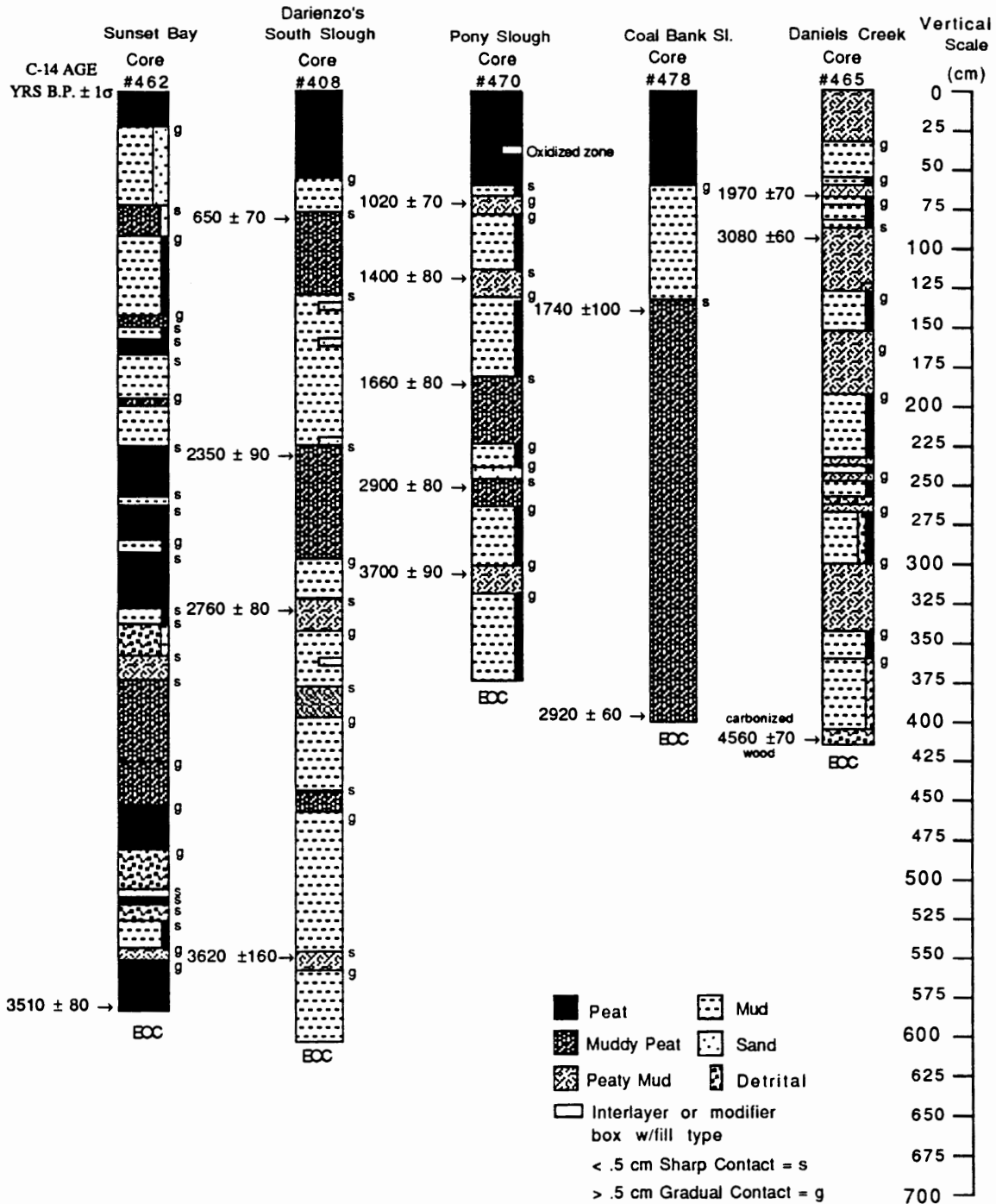


Figure 15. Coos Bay (southern area) radiocarbon dated cores. Elevation corrections for the tops of cores taken in this southern Coos bay area were typically between +0.53 m and +2.65 m above mean sea level ( high marsh, upper intertidal). See appendix B for elevation range and Coos Bay core map for location of southern core sites.

which extends to 290 cm. Peat with sharp upper and sharp lower contacts is evident from 290 cm to 328 cm. At 328 cm there is slightly peaty mud which continues to a depth of 339 cm. From 339 cm to 357 cm there is slightly sandy detrital material which has sharp upper and sharp lower contacts. Peaty mud is seen from 357 cm to 371 cm. At this point there is muddy peat which extends to 450 cm. This muddy peat has sharp upper and gradual lower contacts. At 450 cm it grades down into peat which has a gradual lower contact at 480 cm. From 480 cm the peat grades into detrital material which extends to a depth of 505 cm. At 505 cm there is a thin layer of sand which has a sharp upper contact. At 508 cm there is peat with a sharp upper contact and a sharp lower contact. From 515 cm to 525 cm there is a layer of detrital material. At 525 cm there is slightly peaty mud which extends to a depth 545 cm and has a sharp upper contact and a gradual lower contact. At 545 cm it grades into peaty mud which continues down to 550 cm. The peaty mud grades into peat which continues to the end of the core at 585 cm. The basal date is  $3510 \pm 80$  RCYBP. This core contains at least nine buried peats and/or detrital organic zones.

Cores 401 and 462 were taken from an area at Sunset Bay with a known fault structure first inferred and mapped by Allen and Baldwin in 1944 (Allen and Baldwin, 1944), later mapped by others. This complex area is exposed to the bay but also located at the mouth of a narrow creek valley. Debris

flows down the steep sided canyon and storm surge detrital material washed in from the ocean may have affected the stratigraphy. Even so, these cores show multiple peaty to muddy transitions suggesting episodically buried sequences.

**South Slough Cores - 480, 479, 409, 408**

The South Slough is a tidal marsh 4.2 km (2.6 mi) southeast of the south jetty of Coos Bay (figure 12).

Core 480- This core was taken on the west shore of South Slough 0.8 km (0.49 mi) south of Valino Island. It is 275 cm long and contains peat from the surface down to 35 cm where there is a gradual lower contact. At 35 cm the peat grades down to mud which extends down to 190 cm. At 190 cm the mud grades into a basal sand which continues to the bottom of the core at 275 cm.

Core 479- This 200 cm core was taken 0.3 km (0.18 mi) north of core 480 and consists of peat from the surface to a depth of 31 cm where there is a gradual lower contact. The peat grades into mud which extends to the end of the core at 200 cm.

Core 409- This core was taken by Peterson and Darienzo (1989) on the east side of South Slough at the point where Day Creek enters the slough. This core is 500 cm long. The top portion of the core from the surface to a depth of 57 cm

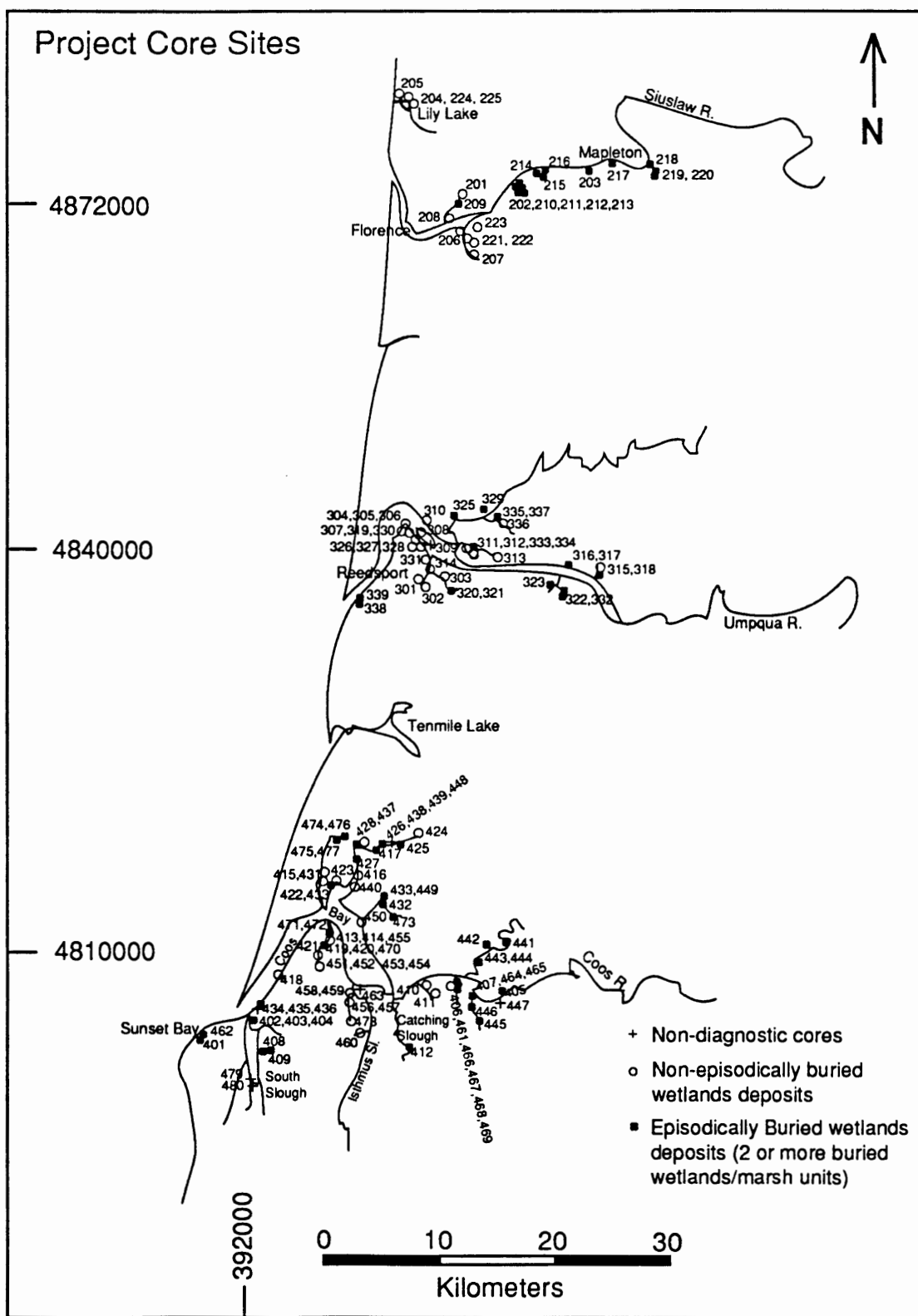
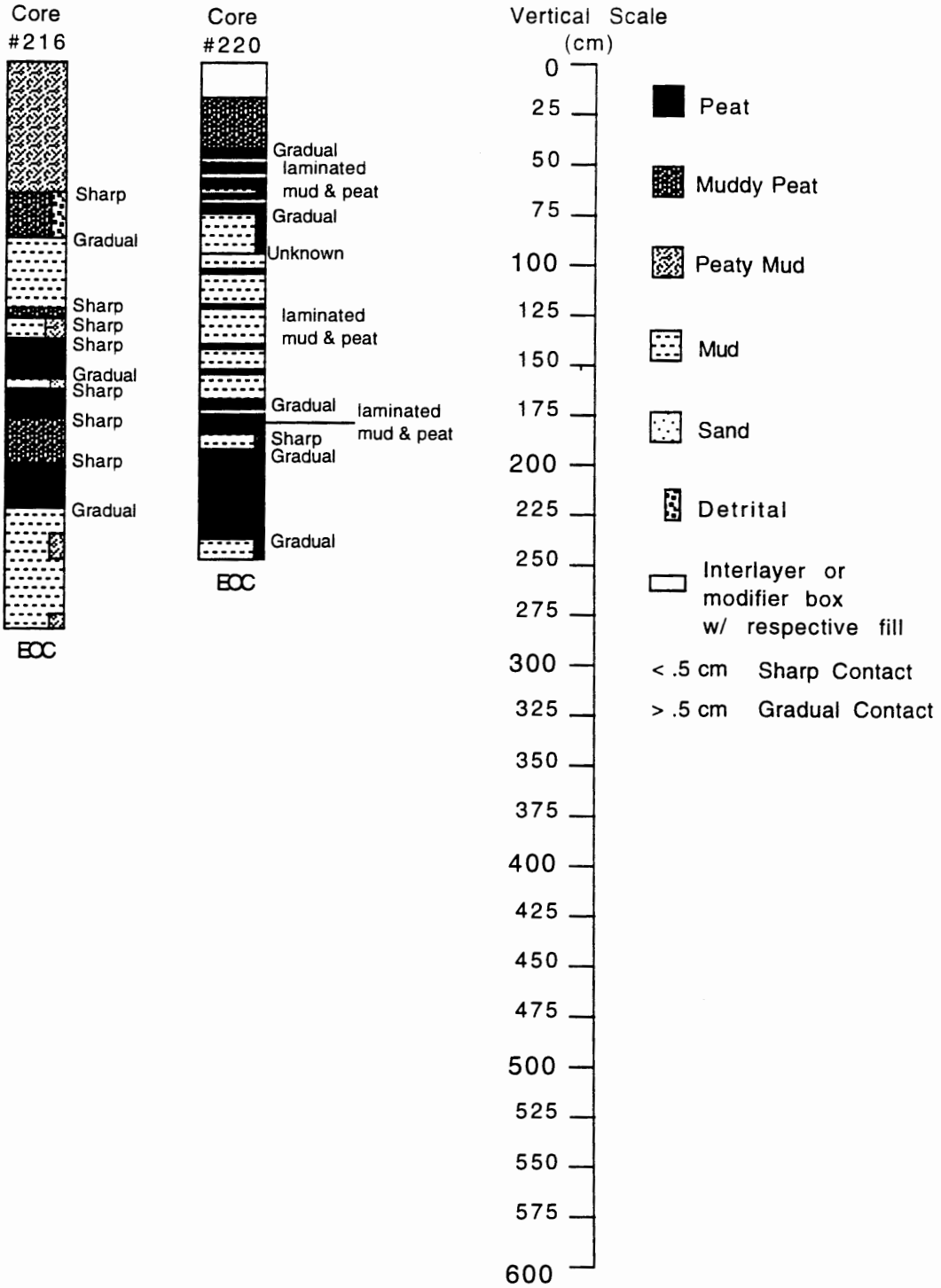
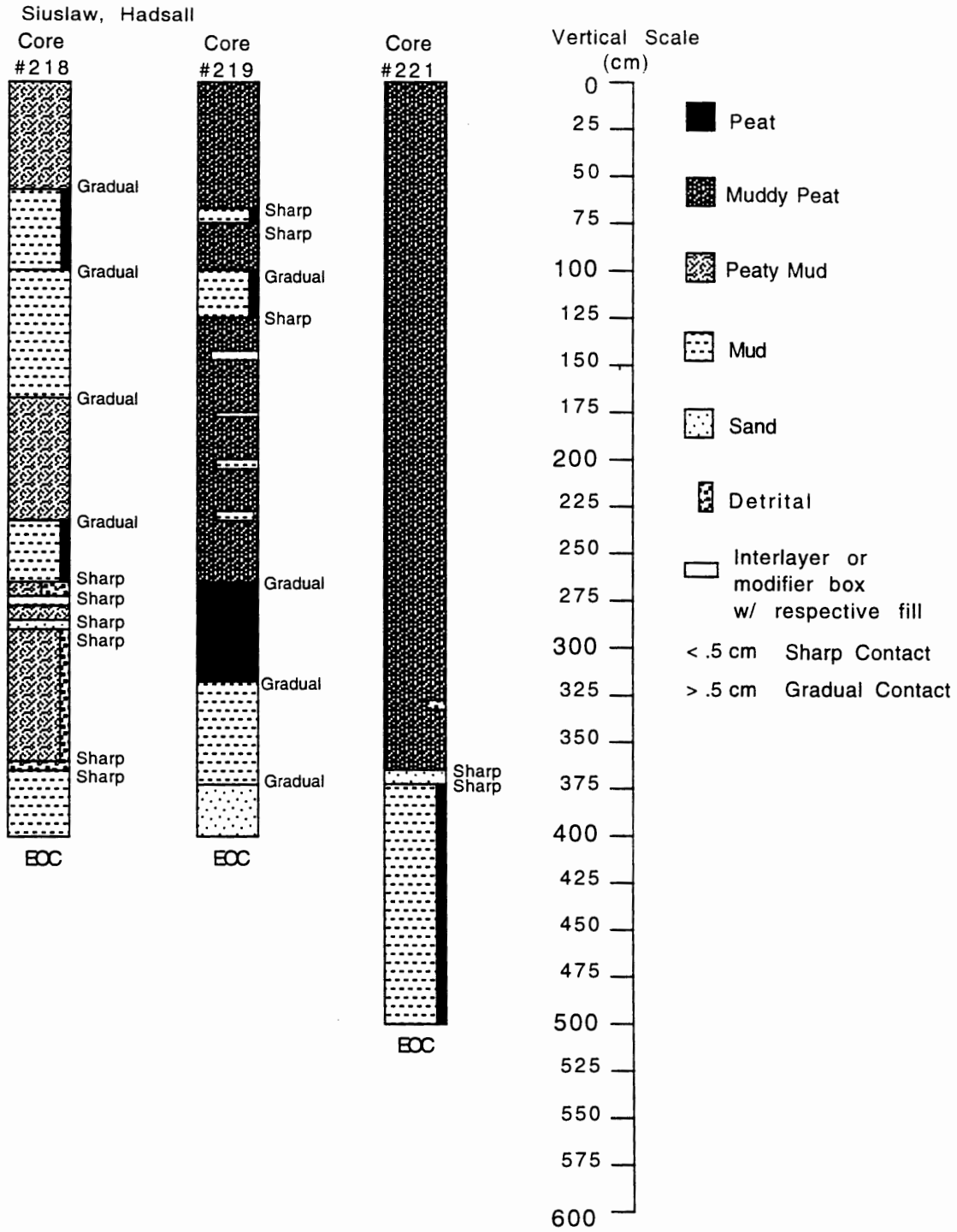


Figure 17. Composite core location map of coastal study area.



Siuslaw, Karnowsky Ck, Hadsall Ck (PC's)







## Pleistocene and Holocene Dunal Landscapes of the Central Oregon Coast: Newport to Florence

**Curt D. Peterson**, Geology Department, Portland State University, Portland, Oregon 97207; petersonc@pdx.edu

**Darren L. Beckstrand**, Cornforth Consultants, 10250 SW Greenburg Road, Portland, Oregon 97223; dbeckstrand@cornforthconsultants.com

**Charley M. Clough**, AMEC Earth and Environmental, 7477 SW Tech Center Drive, Portland, Oregon 97223

**J. Courtney Cloyd**, U.S. Forest Service, P.O. Box 3623, Portland, Oregon 97208; jcloyd@fs.fed.us

**Jon M. Erlandson**, Anthropology Department, University of Oregon, Eugene, Oregon 97403

**Georg H. Grathoff**, Geology Department, Portland State University, Portland, Oregon 97207

**Roger M. Hart**, College of Oceanographic and Atmospheric Sciences, Oregon State University, Corvallis, Oregon 97331

**Harry M. Jol**, Department of Geography and Anthropology, University of Wisconsin., Eau-Claire, Wisconsin 54702; jolhm@uwec.edu

**David C. Percy**, Geology Department, Portland State University, Portland, Oregon 97207; bjpd@pdx.edu

**Frank F. Reckendorf**, Reckendorf and Associates, 950 Market Street NE, Salem, Oregon 97301; frecken.@open.org

**Charles L. Rosenfeld**, Department of Geosciences, Oregon State University, Corvallis, Oregon 97331; rosenfec@geo.orst.edu

**Phyllis Steeves**, U.S. Forest Service, 4077 Research Way, Corvallis, Oregon 97333

**Errol C. Stock**, Griffith University, Brisbane, Queensland 4111, Australia; e.stock@mailbox.gu.edu.au

### ABSTRACT

During this 2 day field trip we will traverse the broad dune sheets (0–100 ka in age) that mantle the narrow coastal plain (1–5 km in width) of the central Oregon coast. We will examine interstratified dunal paleosols and redox-boundary hardpans that control cut-slope stability, ephemeral wetlands, groundwater geochemistry, and archaeological site distributions. We will trek across active dunes, overview dunal archaeological sites, interpret ground-penetrating radar profiles, perform paleosol chronosequencing, and collect a thermoluminescence sample for dating.

### INTRODUCTION AND BACKGROUND

Sustainable development issues in coastal plains of the West Coast are of increasing interest to growing coastal

populations. Narrow coastal plains (1–5 km in width) are largely covered by dune deposits in Washington, Oregon, central California, and Baja California Sur (Fig. 1). Although the dune cover is relatively thin, typically 3–30 m in thickness, it impacts cut-slope stability, surface and groundwater quality, wildlife habitat, and the location of archaeological sites. Regional-scale reexaminations of coastal dunes in western North America are now underway by a large coalition of investigators (<http://nwdata.geol.pdx.edu/SeaGrant/index.html>).

William Cooper's 1958 and 1967 monographs on coastal eolian dunes of Washington, Oregon, and California completed one of the most comprehensive coastal geologic studies in the Pacific Northwest. From a field program spanning 22 years (1919 through 1941) he formulated creative insights about dune morphology and distribution on the West Coast. Since Cooper's seminal work, the technologies of radiocarbon (RC) dating, thermolumines-

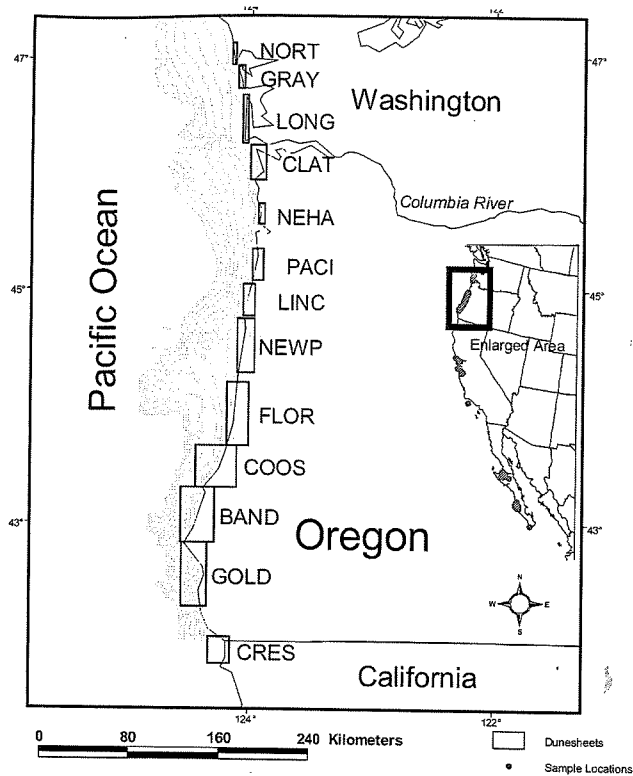


**Figure 1. West Coast dune sites where dune dating (radiocarbon and thermoluminescence) is being performed (dots in Washington, Oregon, California, and Baja California Sur). Square boxes represent areas of dune-sheet mapping in the Pacific Northwest.**

cence (TL) dating, and digital ground-penetrating radar (GPR) have become available to extend our dating and subsurface-imaging capabilities.

Understanding of dunal landscape evolution on the central Oregon coast is also advancing from related studies in other disciplines. The related work includes recent studies of Quaternary sea-level change (Pirazzoli, 1993), coastal neotectonics (Muhs and others, 1992; Ticknor, 1993), coastal paleoclimate (Worona and Whitlock, 1995), and coastal archaeology (Erlandson and others, 1998).

Coastal dune studies in many countries have focused on late Holocene dune development. Dunes originate from posttransgressive remobilization of shelf sand and local redistribution through

littoral drift (Pye and Rhodes, 1985; Short, 1987; Tooley, 1990; Illenberger and Verhagen, 1990). Holocene dune fields of the Oregon coast are generally restricted to embayments or the northern ends of littoral cells. Holocene dune ramps that allowed beach sand to reach sea-cliff tops (2–5 ka) are now largely eroded away, leaving unsupported slopes (Fig. 2). Similarly, the ongoing exposure of buried prehistoric forests that colonized middle Holocene wave-cut platforms (Fig. 3) indicate a net loss of sand from some littoral cells in recent time (Hart and Peterson, 1997).

In contrast to the narrowly restricted active dunes, the widespread stabilized dunes of the central Oregon coast originated in late-Pleistocene time (24–100 ka) (Fig. 4). These widespread dune sheets likely migrated onshore from continental-shelf sand exposed to eolian processes during lower sea-level stands (Fig. 1 and 5). Such lowstand origins have been proposed for some pre-Holocene coastal dunes in southern California (Orme, 1990) and Australia (Thom and others, 1994).

The long geologic histories of the Oregon dune sheets have led to interstratified loose sand and cemented paleosols and hardpans (Fig. 6). These different units complicate predictions of dunal slope stability, wetland regulatory status, and groundwater flow in dunal aquifers (Couch and others, 1980; Reckendorf, 1998). The forested dune sheets previously mapped as marine terrace deposits (Schlicker and others, 1973) climb up the foothills to altitudes of 100–150 m at distances of 1–6 km inland from the coast (Fig. 7a,b). Together, the Holocene and Pleistocene dunal landscapes cover about 80 percent of the coastal plain in the Newport and Florence areas.

This guide to a 2 day field trip between Newport and Florence, Oregon (Fig. 8) identifies about 2 dozen roadside stops where earth scientists can address the age, origin, and stratigraphic development of the dunal landscapes along the central Oregon coast. In addition, many of these stops provide critical exposures that prompt more informed consideration of dunal slope

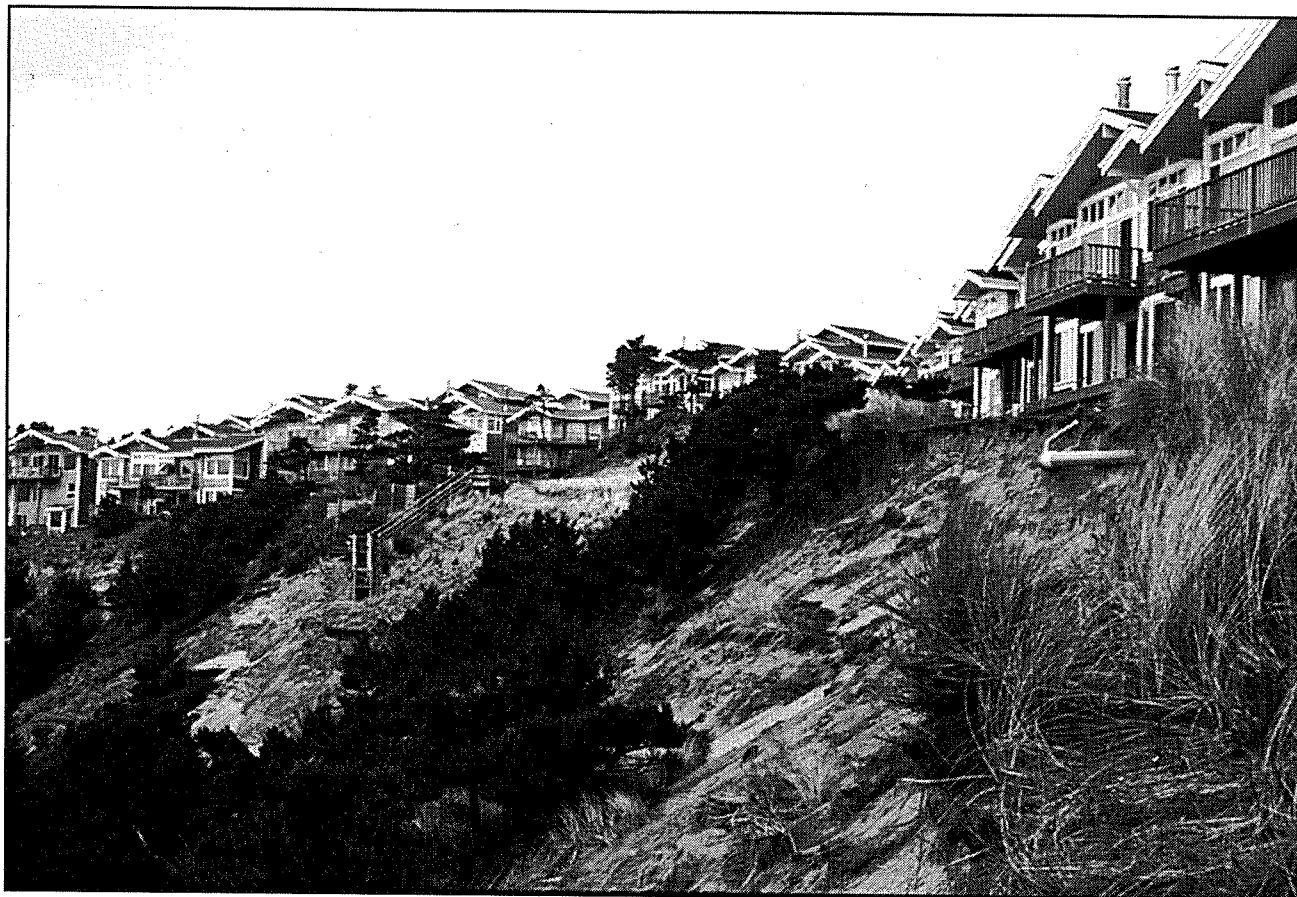


**Figure 2.** Digital image of The Capes development at Netarts Bay, Tillamook County, Oregon. The development extends onto a perched Holocene dune ramp that failed recently, leading to condemned structures and lawsuits.

stability, dunal aquifer management, and sustainable development in the coastal zone. We will appreciate input from field trip participants about specific field trip localities and broader sustainable-development issues on the coastal plain.

## OVERVIEW OF ITINERARY

### Day 1

The formal field trip starts in Newport, Oregon (Fig. 8). The first stop is at a beach-access trail that descends to the base of Pleistocene and Holocene dune deposits exposed in a sea-cliff section. We then complete a traverse to the east (3 km in length) tracing dunal deposits across the city of Newport. The Pleistocene dune sheets, generally ranging from 3 to 30 meters thick, cover marine terraces to the west and hillslope colluvium to the east.

The surface features of uptown Newport, including topographic benches, valleys, and small ridges, reflect both episodic advances of the late Pleistocene dunes and intervening truncation by deflation. We will examine some geotechnical "successes" and "failures" in dealing with dunal cut-slope instabilities at Newport.

From Newport we drive south to Ona Beach for lunch and a brisk walk out to view a stratigraphic record of dunes (0–80 ka). This 30 meter vertical section extends from a basal wave-cut platform up to the Pleistocene–Holocene dunal contact. At this site we will also collect a thermoluminescence (TL) sample for dating one of the dune depositional sequences.

Continuing south toward Seal Rock we complete another eastward traverse (3 km in length) ending at the Pioneer Cemetery on the ridgeline. On a clear day we

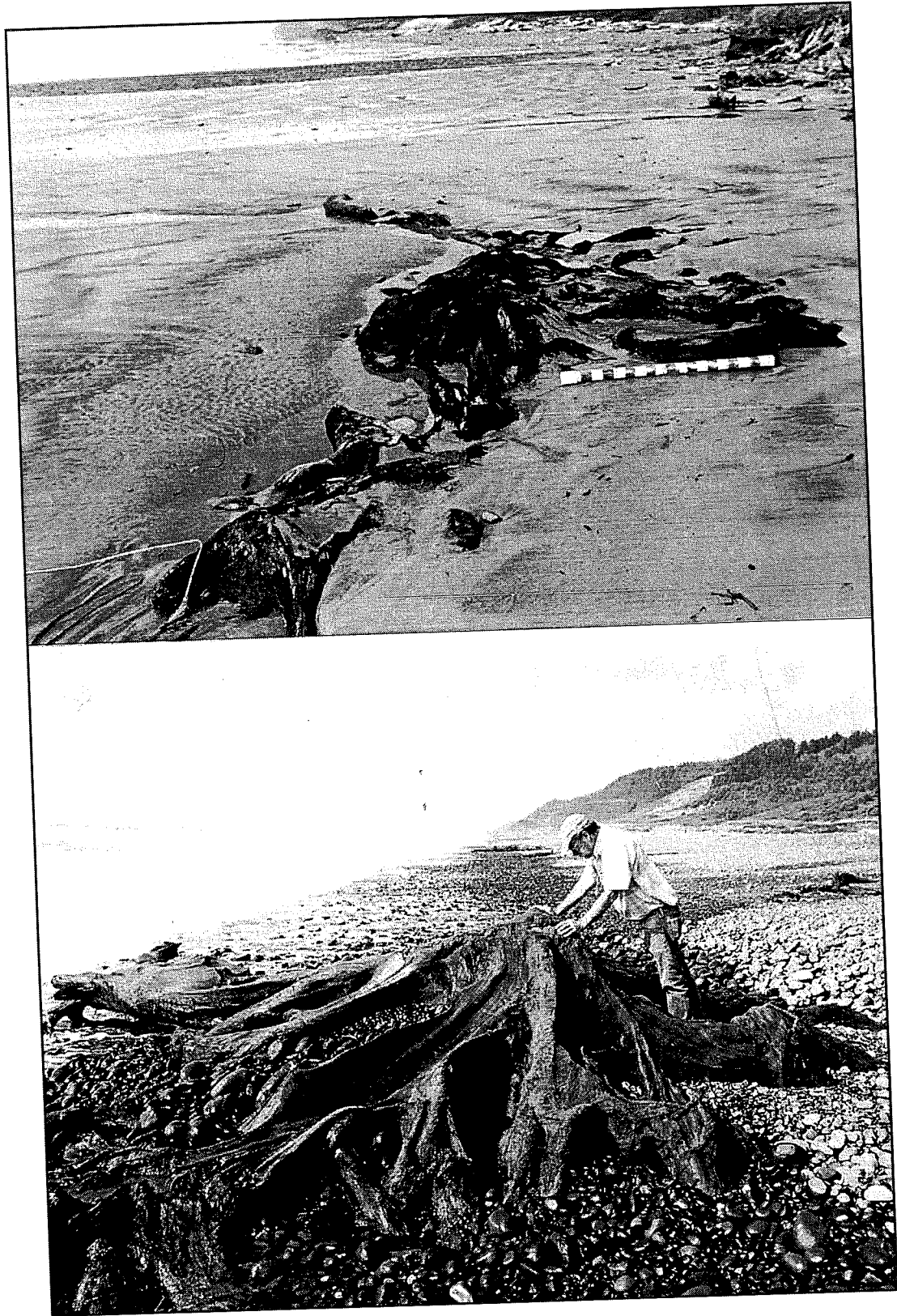


Figure 3. "Mystery" or swash-zone forest stump during summer (upper photo) and winter (lower photo) at the southern end of the Newport Littoral Cell. These forests grew on exposed Holocene wave-cut platforms in middle to late Holocene time, prior to burial by a posttransgressive sand supply during late Holocene time. Progressive exposure of the stumps to marine-life degradation indicates a net loss of beach sand from this littoral cell in latest Holocene time.

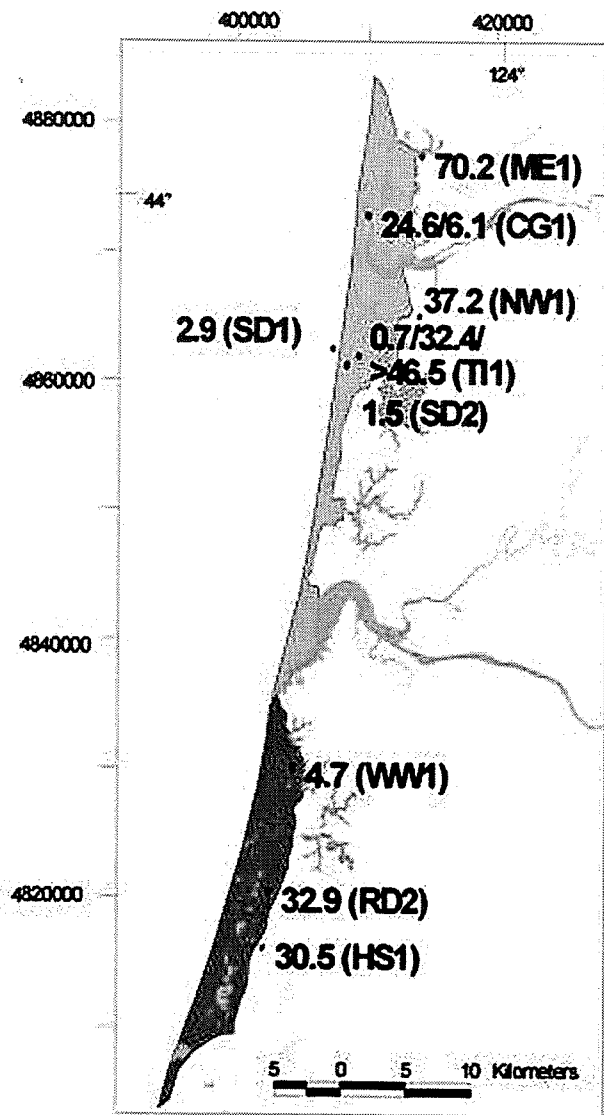


Figure 4. Map of dune ages from thermoluminescence dating (ME1-70.2 ka, CG1-24.6 ka, NW1-37.2 ka, T1-32.4 ka, SD1-2.9 ka, SD2-1.5 ka, WW1-4.7 ka, RD2-32.9 ka, and HS1-30.5 ka) and radiocarbon dating (CG1-6.9 ka, T1->467.5 ka, and 0.7ka) from the Florence and Coos Bay Dune Sheets in the Oregon Dunes National Recreation Area (ODNRA) (from Beckstrand, 2001).

should be able to gaze down the clear-cut dune ramps to the distant sea cliffs. We then can imagine the exposed dune sheets extending west 20–40 km across the inner continental shelf during lowstands of sea level.

Returning to US 101, we will continue south, shortly passing a Native American

shell midden (0.3 ka) at Seal Rock. Short stops will be made to view dune cut-slope failures along US 101, dune-barrage ponds, marine-terrace deposits not covered by dunes, and “mystery” stumps in modern surf zones. Ongoing net erosion of the beach deposits episodically reveals the “mystery” stumps (generally 2–4 ka in age) during the winter months.

Our last formal stop of the day will be at a deflated dune section at Yachats, spanning 0–80 ka in age but only 7 meters in height. After this stop we drive 60 km south on US 101 to Florence. As we drive along the scenic Cape Perpetua to Heceta Head coastline, the tourists will be looking downslope at the crashing surf below, while we will be looking upslope at dunal remnants along the high cliffs.

We have arbitrarily mapped the distal dune sheets as distinct units separated along the coast by major headlands. However, the dune sheets were likely contiguous between major river valleys on the subaerial continental shelf during marine lowstand periods.

#### Day 2

From Oldtown Florence (Fig. 8) we will travel northwest to the Siuslaw Harbor Coast Guard Station. Bay-cliff exposures in this area reveal the contact between the uppermost Pleistocene deflation surface (>24 ka) and the overlying late Holocene dune sheet (<7 ka). We will continue north about 5 km to start another eastward traverse (6 km in length) at the Sutton Creek Recreational Area. Holocene dune cover extends some 2–3 km landward of the modern shoreline at the northern end of the Umpqua Littoral Cell. Holocene shoreline progradation here, possibly 0.5–1 km, accompanied the late Holocene posttransgressive sand surge and northward littoral transport in this cell. We will raise environmental issues about historic dune stabilization, wetland regulation, and barrage-pond water quality at short stops along the traverse.

US 101 marks the onset of late Pleistocene dunes exposed at the surface along this traverse, which continues eastward for

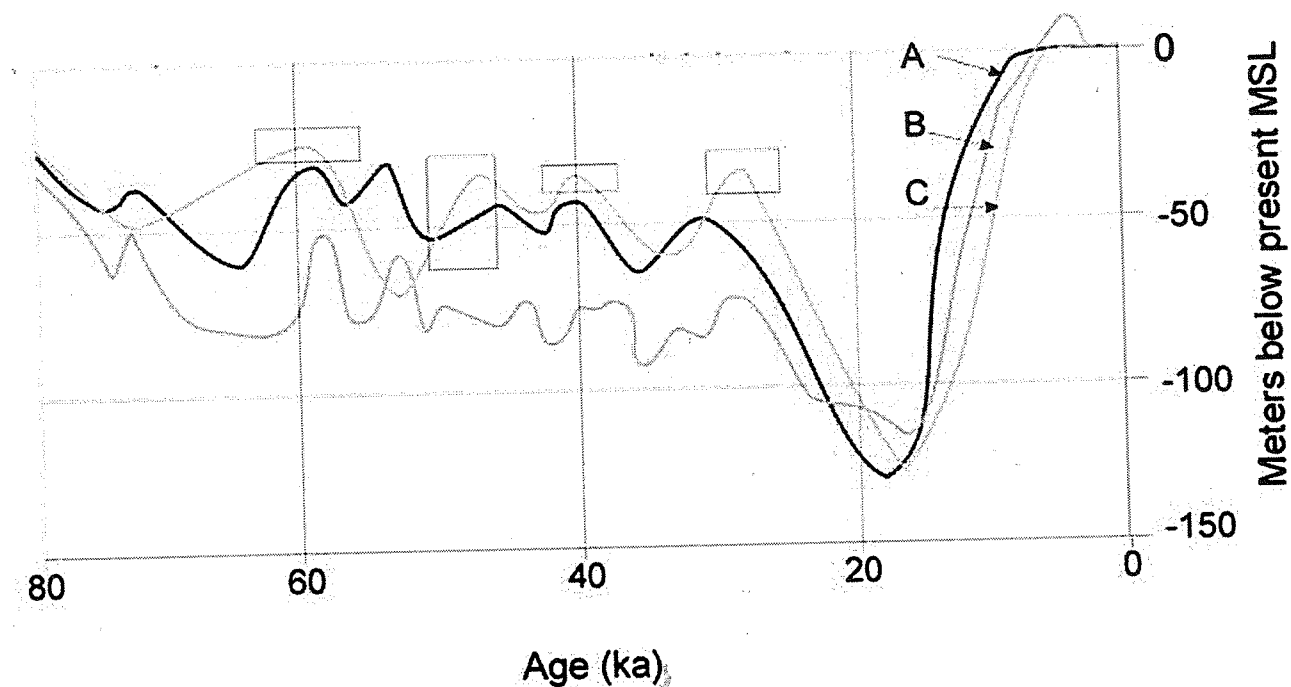


**Figure 5.** Published sea-level curves from a compilation by Pirazzoli (1993). Between 80 and 10 ka, the average sea level was about 50 meters below the present sea level. During the last glacial maximum (about 18 ka), sea level dropped 120–140 meters below the present level.

another 3 km to Mercer Lake. Mercer Lake is one of several smaller barrage lakes that flood pre-Holocene river valleys of the north Florence dune sheet. Gibbsite nodules precipitated in "old" dunal deposits (70 ka) around Mercer Lake, and they will be discussed in terms of interstratal groundwater geochemistry.

A short drive back to Florence and over the Siuslaw River Bridge to South Jetty Road, takes us into the active dune fields of the Oregon Dunes National Recreation Area (ODNRA) managed by the U.S Forest Service. We will complete another eastward traverse here, including an overview of an archaeological site (0.7–1.0 ka) developed on a young, intermittently exposed dunal paleosol (0.5–2 ka). Deep ground penetrating radar (GPR) profiles will be shown from recent surveys along this traverse. The traverse will continue east of US 101 at Woahink Lake to the easternmost extent of the late Pleistocene dunes (37 ka). The Pleistocene dune cover here extends 6–7 km inland from the modern coast (Figure 7b).

At the eastern edge of the Pleistocene dune sheet we will perform a soil-profile analysis for chronosequencing. Several large dunal barrage lakes occur in the southern part of the Florence Dune Sheet. At least one of these barrage lakes, Tahkenitch Lake, contains a nearby (upland) record of Native American occupation (8–0 ka). Efforts are underway to date some of the barrage-lake deposits in the Florence Dune Sheet and to establish the ages of initial impoundment (Jesse Ford, pers. comm., 2001).

The last formal stop of the field trip will be at the modern foredune in the Oregon Dunes National Recreation Area's Siltcoos Access Area. The base of the foredune is dated at 3 ka, indicating little or no net shoreline progradation since that time. However, some landward sand transport occurred until about 1.5 ka at the eastern margin of the existing deflation plain. The Siltcoos foredune site provides opportunities to discuss complex management issues in the ODNRA. Some of these



**Figure 6. "Weeping sands" in late Pleistocene dunes with interstratified dunal paleosols serving as aquitards. Intrastratal groundwater deposition of hydroxides, clay, and other phases at paleosol redox boundaries serves to further cement the paleosol contacts.**

issues include foredune breach experiments, snowy plover habitat, and European beachgrass stabilization of active dunes.

#### **FIELD TRIP ROAD LOG, DAY 1**

From Corvallis, Oregon, drive west 82 km (51 mi) on US 20 to coastal US 101 in Newport. The northern Coast Range drainages provide some of the sand that is ultimately blown onshore to build the dunes. However, dunal sand mineralogies of the central Oregon coast largely reflect volcanic arc and metamorphic provenances drained by larger rivers to the south such as the Umpqua, Rogue, and Klamath Rivers. Commingling of the different provenance

mineralogies occurs on the inner continental shelf, which is a source of sand to the larger dune fields (Scheidegger and others, 1971; Beckstrand, 2001).

0.0 km (0.0 mi) Field trip starts at the intersection of US 20 and US 101 in Newport, Oregon (Fig. 8). Continue across the intersection due west 0.7 km (0.4 mi) on W Olive Street.

0.7 km (0.4 mi) Reach Stop 1 at the City Park (Donald A. Davis Park) above the sea cliff.

#### **Stop 1: Donald Davis City Park Beach Trail (rest rooms)**

From the parking area we will follow the paved trail past the flagpole as it winds down the sea cliff to the beach. We will examine the dune sequences in the sea cliff including from bottom to top (a) the wave-cut platform cut into the local bedrock, (b) Pleistocene dunes, and (c) a thin mantling of late Holocene dunes (regional dates of 1–3 ka by radiocarbon dating) above a conspicuous paleosol. The Newport wave-cut platform (lowest exposed platform) is dated at 80–85 ka by mollusk aminostratigraphy (Kennedy and others, 1982) This terrace age is thought to represent the last substantial marine highstand (isotope stage 5a) forming the Whisky Run Terrace of southwest Oregon (Muhs and others, 1992). The late Pleistocene dune sequence contains different types of paleosols as follows (1) Bw horizons (iron-stained accumulation), (2) Bh horizons (humate accumulation), (3) Bg horizons (chemically reduced glade or "gray" layers), and (4) Bt horizons (clay accumulation). The late Holocene dunes contain only Bw and Bh horizons, whereas the late Pleistocene sequences also include Bg and Bt horizons (Table 1).

The late Holocene dunes above the late Pleistocene topsoil must have originated from broad beaches and extensive dune ramps that climbed above the middle Holocene sea cliffs. The sea cliffs are now once again eroding, thereby undercutting both the Pleistocene and Holocene dune cover. Unstable dunal sea cliffs seem to fail

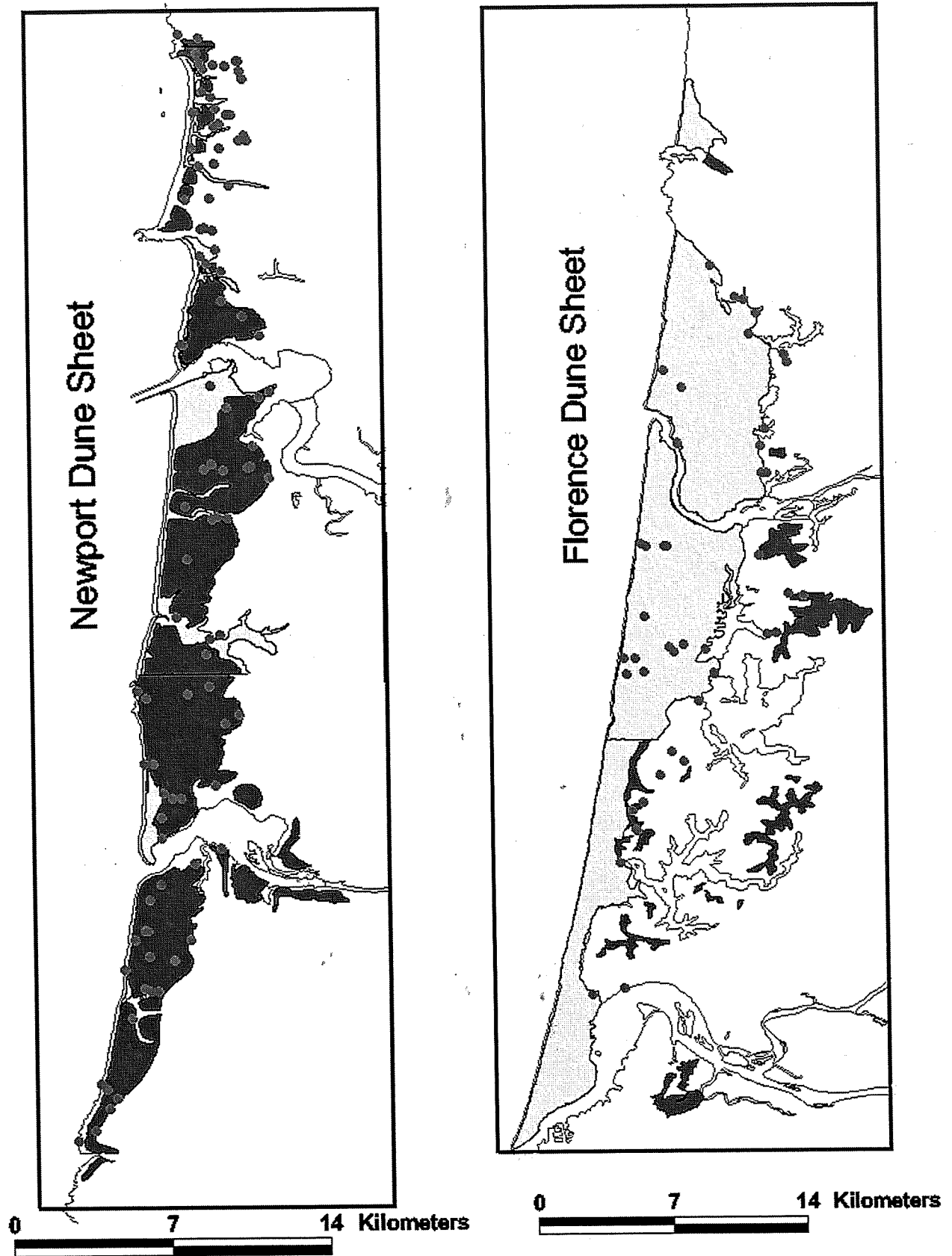


Figure 7. Quaternary dune and marine terrace deposits digitized from published geologic maps (<http://nwdata.geol.pdx.edu/SeaGrant/index.html>) showing dots where dune deposits have been profiled in the Newport (Figure 7a) and Florence (Figure 7b) Dune Sheets. Shaded units are shown in the legend.

unpredictably, due in part to the variably cemented Pleistocene dune strata. Creep along seaward-dipping failure plains in the shallow bedrock units further complicates the shoreline-erosion process in this area (George Priest, pers. comm., 2001).

2.3 km (1.4 mi) From Stop 1 return to the intersection of US 101 and US 20, then continue east on US 20 (E Olive St) 0.8 km (0.5 mi) to a stoplight intersection with NE Harney, and turn north (left) on NE Harney.

2.7 km (1.7 mi) Continue north 0.4 km (0.2 mi) on NE Harney to a stop-sign intersection with 7th Street. Turn east (right) on 7th Street.

2.9 km (1.8 mi) Continue up the hill on 7th Street 0.2 km (0.1 mi) to Stop 2 at the Newport Middle School parking lot.

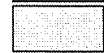
#### Stop 2: Newport Middle School Parking Lot

From the parking lot and playing fields of the Newport Middle School we will view the engineered dunal slopes to the east. Initial grades were too steep, resulting in rilling, gulying, and small slumps after winter rains. Mitigation steps included drainage-monitoring wells, slope-grading, geotechnical fabric covers, and reseeding.



### Legend

#### Dune Type

	<b>qmt</b>
	<b>qmth</b>
	<b>qmtl</b>
	<b>qmtm</b>
	<b>qmtu</b>
	<b>qs</b>

#### Shoreline

#### Dunesheets

#### Counties

**Side Trip:** A side trip can be made to a dunal liquefaction site near the top of Big Creek Road in north Newport. From 7th Street continue several blocks west to Eads Road, then turn north (right) on Eads Road, and continue around Sam Case Elementary School to connect with Big Creek Road. The liquefaction site is at a Pleistocene dune outcrop in a road cut (west) at the intersection with the Frank Wade City Park entrance. Clastic dikes (>20 cm width) at the base of the exposed section transition to convolute bedding (1–3 m in thickness) in the middle of the section. The scale and setting of these features indicate significant ground shaking. A thermoluminescence (TL) date of the dune deposit (predating the liquefaction) is pending. Similar coseismic liquefaction features are reported from dune deposits above marine terraces that are exposed in nearby sea cliffs (Peterson and Madin, 1997). Return to Stop 2.

3.2 km (2.0 mi) From Stop 2 return to NE Harney Street and turn south (left) to intersection with 3rd Street. Turn east (left) on 3rd Street.

4.2 km (2.6 mi) Continue east 1 km (0.6 mi) on 3rd Street, viewing dune deposit exposures in road cuts to Stop 3 at the Newport City Water Tank.

#### Stop 3: Newport Water Tank, 3rd Street Road Cut

After pulling off the road across from the Newport water tank, we will walk 50 m east (uphill) on 3rd Street to examine dune-deposit exposures in the north road cut. Stop 3 is within 0.5 km of the eastern limit of the preserved dune-sheet deposits in this area (Figure 7a). The Newport Dune Sheet maintains about the same width to the south, but it narrows to the north. The next dune sheet north, the Lincoln City Dune Sheet, averages only about 1 kilometer in width. Pleistocene dune sheets farther north of Lincoln City are increasingly narrow and discontinuous to the north. These trends suggest diminishing shelf-sand supply north of the Stonewall-

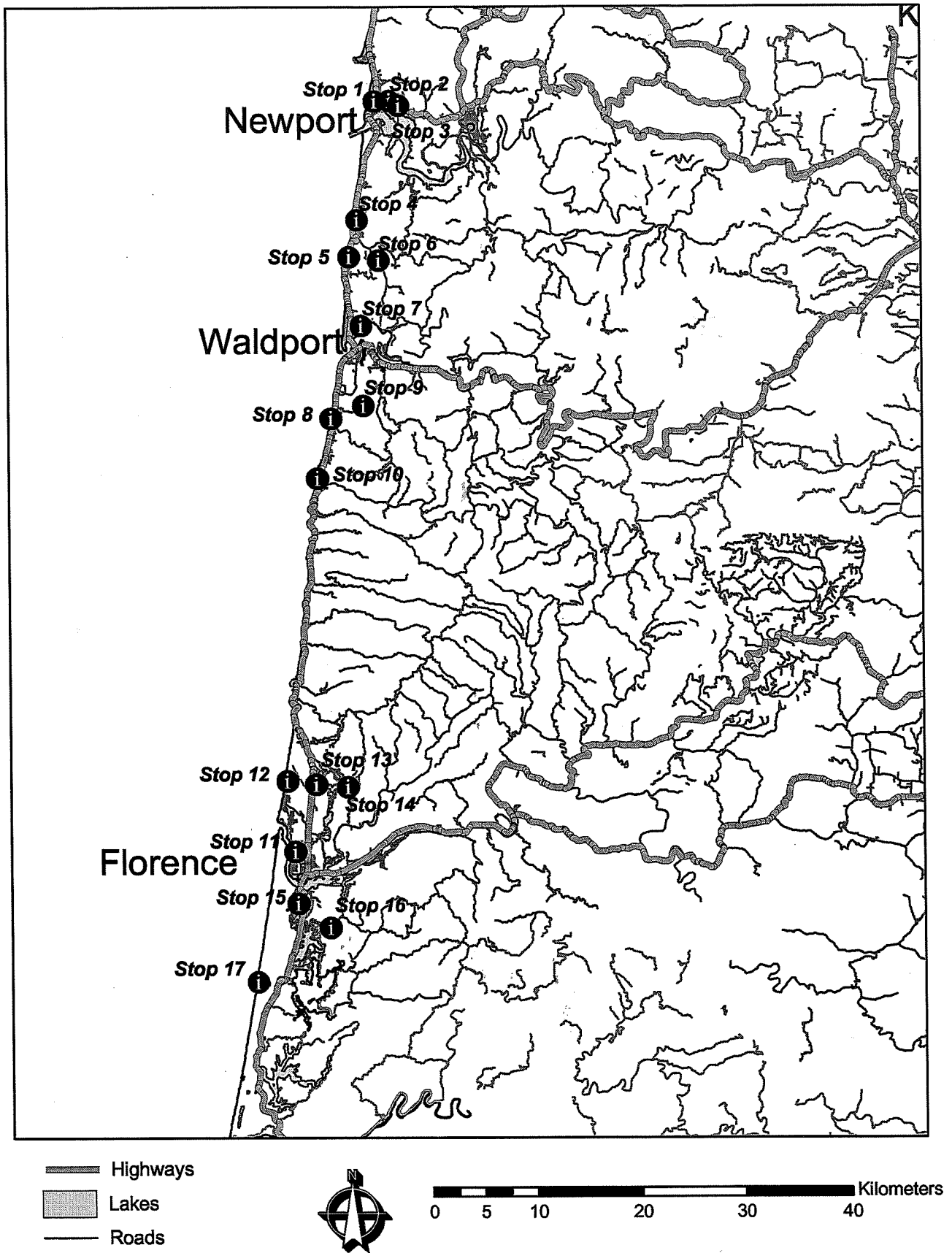


Figure 8. The study area roads and field trip stops (black symbols numbered in the order of the stops).

Florence Pleistocene dune sheets were likely contiguous between major river valleys on the inner continental shelf during marine lowstands. Small Holocene dune fields, which ramped up the middle Holocene sea cliffs, are now being undercut by net erosion along the small pocket beaches.

103.5 km (64.3 mi) At a distance of 26–26.5 km (16.1–16.5 mi) south of Yachats look for viewpoint turnouts on the southwest side of US 101 that overlook the northern end of the Florence Dune Sheet.

Lilly Lake, one of a half dozen dune-barrage lakes in the area, is at the foot of the Heceta Head headland and has a basal peat date of 3 ka (Briggs, 1994). Late Holocene peat and forest remnants have been observed at the modern beach just south of Lilly Lake. These wetland deposits exposed at modern beaches reflect some net erosion of the shoreline in recent time. A marine terrace back edge of unknown age is identified by sea stacks east of Lilly Lake. The sea stacks are on US 101 some 29 km (18 mi) from Yachats. Pleistocene dunes generally surface east of US 101, and they climb the foothills to heights of 100 to 150 m at distances of some 5–6 km inland from the present coast (Fig. 7b).

118 km (73.3 mi) Continue south 15 km (9.3 mi) on US 101 to Florence on the Siuslaw River, which marks the end of Day 1.

## FIELD TRIP ROAD LOG, DAY 2

0.0 km (0.0 mi) From the Oldtown Florence Loop under the bridge drive northwest 0.4 km (0.2 mi) on Kingwood Street to the intersection with Rhododendron Drive, turn west (left) on Rododendron Drive (Fig. 8).

4.9 km (3.0 mi) Continue 4.5 km (2.8 mi) northwest on Rhododendron Drive to the Coast Guard station, just past (north of) the 35th Street intersection. Turn west (left) off of Rhododendron Drive into the Coast Guard station and drive northwest 0.1 km (0.05 mi) to the visitors' parking lot for Stop 11.

### Stop 11: Siuslaw Coast Guard Station

The access to this stop requires advance permission from the U.S. Coast Guard. The contact between overlying Holocene and underlying Pleistocene dune deposits can be viewed at several bay-cliff localities 0.5–1 km north and south of the Coast Guard station. Several key thermoluminescence (TL) and radiocarbon (RC) dates have been taken from dunal deposits at the Coast Guard Station site (Fig. 4). The bay-cliff exposure along this part of the Siuslaw River reveals a broad contact between a late Pleistocene deflation surface, about 24 ka (thermoluminescence), and overlying Holocene dunes, younger than 7 ka (radiocarbon). A Holocene radiocarbon-date sample at the contact (6,900±700 RCYBP Beta#84373) was taken from one of many stumps that were buried in situ, vertically standing, by the advance of the Holocene dunes. The radiocarbon date from the standing stump represents an approximate age of tree death that predates the major influx of Holocene dune sand.

5.2 km (3.2 mi) From Stop 11 return to Rhododendron Drive, then turn south (right) on Rhododendron Drive then abruptly (left) at the 35th Street intersection.

6.6 km (4.1 mi) Continue east 1.4 km (0.9 mi) on 35th Street, to reach the intersection with US 101. En route, note the recently active parabolic dunes. The elimination of virtually all active dunes in the Florence area by vegetative stabilization and other methods is both imminent and controversial (see discussion topics at next stop). Turn north (left) on US 101.

11.8 km (7.3 mi) Continue north 5.2 km (3.2 mi) on US 101 to Campground Vista Road (Sutton Creek Campground Road) intersection. Turn west (left) on Campground Vista Road.

15.0 km (9.3 mi) Continue west 3.2 km (2.0 mi) on Campground Vista Road to Holman Vista Parking Lot (Sutton Beach Access) for Stop 12.

**Stop 12: Holman Vista (Sutton Beach Access) rest rooms**

At this stop we initially will examine one of the few dunal isopach maps in Oregon. Based on a seismic-refraction survey, three dunal aquifer layers are identified in the Florence Dunal Aquifer (Couch and others, 1980). For example, at the intersection of Campground Vista Road and US 101 the isopach map indicates (1) 6 m of unsaturated Holocene dune sand above (2) 20 m of saturated Holocene dune sand above (3) 20 m of semiconsolidated Pleistocene dune sand above (4) bedrock. The maps indicate substantial spatial variability of the different units' thickness throughout the dunal aquifer.

After discussing the dunal isopach map, we will walk out to the modern foredune (beach access trail) to view a variety of dunal habitats. We will examine the effects of nonnative vegetation such as European beachgrass *Ammophila arenaria* on different dunal environments. Until a decade ago the major goal of dune managers was the stabilization of active dunes (Carlson and others, 1991). However, environmental, recreational, and community sentiments are changing toward an appreciation of active and semiactive dunal landscapes. We will discuss efforts to recreate an active-dune habitat for threatened species such as the Snowy Plover. We also will discuss the potential impacts of vegetative stabilization on other recreational and aesthetic uses of active-dune landscapes.

18.2 km (11.3 mi) From Stop 12 return east 3.2 km (2.0 mi) on Campground Vista Road to the US 101 intersection. En route, view dune pine and rhododendron forests, dunal ponds, and wetlands on the Holocene dune fields. Turn north (left) on US 101.

18.4 km (11.4 mi) Continue north 0.2 km (0.1mi) on US 101 to the Mercer Lake Road intersection. Turn east (right) on Mercer Lake Road.

18.5 km (11.5 mi) Continue east 0.1 km (0.05 mi) on Mercer Lake Road to the *Darlingtonia*

Bogs State Park on the south side of the road for Stop 13.

**Stop 13: *Darlingtonia* State Park (rest rooms)**

At this stop we will take a short (50m long) boardwalk to see some *Darlingtonia* bogs. *Darlingtonia* (pitcher plant) is a carnivorous plant that relies on the digestion of trapped insects for nutrients that are low in abundance in the bog soils. At this site we will discuss issues concerning federal regulation of dunal wetlands. Wetland species thrive in dunal bogs following rainy seasons, but they dry out at ephemeral wetland sites during drought periods. The ephemeral wetlands of dunal deflation hollows and gullies are temporarily formed by perched groundwater above paleosol aquitards. Federal regulations restrict development in the sensitive wetlands. Disputes arise when developers purchase land, but are then restricted from developing it when wetland species rejuvenate during wet years.

20.7 km (12.9 mi) Continue east 2.2 km (1.4mi) on Mercer Lake Road to a turnout on the northwest side of the road. The small turnout at Stop 14 is adjacent to a prominent road cut at a sharp road bend on the southeast side of Mercer Lake. Watch for traffic hazards at this sharp road bend.

**Stop 14: Mercer Lake Road Cut**

From the turnout at the road bend at this stop we will carefully cross the road to examine gibbsite nodules and interstratal groundwater cementation of late Pleistocene dunes that date back to 70 ka (thermoluminescence) (Fig. 4). The top of this dune section has been truncated by mass wasting, and the lower units extend below the Mercer Lake water level. The full extent of this early dune advance is not known. However, younger late Pleistocene dunes, with less interstratal cementation, reach farther inland and to higher altitudes (see Side Trip below). The precipitation of gibbsite  $Al(OH)_3$  in the coastal dunes came as a surprise to us, as this phase usually reflects extreme weathering in laterite. The

gibbsite occurs in the coarser sand where it precipitates as nodules or in cavity fills (1–2 cm diameter). The precipitation of gibbsite rather than kaolinite requires a low dissolved silica concentration, which was unexpected in these quartz-rich sand dunes (Beckstrand, 2001; Grathoff and others, 2001). Groundwater is apparently removing large amounts of Fe and Si from the aquifer, but the sinks or discharge areas of those two elements are not known. In addition to the gibbsite nodules, some late Pleistocene dune sections include gibbsite fracture fills, gibbsite replacement of lithic clasts, and gibbsite sheets between bedding planes.

**Side Trip:** An interesting side trip can be made from here to one of the higher altitude dune deposits in the Florence area. From Stop 14 continue 0.1 km (0.05 mi) east on Mercer Lake Road to an unmarked intersection. Turn south (right) on the gravel road (which turns into Chapman Road) and follow it 0.6 km (0.4 mi) uphill to an intersection with View Road. Alternatively, find another route to View Road. Turn east (left) on View Road, and then make an abrupt turn north (left) on Ocean View Road. Continue uphill 0.2 km (0.1 mi) and look for dune deposits in an east-side road cut near the top of Ocean View Road. The thin topsoil development and weak cementation of the Cox horizon here suggests a younger age for these late Pleistocene dunes than those of the Mercer Lake deposit at the bottom of the north slope at Stop 14. Return to Stop 14.

23.0 km (14.3 mi) From Stop 14 return 2.3 km (1.4 mi) west on Mercer Lake Road to the US 101 intersection. Turn south (left) on US 101.

30.5 km (18.9 mi) Continue south 7.5 km (4.7 mi) on US 101 to the Oregon 126 intersection in Florence.

33.0 km (20.5 mi) Continue south 2.5 km (1.5 mi) on US 101 through Florence, and over the Siuslaw River Bridge to the South

Jetty Road intersection. Turn west (right) on South Jetty Road.

36.3 km (22.5 mi) Continue west 3.3 km (2.1 mi) on South Jetty Road to a north bend (right) in the road at the modern foredune. Turn around at the gravel-road intersection.

Solid-stem auger coring at this site recovered late Holocene beach shells and gravel at 7 m depth. Little or no net shoreline progradation has occurred at this site since the deposition of the beach shells (shell radiocarbon sample yet to be dated). Ground penetrating radar profiles, vibracores, and geoprobe cores from the adjacent deflation plain record subhorizontal deflation surfaces to at least 10 m depth. In this area the position of the middle Holocene paleoshoreline back edge has not been established. However, a deflation-truncated paleosol was encountered at 10 m depth at the eastern margin of the deflation plain (Goose Pasture Staging Area) about 1 km east of the foredune. Deeper GPR profiling will be required to establish the Holocene shoreline back edge, somewhere between the modern foredune and the Goose Pasture Staging Area.

38.5 km (23.9 mi) Return east 2.2 km (1.4 mi) on South Jetty Road to the South Jetty Staging Area entrance road south (left turn) for Stop 15.

**Stop 15: South Jetty Road Staging Area 1 (rest room and lunch)**

After lunch we will take a brisk walk to an overview of the South Siuslaw Dune archaeological site. This informal overview is 50 north of the entrance day-pass station, which was passed on the way into the South Jetty Staging Areas. The archaeological site, dated at 0.7–1.0 ka (Minor and others, 2000) was developed on a weak paleosol that is being progressively buried and exposed on opposite sides of a deflation corridor between active transverse dunes. The deflation corridor can be viewed toward the base of the northward-descending dune field. Abundant fish bones, small spear points, and other artifacts are scat-

tered on the paleosol. Charcoal layers in the paleosol date from 0.5-2.3 ka (radiocarbon). Another paleosol 0.5 km to the east of the 0.5-2 ka paleosol dates at 4 ka. It is not known what caused the localized vegetative stabilization of the dunes during the temporary periods of soil development recorded at these active-dune sites.

Ground penetrating radar profiling was performed to test whether the buried cultural horizon, that is paleosol (0.5-2 ka), could be mapped under the active dunes. We will examine the GPR profiles of the cultural site from the overview. The GPR records show that the paleosol climbs to the south, as photographed in previous years of exposure, and that it merges with a perched groundwater surface at several meters depth. Both the paleosol and groundwater surface dip northward toward the Siuslaw River. Several dune reactivation surfaces are imaged at much greater depths in the subsurface. A continuous high-amplitude basal reflection occurs at a subsurface depth of 40 m. It is not known whether this basal reflection represents the Holocene-Pleistocene dunal contact, a fluvial terrace cut into the dunal substratum, or some other structure.

39.6 km (24.6 mi) Return 1.1 km (0.7 mi) to US 101 intersection. Turn south (right) on US 101.

42.1 km (26.1 mi) Continue south 2.5 km (1.5 mi) on US 101 to intersection with Woahink Road. Turn east (left) on Woahink Road.

45.2 km (28.1 mi) Continue east 3.1 km (1.9 mi) on Woahink Road to Stop 16 at dune deposits exposed in a north-side road cut. En route, examine oversteep cutbanks of Woahink Road and the subsequent slope failures of late Pleistocene dune deposits, some 1.6 km (0.9 mi) from the US 101 intersection.

#### **Stop 16: Woahink Road Cut Exposure**

At this stop we will briefly examine and record a soil profile taken in a road cut

of the late Pleistocene dune deposits. This locality is near the eastern limit of late Pleistocene dune advance, and has been thermoluminescence (TL) dated at 37 ka (Figures 4 and 7b). Pleistocene dune-soil chronosequencing has been attempted in the study area, based on traditional methods of soil color, texture, and structure. However, the traditional indexes of soil development have not correlated well with measured deposit age (Beckstrand, 2001). Problems likely arise from soil truncation by deflation, loess deposition on existing soils, and variable redox conditions from changing groundwater level, among others.

For this study we have had success in using a combination of measurements taken from the preserved accumulation horizons in the dune topsoils. The measurements include (1) type of soil accumulation horizon (Bw, Bh, Bg, Bt, Bs/Bc); (2) thickness of preserved accumulation zone (<5, 5-20, 20-60, 60-120, >120 cm); (3) maximum apparent consolidation (loose, cohesive, peds, blocky, Cox-cemented); and (4) maximum consolidation measurements from penetrometer (1, 2, 3, 4, 5 kg/sq cm). Each of these parameters is scored (1-5), summed, and averaged by the number of parameters to yield a normalized accumulation horizon index (NAHI) of 1-5. Low NAHI values (1-2) generally correspond to late Holocene dune topsoils, whereas high NAHI values (4-5) typify Pleistocene dune topsoils. Where truncation has occurred at incomplete soil profiles, the parameter of accumulation-horizon thickness is not used. Where dune reactivation has buried soils producing multiple paleosols, the NAHI index provides only a limiting relative-age estimate. Ultimately, luminescence or radiocarbon dating is required to constrain the absolute age of the dune deposits. However, the NAHI system used in this study has proved useful to geologists, engineers, and archaeologists in discriminating between Pleistocene and Holocene dune deposits.

48.3 km (30.0 mi) Return west 3.1 km to US 101 intersection. Turn south (left) on US 101.

51.4 km (31.9 mi) Continue south 7.1 km (4.4 mi) on US 101 to intersection with Siltcoos Road (Siltcoos Campground and Beach Access). Turn west (right) on Siltcoos Road.

53.8 km (33.4 mi) Continue west 2.4 km (1.5 mi) on Siltcoos Road to Stop 17 at the Siltcoos Recreation Area foredune parking lot and beach access trail.

**Stop 17: Siltcoos Recreation Area  
Foredune (rest rooms)**

This is the last stop of Day 2 in the formal Field Trip Guide. We will walk a couple hundred meters north from the parking lot to a "foredune breach" experiment site. The artificial breach was completed a couple of decades ago to allow beach sand to be blown through the beachgrass-stabilized foredune, thereby rebuilding dunes on the deflation plain. We will observe and discuss the results of the experiment, particularly with respect to modern beach-sand supply. The basal foredune deposits have been vibracored and thermoluminescence dated (3 ka) at this locality. Deflation-plain deposits (dune sand) were also vibracored and TL dated (1.5 ka) at sites at the eastern margin of the existing deflation plain. Historic photos demonstrate at least 100 m of recent eastward deflation. The deflation occurs to groundwater level, and it leaves interannual records of "trailing linear-edge deflation troughs". Landward from the deflation plain, or about 1.5 km east of the foredune, we will observe Tree Island #1, where exposed paleosols date to late Pleistocene time, greater than 32 ka (thermoluminescence and radiocarbon)(Fig. 4). These exposed paleosols indicate a relatively thin veneer of Holocene sand above the late Pleistocene dune ridge. Current deflation of the late Pleistocene paleosols at the Tree Island site, and in nearby parabolic-dune deflation corridors, reflect the remobilization of the underlying late Pleistocene dune deposits to form new Holocene dunes.

We hypothesize the following scenario for dune development in this area: Late

Pleistocene dune deposits by 30 ka accumulated as a broad high ridge (about 100 m above modern sea level) landward from a broad deflation plain (near present sea level). Early to middle Holocene transgression ravined the late Pleistocene deflation-plain deposits. Middle Holocene shoreline progradation followed posttransgression sand supply from onshore wave transport for several thousand years. Surplus sand was blown inland, mantling and locally reactivating the late Pleistocene dune ridge. With decreasing sand supply in latest Holocene time, the shoreline position stabilized or began to retreat. However, shoreward deflation continued to supply small transverse and parabolic dunes on the seaward side (Tree Island area) of the large dune ridge. Large areas of unstable active dunes continued to resist vegetative stabilization into late historic time (Cooper, 1958; Hunter and others, 1983). Nonnative beachgrass and shore pine planted in the middle part of the 1900s isolated and stabilized the active dunes. Deflation east of the foredune lowered the Holocene dune cover to the groundwater-surface level. Ongoing deflation continues to extend the deflation-surface wetlands (bogs) to the east. Finally, incipient European beachgrass colonization of the transverse and parabolic dunes on the large dune ridge has begun within the past couple of decades. The spread of European beachgrass onto the western slopes of the large dune ridge foretells the likely end of active dunal landforms in the Oregon Dunes National Recreation Area.

Several means of reactivating the vegetation-stabilized dunes are now under study in the ODNRA. These approaches to European beachgrass control include large-scale mechanical removal, expanded all-terrain vehicle (ATV) recreation, herbicides, burning, and handpicking. We will discuss the costs and relative effectiveness of these methods, and whether they can be sustained over large areas.

**Side Trip:** A short drive can be made from the Siltcoos Recreational Area entrance to the ODNRA Dunes Overlook Station by going south 4.1 km (2.5 mi) on US 101. The

U.S. Forest Service provides a handicap-accessible overlook of the dunes. On a clear day the view extends from the deflation plain landward of the foredune to climbing parabolic dunes "precipitating" (Cooper, 1958) into upland forests perched on late Pleistocene dunes. The late Pleistocene dunes are themselves ramped up against foothills of the Coast Range. Signboards at the overlook outline dune forms, habitats, and wildlife. Return to Stop 17.

**Side Trip:** A further side trip can be made to the Tahkenitch Landing archaeological site at Tahkenitch Lake, another 3 km (2 mi) south of the ODNRA Overlook. Three periods of dunal landscape development have been proposed for the Tahkenitch Lake area based on animal remains and other artifacts at the site (Minor and Toepel, 1986). The periods are (1) fishing camp—saline species in an estuary of the Tahkenitch Valley (8-5.2 ka by radiocarbon), (2) village—saline species and whalebones in a shallow estuary of the Tahkenitch Valley (5.2-3 ka), and (3) canoe landing—dune-barrage lake (3-0 ka). A controversy has arisen over the origin of the whalebones. If the whales swam up a moderately deep estuary to the site in late Holocene time, then the large dunes blocking the valley could not have developed until very late Holocene time. If the whalebones were scavenged from the beach and transported to the site, then the large dunes blocking most of the Tahkenitch Valley might have been in place by middle Holocene time. Analysis of long core records from the Tahkenitch Lake deposits could help resolve the timing of the estuary-to-lake transition. Return to Stop 17.

68.3 km (42.4 mi) From Stop 17 return east 2.4 km (1.5 mi) to the intersection with US 101. Turn north (left) on US 101, and continue north 12.1 km (7.5 mi) to the intersection of US 101 with Oregon 120 in Florence. End of field trip guide.

#### ACKNOWLEDGEMENTS

This field trip guide is based in large part on field mapping performed by us, by

study collaborators, and by student field assistants. Some of the student assistants include C. Alton, J. Brasseur, B. Burris, S. Cowburn, J. Jones, C. Knoepp, G. Peterson, S. Wacaster, and R. DeChaine. Support for this research has been provided by Griffith University, Brisbane, Australia (1996-present); the USFS Siuslaw National Forest (1997-present); the Oregon Dunes National Recreation Area (1996-1999); Oregon Department of Transportation (1999-present); Oregon Sea Grant 2000-02 (R/SD-04 NA650K); and Oregon Sea Grant 2002-04. George Moore provided editorial suggestions for the improvement of this field trip guide.

#### REFERENCES

- Beckstrand, D.L., 2001, Origin of the Coos Bay and Florence Dune Sheets, south central coast, Oregon: Portland State University MS Thesis, 192 p.
- Briggs, G.G., 1994, Coastal crossing of the elastic strain zero-isobase, Cascadia margin, south central Oregon coast: Portland State University MS Thesis, 251 p.
- Carlson, J., Reckendorf, F., and Ternyik, W., 1991, Stabilizing coastal sand dunes in the Pacific Northwest: USDA Soil Conservation Service, Agriculture Handbook 687, 53 p.
- Cooper, W.S., 1958, Coastal sand dunes of Oregon and Washington: Geological Society of America Memoir 72, 169 p.
- Cooper, W.S., 1967, Coastal dunes of California: Geological Society of America Memoir 104, 131 p.
- Couch, R., Cook, J., Gerald, C., Troseth, S., and Standing, W., 1980, Seismic measurements of the dunal aquifer of Florence, Oregon: Final Report to the Lane Council of Governments, Eugene, Oregon, 41 p.
- Erlanson, J.M., Tveskov, M.A., and Byram, S., 1998, The development of maritime adaptations on the southern Northwest Coast: *Arctic Anthropology*, v. 35, p. 6-22.
- Grathoff, G.H., Peterson, C.D., and Beckstrand, D.L., 2001, Coastal dune soils in Oregon, USA, forming allophane and gibbsite: 12th International Clay Conference Proceedings, Argentina, 8 p., in press.
- Hart, R., and Peterson, C.D., 1997, Episodically buried forests in the Oregon surf zone: *Oregon Geology*, v. 59, p. 131-144.
- Hunter, R.E., Richmond, B.M., and Alpha, T.R., 1983, Storm-controlled oblique dunes of the Oregon coast: *Geological Society of America Bulletin*, v. 94, p. 1450-1465.
- Kennedy, G.L., Lajoie, K.R., and Wehmler, J.F. 1982, Aminostratigraphy and faunal correlations of late Quaternary marine terraces: *Science*, v. 299, p. 545-547.
- Illenberger, W.K., and Verhagen, B.T., 1990, Environmental history of dating of coastal dunefields: *South African Journal of Science*, v. 86, p. 311-314.

## Stop 1. Bastendorff Beach

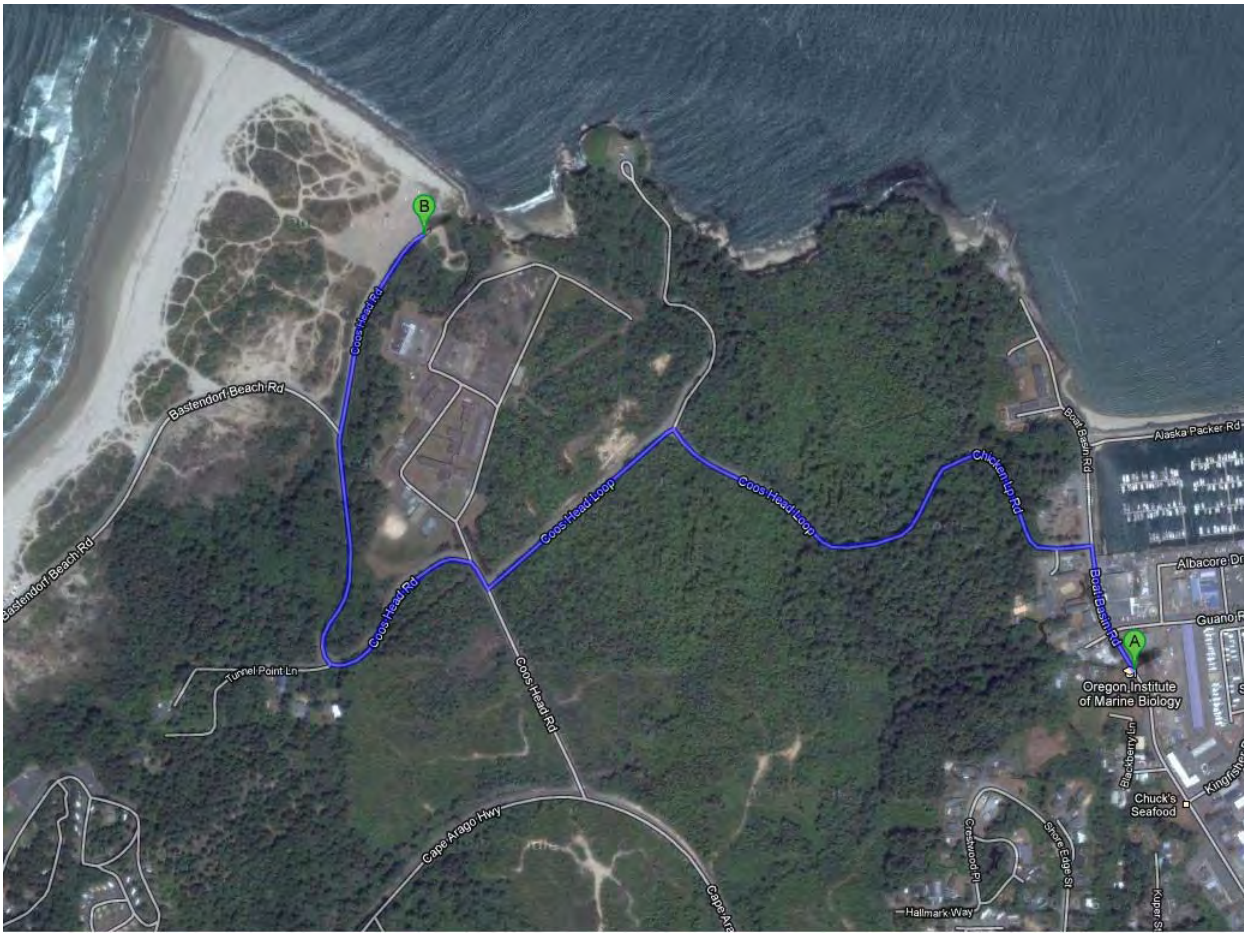


**Figure 1-1. Navigation**

Leaving OIMB, our first stop is Bastendorff Beach, a short drive over Coos Head.

### **Oregon Beach dynamics**

The Oregon Coast is highly active, with one of the most energetic wave climates (Figure 1-2) in the world, and all of that energy pushes a lot of sand around. We all learned about longshore drift in Geo 101, but the pattern in Oregon is fundamentally different. Oregon's coast is broken into a series of "pocket beach" littoral cells, long stretches of dune or bluff-backed beach bounded by rocky headlands that extend into water that is deep enough to block sediment transport around the ends of the headlands. There are also large differences in the direction and energy of summer versus winter waves (Figure 1-3); highly energetic winter waves erode the beaches and move sand offshore to form sand bars, while gentler summer waves restore the sand to the beaches. Within each cell, sand also moves north or south depending on the prevailing wave directions and in response to climate events such as El Niño's. Here at Bastendorff beach we see evidence for this intra-cell movement in the form of dramatic accretion of the beach since the construction of the south jetty in the early 1900's. The beach rapidly accreted (Figure 1-3) until about 1967, and has reached some state of equilibrium since then. The abandoned sea cliff is now hidden behind the forest of shore pines, but is clearly visible on lidar. Also typical of the Oregon Coast, the backshore at Bastendorff beach has been rapidly and effectively stabilized by

European dune grass, a non-native species that have substantially changed dune characteristics in the last century.

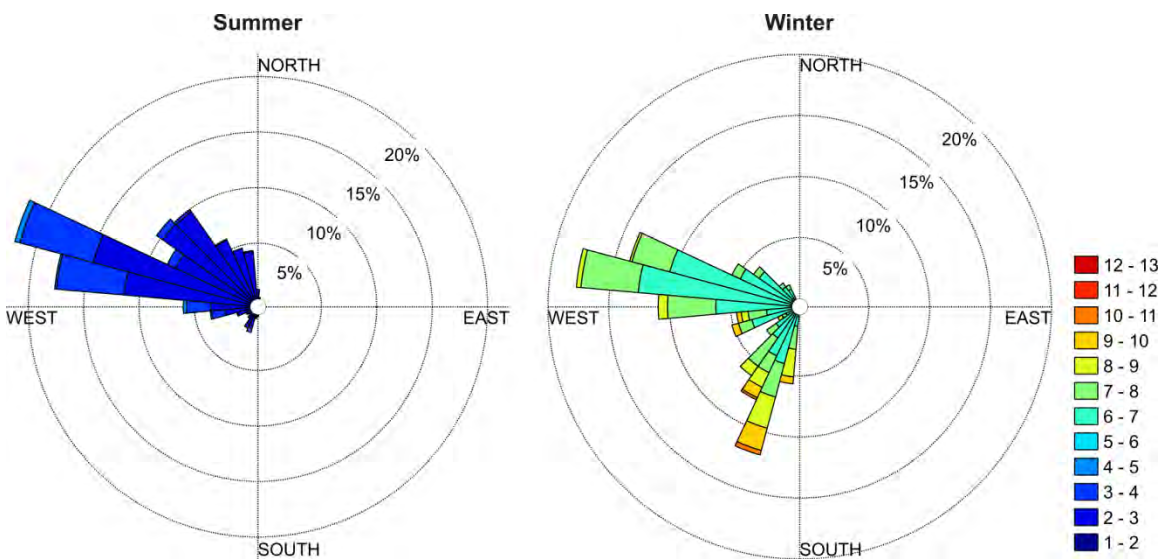
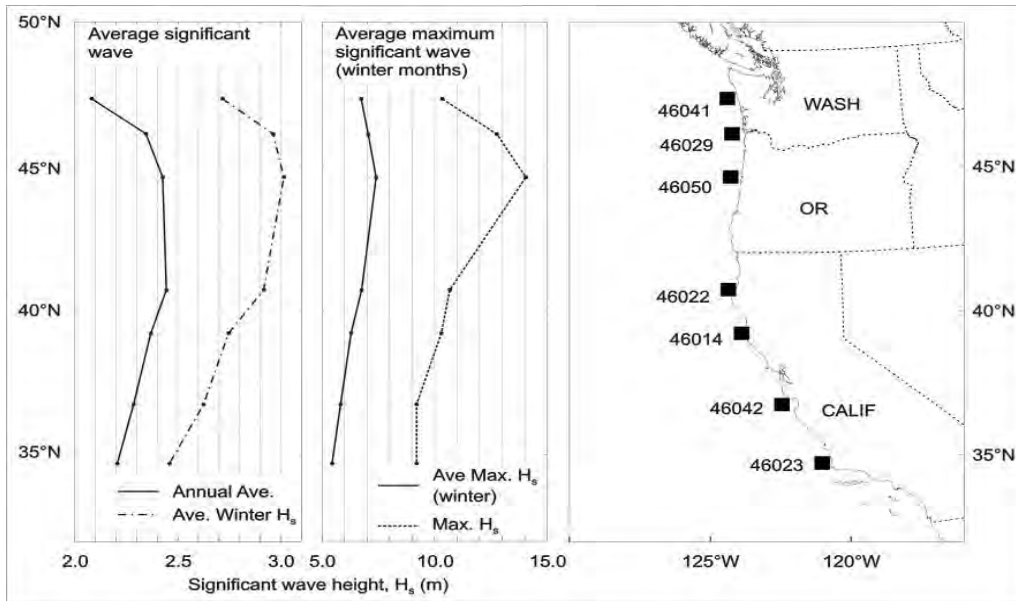


**Figure 1-2.** Top: Wave heights on the US west coast. Bottom: Winter vs summer wave directions offshore from the central Oregon coast. Colored scale indicates the wave height in meters.

The introduction of European beach grass, (*Ammophila arenaria*) in the early 1900s for the purposes of dune stabilization and its eventual proliferation along the coast, has without doubt single-handedly transformed the character of the coast, particularly since the late 1930s. For example, the first state-wide aerial photographic survey of the coast in 1939 clearly shows that the majority of the dunes and barrier spits on the coast were completely devoid of vegetation. At that time, the expanse of low lying hummocky dunes allowed sand to be transported significant distances inland, where the dunes piled up against marine terraces where present, or inundated forest communities. With the introduction of European beach grass, particularly in the late 1960s and early 1970s when extensive dune planting programs took place, the dunes and barrier spits have subsequently become stabilized, building foredunes that now range in height from 10- 16 m.

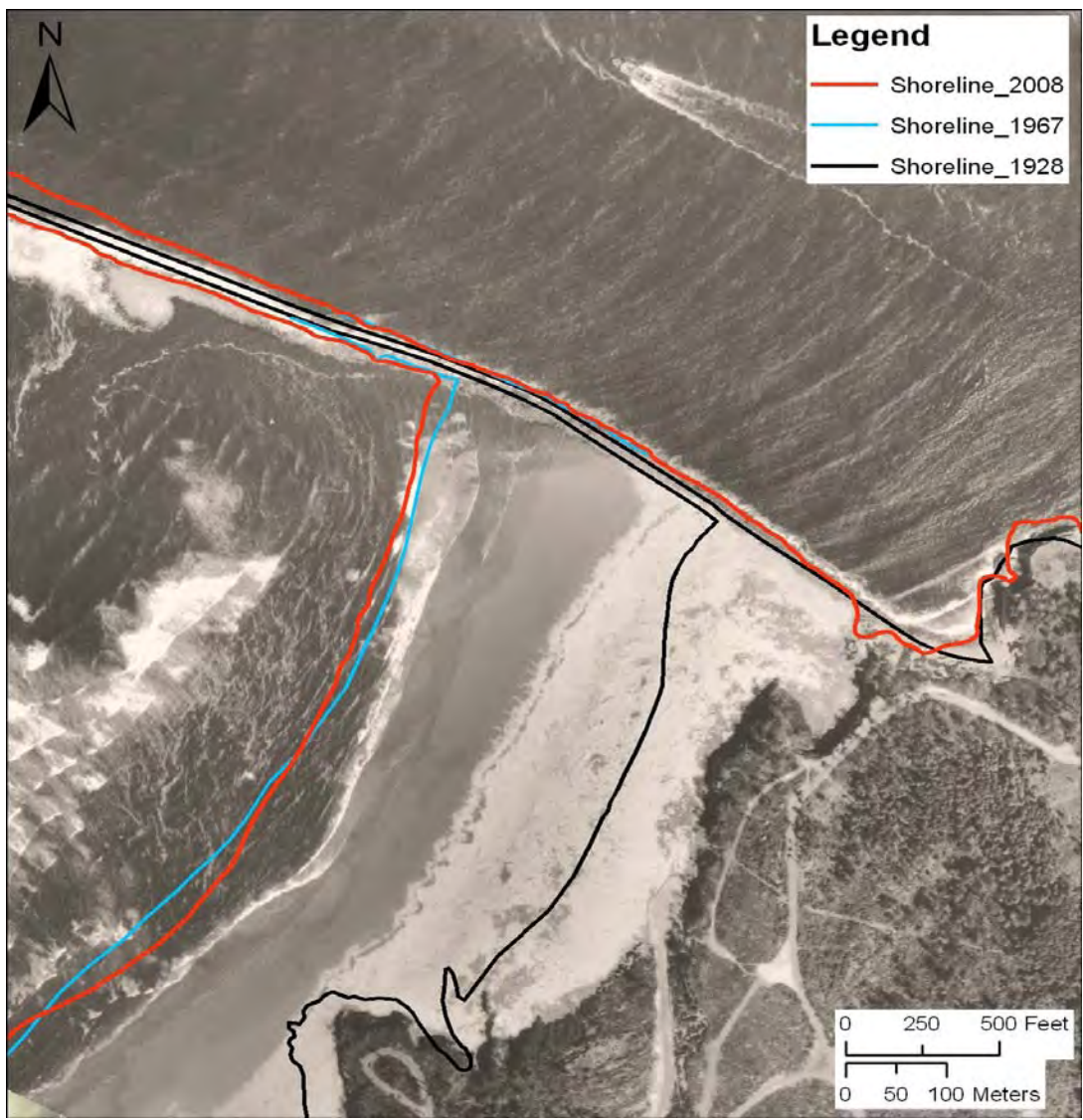


**Figure 1-3.** Historic shorelines at Bastendorf Beach, photo is from 1939.

Periodic extreme storms, such as occur during El Nino or La Nina events can cause dramatic erosion within littoral cells, and in some cases appear to actually move sand out of the cell, or into water so deep that summer waves cannot return it. Understanding beach erosion and dynamics therefore requires detailed quantitative data, so that one can begin to sort out the cyclic changes from the permanent changes. Jonathan Allan, DOGAMI’s coastal geomorphologist, has pioneered this effort, using serial lidar and repeat RTK-GPS surveys to track beach changes. There are several iterations of coastal lidar currently available, and although the earlier data are much lower resolution and accuracy than current Oregon Lidar Consortium data, they are sufficiently accurate in the relatively flat and well-exposed beach areas to allow for quantitative comparison. However, beach changes take place at far shorter intervals than the time between lidar flights, and weather precludes lidar collection during most of the winter, when changes are greatest. To get around this, Jon has established a series of monitoring profiles up and down the coast where he does repeat RTK-GPS surveys with sufficient accuracy to detect changes in elevation of 4-5 cm, a small fraction of the typical 1-3m seasonal change in beach elevation.

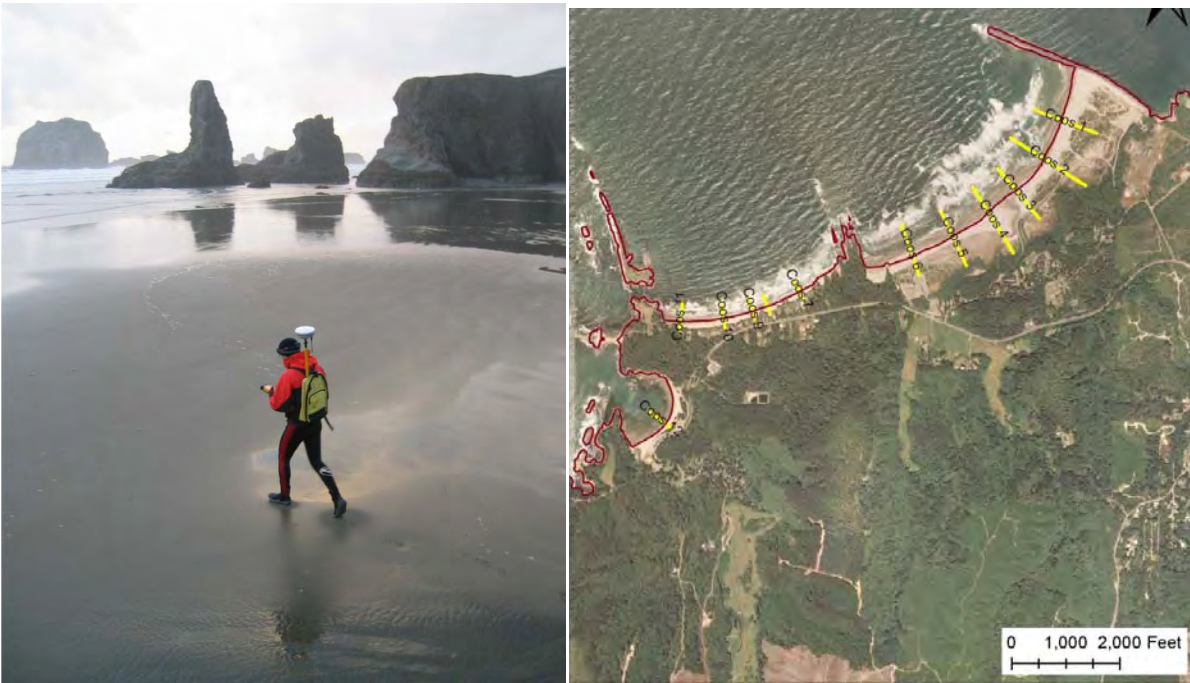


**Figure 1-4.** RTK-GPS beach profiling and location of transects at Bastendorf Beach. Data for these sites and many others are available at: <http://www.nanoos.org/nvs/nvs.php?section=NVS-Products-Beaches-Mapping>.

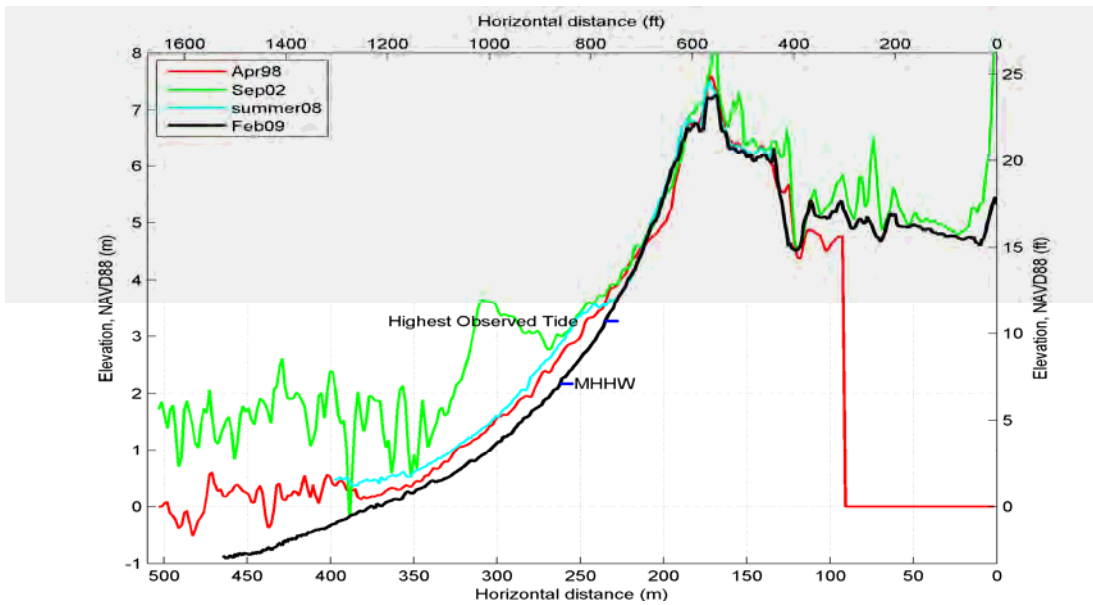


**Figure 1-5:** The Coos 2 profile site indicating the generally low backshore elevations that suggest that the beach probably prograded rapidly seaward following jetty construction, while the high contemporary foredune indicates that the shoreline has stabilized.

For those interested in rocks, the shoreline behind the beach is composed of a sequence of steeply E-dipping Eocene and Oligocene marine sedimentary rocks, overlain just at our stop by Miocene marine mudstone with a significant angular unconformity.

## Stop 2: Shore Acres State Park



**Figure 2-1. Navigation**

Leaving Bastendorf Beach, Stop 2 at Shore Acres State Park is a short drive down the Cape Arago Highway. There is a \$5 per car day use/entry fee required at Shore Acres.

Shore Acres is an iconic bit of Oregon coastal scenery. Thick sandstone beds of the lower Coaledo Formation dip moderately inland, forming beautifully sculpted ramparts against which huge waves crash (Figure 2-2). The broad flat surface on which the park is located is the lowest of a well-defined sequence of marine terraces that are present in the Coos Head-Cape Arago region. As we all remember from Geomorph 101, marine terraces form during times of stable or slowly rising sea level, as waves erode the shoreline, carving a submarine wave-cut platform as erosion progresses inland. The platforms end at the paleo-sea cliff commonly referred to as the shoreline angle or backedge, and are covered with nearshore marine sediments of varying thickness. As sea level cycled during the Pleistocene, tectonically rising coasts preserved a stair step sequence of terraces like those we see here. These terraces were dated by McInnelly and Kelsey (1990) and then mapped in detail by Madin, McInnelly and Kelsey (1995). The terraces are:

- Whisky Run (80 ka, Stage 5a)
- Pioneer (105 ka, Stage 5c )
- Seven Devils (125 ka Stage 5 d or e? )
- Metcalf (200-250 ka, Stage 7)

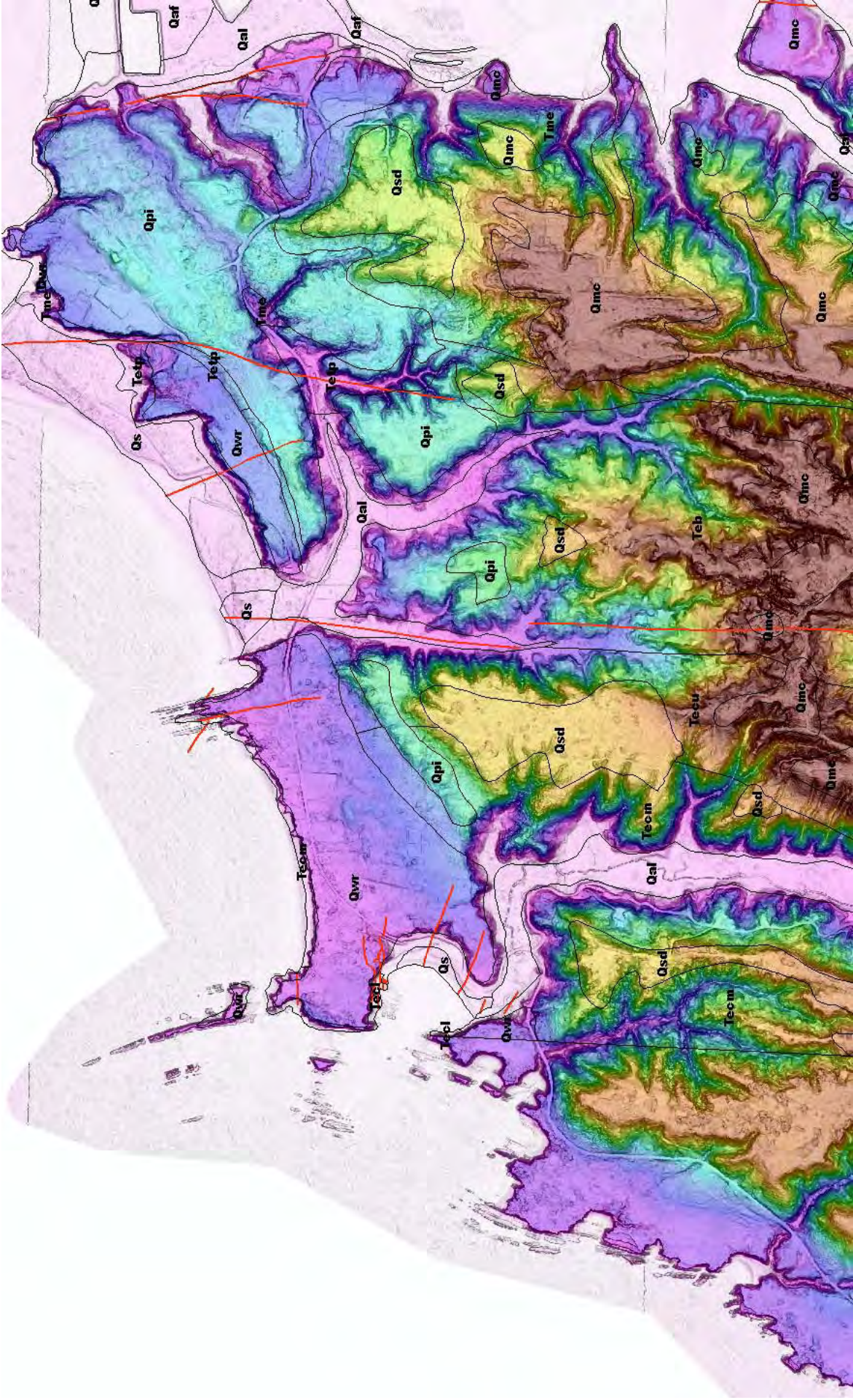
An older Arago terrace may or may not exist. On the lidar image (Figure 2-3) we can clearly see the flat Whiskey Run surface (Qwr, generally violet and blue elevation colors) and its well-defined backedge, the Pioneer Terrace ( pale blue elevation tint) is quite dissected with little of the backedge preserved, as is the Seven Devils terrace (yellow elevation



Figure 2-2. Shore Acres Park, note people for scale.

tint), and the Metcalf terrace (brick red elevation tint) is even more deeply eroded (and tilted) and is largely preserved capping ridges

We are standing on the Whiskey Run terrace and all along the edge of the modern sea cliff you can see the exposed wave cut platform and the very thin terrace cover sediments. The marine terraces are rapidly formed planar surfaces that define sea level at a particular stage, so they are excellent markers for tectonic deformation. Figures 2-3 and 2-4 show a cross section of deformation through this area, as well as calculated uplift rates for the various terraces. Care must be taken to work with the wave-cut platform, not the terrace surface, because the thickness of the terrace cover sediments varies widely.



**Figure 2-3.** Lidar image (slopesshade and colored elevation gradient) and geologic map of Coos Head. Geologic units are Qaf, artificial fill; Qal, beach deposits; Qal, alluvium; Qvr, Whisky Run terrace; Qpi, Pioneer terrace; Qsd, Seven Devils terrace; Qmc, Metcalf terrace; Tme, Empire Formation; Totp, Tunnel Point Formation; Teb, Bastendorf Shale; Tecu, upper Coaledo Formation; Tecm, Middle Coaledo Formation; Tecl, lower Coaledo Formation.

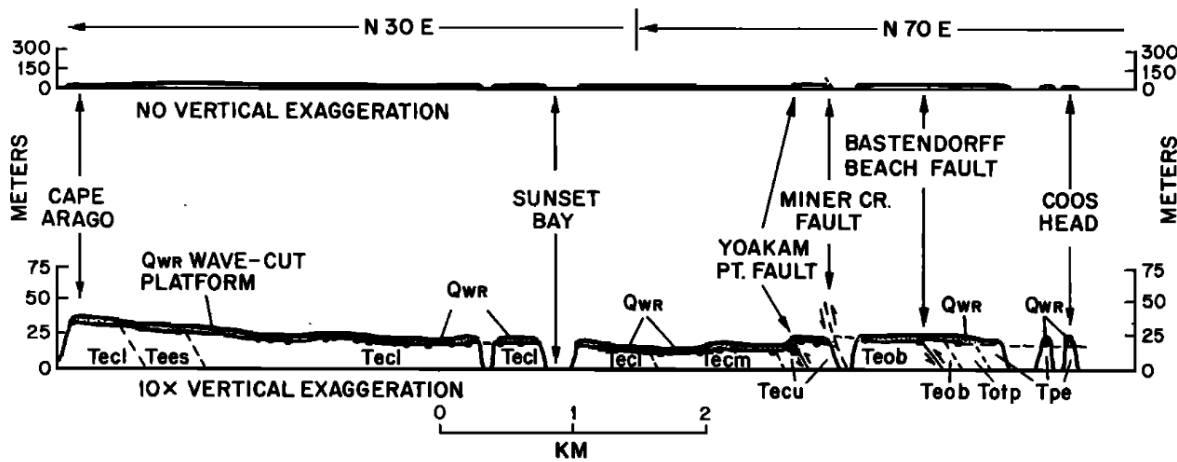


Fig. 7. Post-80 ka deformation of the Whisky Run wave-cut platform is illustrated in this coastwise transect from Cape Arago to Coos Head (view to northwest and north-northwest). Solid circles are altimeter survey locations. Data are projected onto a line that trends N30°E from Cape Arago to Sunset Bay, then N70°E to Coos Head. The gradual descent of the Whisky Run Wave-cut platform from Cape Arago to Coos Head is interrupted repeatedly by flexural-slip faults at Yoakam Point, Miner Creek, and Bastendorff Beach. Geologic units are same as previous figure.

Figure 2-4. Deformation of Whisky Run terrace between Cape Arago and Coos Head

TABLE 2. Marine Wave-Cut Platforms at Cape Arago: Ages, Uplift Rates, Tilt Rates, and Horizontal Strain Rates

Wave-Cut Platform	Estimated Age, ka	Maximum Elevation, <sup>a</sup> m	Shore-Normal Distance From Shoreline Angle, km	Original Gradient of Platform, m/km	Original Depth of Platform, m	Paleo-Sea Level, <sup>b</sup> m	Sea Level Model <sup>c</sup>	Maximum Uplift Rate, <sup>d</sup> m/kyr	Elevation of Shoreline Angle, m	Uplift Rate at Shoreline angle, m/kyr	Maximum Observed Tilt, <sup>e</sup> rad	Tilt Rate rad/yr	Horizontal Strain Rate, <sup>f</sup> yr <sup>-1</sup>
Whisky Run	80	35	0.2	20	4	-19 ± 5	NG	0.73 ± 0.07	31	0.63 ± 0.07	2.3 × 10 <sup>-3</sup>	2.9 × 10 <sup>-8</sup>	0.44 × 10 <sup>-7</sup>
	80	35	0.2	40	8	-19 ± 5	NG	0.78 ± 0.07	31	0.63 ± 0.07			
	80	35	0.2	20	4	-5 ± 2	CA-JP	0.55 ± 0.03	31	0.45 ± 0.03			
	80	35	0.2	40	8	-5 ± 2	CA-JP	0.60 ± 0.03	31	0.45 ± 0.03			
Pioneer	105	68 <sup>g</sup>	0	NA	0	-9 ± 3	NG	0.73 ± 0.03	68	0.73 ± 0.03	5.7 × 10 <sup>-3</sup>	5.4 × 10 <sup>-8</sup>	0.83 × 10 <sup>-7</sup>
	105	68 <sup>g</sup>	0	NA	0	-2	CA-JP	0.67	68	0.67			
Seven Devils <sup>h</sup>	125	100	0.2	20	4	+6	both	0.78?	98 <sup>g</sup>	0.74?	8.1 × 10 <sup>-3</sup> ?	6.5 × 10 <sup>-8</sup> ?	1.0 × 10 <sup>-7</sup> ?
	125	100	0.2	40	8	+6	both	0.82?	98 <sup>g</sup>	0.74?			
Metcalf <sup>h</sup>	200?	169	0	NA	0	B+2		0.84?	169	0.84?	17 × 10 <sup>-3</sup> ?	8.5 × 10 <sup>-8</sup>	1.3 × 10 <sup>-7</sup> ?

<sup>a</sup>For Whisky Run and Seven Devils platforms, the maximum elevation near Cape Arago is 200 m seaward (westward) of the paleoshoreline angle. For Pioneer and Metcalf platforms the maximum elevation near Cape Arago is at the paleoshoreline angle. All platforms are landward tilted at Cape Arago.

<sup>b</sup>Relative to present sea level.

<sup>c</sup>NG, New Guinea model [Chappell and Shackleton, 1986]; CA-JP, California-Japan model [Machida, 1975; Muhs et al., 1988]; B, Bermuda data for 200 ka high stand [Harmon et al., 1983].

<sup>d</sup>Uncertainties for Whisky Run and Seven Devils wave-cut platforms: (1) paleo-sea level, (2) paleo-water depth during the 80 and 105 ka sea level high stands for the present point of maximum elevation.

<sup>e</sup>For all terrace platforms, tilt is measured from the vicinity of Cape Arago N60°E to the vicinity of South Slough. Tilts measured parallel to the N60°E down-dip direction.

<sup>f</sup>See assumptions for derivation of strain rate in text.

<sup>g</sup>Elevation is extrapolated from known distance measured in downdip direction and using average platform tilt.

<sup>h</sup>The estimated ages of the Seven Devils and Metcalf platforms are minimum ages and not constrained by isotopic data. Therefore all calculated rates based on these ages are maximum rates and are queried because of the large uncertainties.

MCINNELLY AND KELSEY: TECTONIC DEFORMATION, COASTAL OREGON

Figure 2-5. Measured deformation rates for terraces between Cape Arago and Coos Head.

Note also that the offshore rocks here very clearly define the structure of the steeply dipping and folded marine strata. All along this stretch of coast, the geologic structure has a strong influence on the shape of the coastline, for instance Sunset Bay has formed where a series of scissor faults perpendicular to the bedding have weakened the resistant sandstone rips enough to allow wave erosion to penetrate inland and then spread where it encounters mudstone and siltstone.

Figure 2-6 shows a 2ft contour map of the Shore Acres area and the paleo sea cliff behind it. There are two large alluvial fans that emanate from very small gullies in the sea cliff, and are built out onto the Whisky Run terrace surface. George Priest from the DOGAMI Newport field office has been mapping the Oregon coast in detail for years, and he sees evidence that Western Oregon endured a much colder and wetter climate than today from shortly after the last high sea stand ~80,000 years ago until ~10,000 years ago. During much of this period sea level was ~200-400 feet lower than today with annual rainfall probably approaching that of southeast Alaska, hundreds of inches per year. Cascadia subduction zone earthquakes shook the region about every 500 years, sometimes occurring during winter when slopes

were least stable. As a result, numerous deep bedrock slides and debris flows covered most steep slopes. These old landslides and colluvial deposits now form a more or less continuous, semi-consolidated deposit in many areas. These unusual fans may be the result of that extremely wet and active period.

Finally, here is an opportunity to make a point about using lidar for geologic maps, and I can beat up on this map because it is mine (from 17 years ago). Compared to the lidar geomorphology, a few of the contacts in Figure 2-3 are pretty good, but most are off by tens of meters or more. I also completely missed the obvious extension of the Whisky Run terrace and backedge to the east of the fault that extends under Bastendorf Beach, and completely missed the landslide at the back of the beach, as well as two additional faults crossing the Whisky Run terrace near Sunset Bay. The moral of the story is that if you are making a geologic map, get lidar first, so future generations don't make fun of your work in field trip guides.

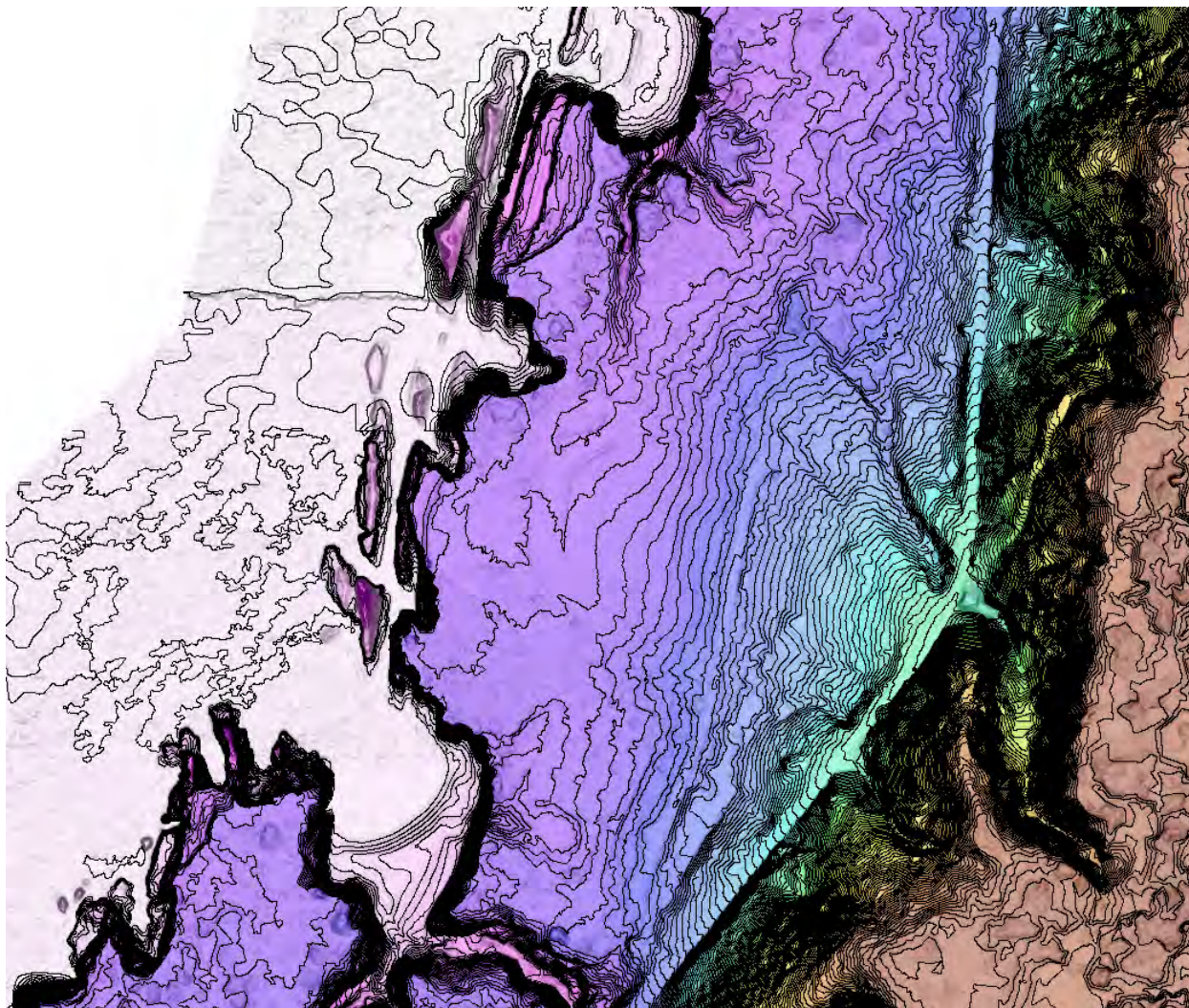


**Figure 2-6.** 2 ft lidar contours on color elevation gradient and slopeshade at Shore Acres State Park.

### Stop 3: Seven Devils Road

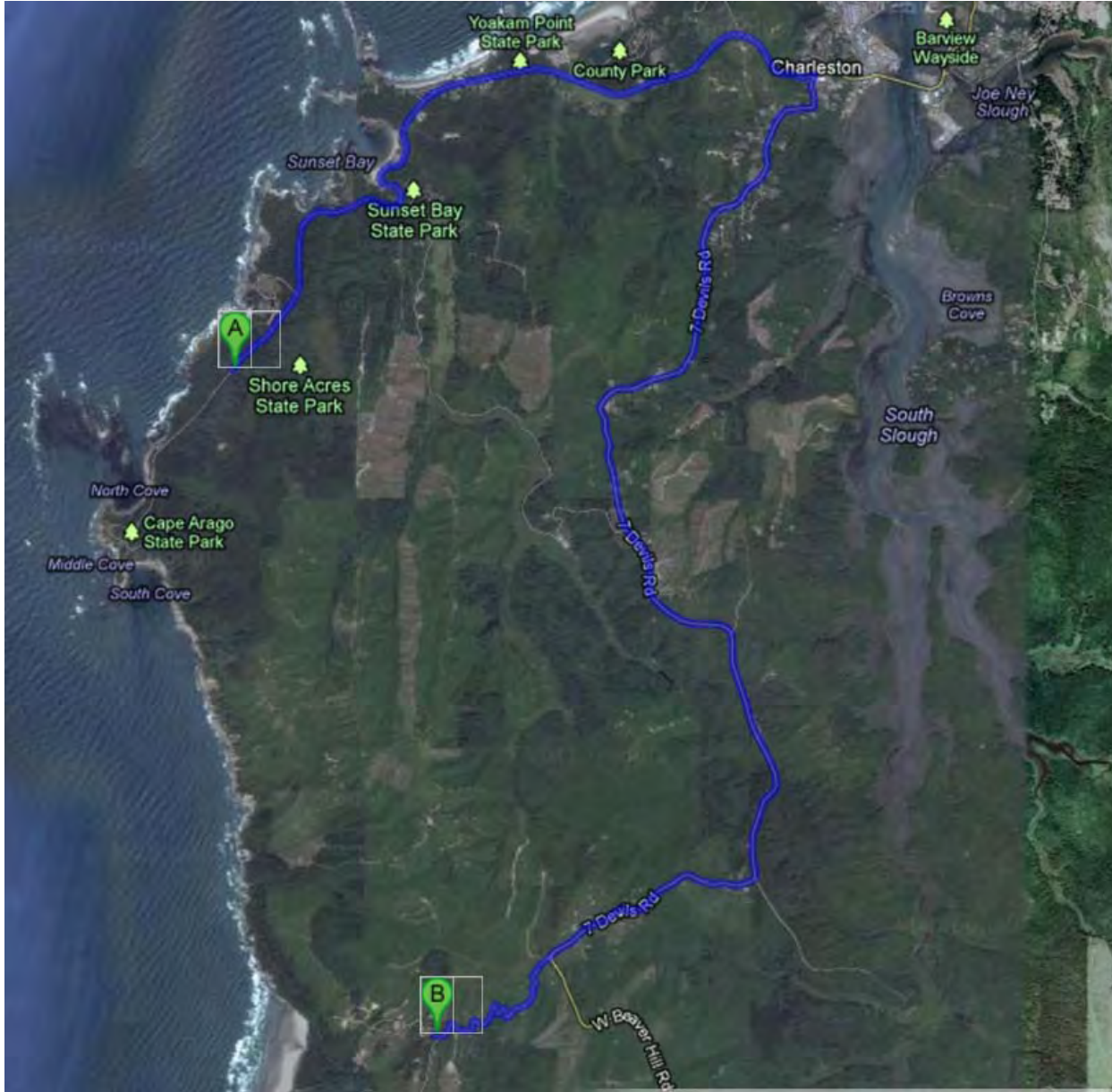


**Figure 3-1.** Navigation

From Shore Acres to stop 3 is about a half hour drive. We retrace our steps to Charleston then climb quickly up through the marine terrace sequence to get on top of a series of ridges that separate South Slough from the Pacific. These ridges (Figure 3-2) are all capped with Metcalf terrace, which appears as bleached or iron-stained weakly cemented sand. The ridges are all strike ridges held up by the same steeply E-dipping marine strata we saw at Bastendorf beach, with valleys occupying the mudstone intervals. South Slough was long believed to occupy the axis of a large N-trending syncline, but more recent geologic mapping, coupled with gas-exploration seismic shows that in fact there is a thrust fault up the Slough, and our route along Seven Devils road is actually on the anticline formed on the upper plate of the thrust sheet.

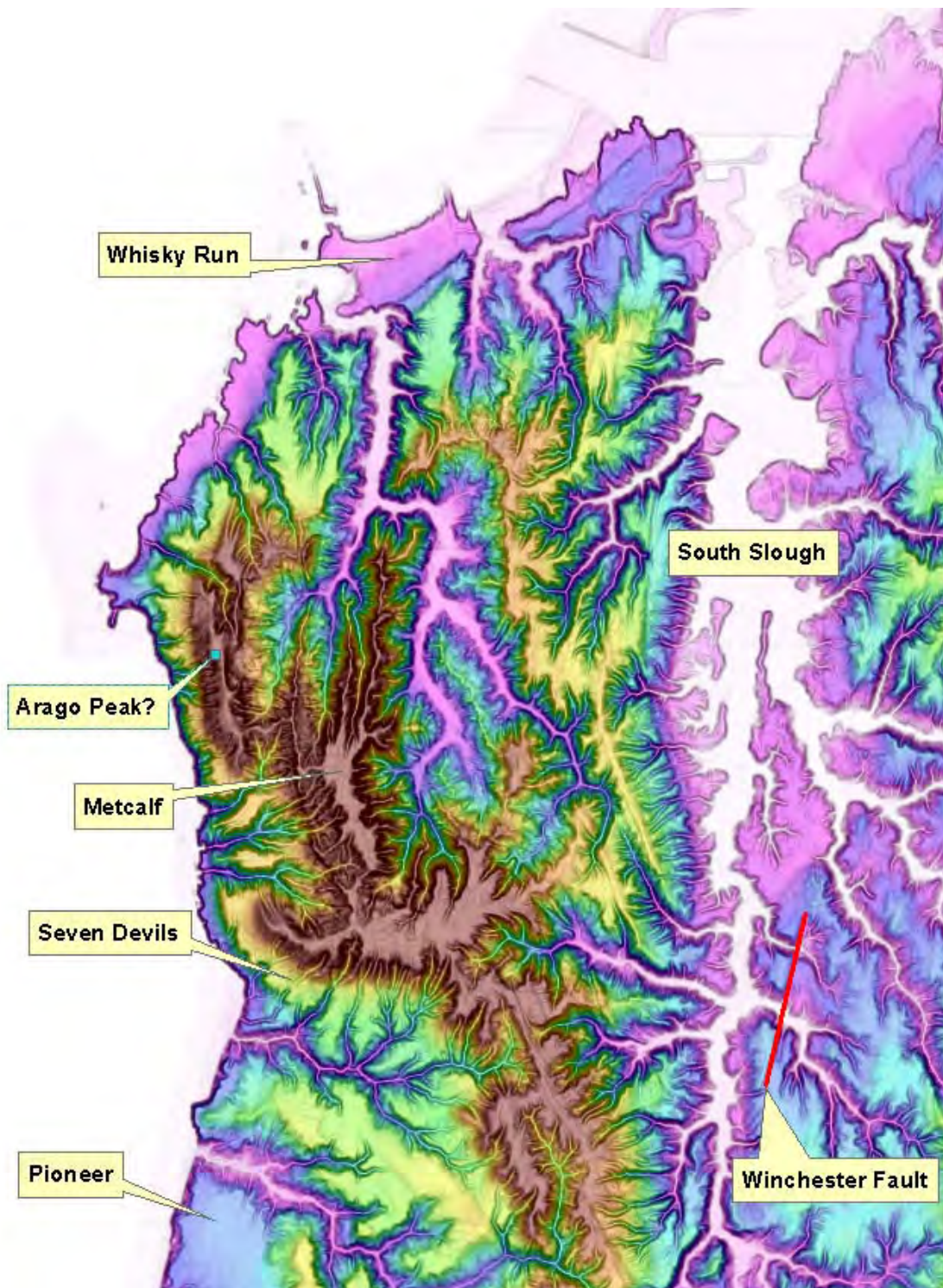


**Figure 3-2.** Topography along Seven Devils Road.

We turn off the pavement and descend the steep and winding section of Seven Devils road, drive carefully. Everyone but the driver can gawk at the excellent road cut exposures of lower Coaledo Formation sandstone. You may also be able to see the Metcalf wave-cut platform just as we start down; the Metcalf cover sediments here are quite thin.

We will descend to the Seven Devils Terrace and drive across it, stopping just where we start to descend again to look at good exposures of the Seven Devils wave cut platform. Here the platform is cut in lower Coaledo, which is a nearshore

## 2013 Bretz Club Field trip Guide, Part Deux: *Kentucky Falls extravaganza*

### **Saltate, meander, and plummet: Sediment pathways in the Oregon Coast Range**

**Saturday, 27 April 2013**

**Led by Josh Roering, Jill Marshall, Kristin Sweeney, University of Oregon**

**Notes:** The field trip entails a 4-mile round-trip hike. Bag lunches will be provided by OIMB for Bretz registrants. We'll make several stops along the way and then break for lunch at the base of Lower Kentucky/North Fork Smith River Falls. After lunch there will be one or two more stops. If you need to leave early to get home, feel free to head up the trail to your car at any time. We'll provide a handout with directions for getting from the parking lot to Hwy 126, which is the shortest route for most people to get home. Otherwise, please ask of questions and be safe in this beautiful spot!

#### **Stops and themes for discussion**

1. Parking lot: General site background and logistical discussion.
2. Mid-way b/w parking lot and Upper Kentucky Falls:
  - a. Note and discuss: tree throw pit/mound features.
  - b. Small-order catchment dynamics: colluvial infilling and excavation by debris flows
3. Base of Upper Kentucky Falls:
  - a. Petrology of Oligocene intrusions
  - b. Incision and retreat of knickpoints
  - c. Physical and chemical alteration of bedrock
  - d. Baselevel controls in the Oregon Coast Range
4. Wooden Bridge over Kentucky Creek
  - a. Sediment transport and suspended sediment concentration vs. discharge relationships in a threshold-dominated landscape.
5. Downstream of bridge
  - a. Gargantuan Tree throw pit/mound
  - b. Discuss role of bioturbation in soil production
6. Base of Lower Kentucky Falls/North Fork Smith River Falls
  - a. LUNCH STOP
  - b. Discuss waterfall retreat and landscape adjustment in the upstream watershed
7. Return upstream: Historic bridge remains and logging camp
  - a. Intrepid path (traverse to top of falls and upstream to historic bridge remains)
    - i. Requires steep hillside slog and shallow stream walking
  - b. Standard path
    - i. Back up trail to wooden bridge and wait there for a bit of gentle bushwhacking
  - c. Discuss
    - i. Logging and legacy of land-use practices, in-stream structures
    - ii. Landscape evolution and adjustment upstream of knickpoint
      1. Hillslope soils
      2. Valley width
8. Return to vehicles and head home...drive safely!

## **A Brief Summary of Oregon Coast Range Geology, Geomorphology, Tectonics, and Climate**

Spanning 200 miles along the Pacific, the Oregon Coast Range is defined by a 30-40 mile wide swath of moderately high mountains. The range averages 1,500 feet in elevation and has a maximum elevation of 4,097 feet at Mary's Peak. Slopes and drainage basins are consistently steep through the range, approaching 50° in many localities. Pacific storms buffet the range in the wet, winter months and support thick forests of Douglas fir and hardwood species. The average annual rainfall in the range is over 100 inches per year. Several rivers flow west across the Oregon Coast Range and empty into the Pacific. These rivers generally flow across sedimentary or volcanic bedrock and do not have significant storage of sediment in river bars or banks. Once home to an abundance of trout, salmon, and other fish, rivers and streams in the Coast Range now harbor a small fraction of the original aquatic population.

The Oregon Coast Range is a belt of uplifted land lying along the Pacific Coast of Oregon. The uplift is a result of plate convergence. About 400 km west of the Coast Range lies the spreading center, which separates the Pacific plate (which extends to just east of Japan) and the Juan de Fuca plate, which descends under the North American Plate along the Cascadia subduction zone. The Coast Range overlies the subducted Juan de Fuca plate and lies about 150 to 200 km to the east of the Cascadia subduction zone. The region seaward of the location of volcanism is referred to as the "forearc" and that the materials found in the forearc are comprised of rocks scraped off the descending the subducting slab ("accretionary wedge") and of rocks deposited within the basins ("forearc basins") created by deformation of the accretionary wedge.

The Oregon Coast Range is composed of accreted oceanic sediments. The oldest rocks, the Siletz River volcanics, are oceanic crust formed during the Paleocene to middle Eocene (about 60 to 45 million years ago). Deposited synchronously with these volcanics but also overlying them and intruded by them is a regionally extensive marine sandstone and siltstone. Commonly referred to as the Tyee formation this unit is mostly formed by repeated deposition of dense currents of sediment (turbidity currents) derived from uplifted terrestrial sources. Our study sites lie entirely within this unit. Successively younger deposits of sediments and volcanics are found to the east of the coast range and along the coast. Overall the rocks are gently folded and have a slight westward dip (Kelsey et al., 1996).

During the Oligocene (-25 million years ago), uplift of sedimentary basins in Oregon resulted in the westward migration of the coastline from as far east as Idaho towards the present position. Synchronous with uplift, giant fissures in northern Oregon brought lava flows up from the subducting plate. Dikes and sills also intruded into the Eocene and Miocene sedimentary rocks that make-up most of the Coast Range today. These isolated volcanics tend to resist weathering and erosion more than the surrounding sedimentary rocks and constitute some of the prominent peaks in the Coast Range. Continued uplift of the coast has led to the development of marine terraces along the Oregon coast. These features record the history of sea level change and uplift, and specifically they record differential uplift along the coast that may result from faulting.

The Juan de Fuca plate is being subducted at about 4 cm/yr (De Mets, et al., 1990). It dips beneath the Coast Range at about 13 to 16 degrees (Trehu et al., 1994). One of the most peculiar and troubling aspects of the Coast Range is the low seismicity of the region in recorded time. Concerns about potential seismicity associated with the Cascadia subduction zone has prompted many researchers to search for evidence of historical earthquakes in the region (e.g. Atwater, 1987). Deformation of local coastal

marshes and Quaternary terraces has been interpreted as a response to pre-historic earthquakes. Geological evidence now suggests that instead of frequent lower magnitude events the Coast Range occasionally experiences very high magnitude earthquakes (order 9.0), the most recent perhaps having occurred 300 years ago (Verdonck et al., 1995). One question we will consider is whether these rare, but very large magnitude earthquakes leave a geomorphic imprint on the landscape.

Studies of fluvial strath terraces (Personius, 1995) and marine terraces (Kelsey et al., 1996) have been used to examine the spatial and temporal pattern of Quaternary rock uplift of the Coast Range. Inferred patterns of stream incision rates appear to roughly balance rock uplift rates, i.e. the rivers keep pace with uplift during the late Quaternary. A complex pattern is suggested, with generally more rapid incision in the north. Resurveys of targets and analysis of tide gauge records during the past 50 years enables an estimate of contemporary vertical deformation. These rates are in the south as much as 10 times higher than late Quaternary rates inferred from stream incision rates. As Mitchell et al. (1994) argue these data, which represent a period of little seismicity record significant strain accumulation, which implies the build up of a large seismic hazard.

Since the 1960's, many researchers have investigated the hypothesis that rates of tectonic deformation and long-term average erosion are strongly related. Many studies have addressed the balance of erosion and tectonic uplift in the central and southern Oregon Coast Range. In this part of the range, the topography has a characteristic morphology, with convex ridge tops dominated by soil creep processes and steep sideslopes, where small soil slips and landslides dominate (Roering et al., 1999). Near the terminus of steep, sideslopes, in steep, unchanneled valleys (topographically-defined hollows), soils accumulate and thicken over long time periods. These convergent parts of the landscape also tend to become saturated during rainfall events. The combination of thick soil and frequent saturation tends to favor these parts of the landscape for episodic shallow landsliding. As a result, hillslope erosion rate is highly stochastic over human timescales, but when averaged over thousands of years the landscape appears to be eroding at roughly the same rate, 0.1 to 0.2 mm/yr (Heimsath et al., 2001). Reneau and Dietrich (1989) estimate average hillslope erosion rates of 0.07 mm/yr over the last 4,000 to 15,000 years from analysis of colluvial deposition in hollows or topographic depressions. Sediment yield measurements from several Coast Range basins indicate similar rates of erosion between 0.05 and 0.08 mm/yr (e.g. Brown and Krygier, 1971; Beschta, 1978). These findings suggest that the portions of the landscape in the Oregon Coast Range are lowering at a similar rate of 0.05 to 0.2 mm/yr. These studies do not reflect millennial-scale variations in process rates related to climate change. Recent evidence (Long et al., 1998, Roering and Gerber, 2005) suggests that episodic fires may be a significant mechanism of sediment production because the incineration and removal of vegetation on steep slopes can cause extensive transport via dry ravel (bouncing, sliding, and rolling of grains). In the early Holocene (~8,000 ya), fires were much more frequent (~110-yr return interval) than recent times, suggesting that the soil mantle may have been much thinner and less continuous than today.

In the Oregon Coast Range, stream incision or (fluvial bedrock incision) rates are spatially variable, but approach 0.2 mm/yr to 2.0 mm/yr in regions where estimated hillslope erosion rates are 0.1 mm/yr (Reneau and Dietrich, 1991). This disparity may indicate that the Oregon Coast Range is not in strict dynamic equilibrium. Alternatively, the factor of 2 to 3 difference may reflect errors associated with measurements, dating errors, or it may reflect tectonic or climatic factors that cause these rates to be disparate on a short time scale. Although, deep-seated landslides make-up 30% of the land surface in certain portions of the Oregon Coast Range, their role in landscape evolution is unclear. In areas with a high frequency of large landslides, local topographic relief is depressed, suggesting that these features

may limit topographic development. The notion of steady state topography in the Oregon Coast Range requires further examination.

Analysis of pollen and plant fossils from Little Lake, Oregon, provides a record of climatic history in the Oregon Coast Range (Worona and Whitlock, 1995). The following table indicates the climatic trends. The Oregon Coast Range supported few if any glaciers during the last major glacial period, which has important implications for geomorphic and tectonic interpretations (Baldwin, 1993). Notably, Reneau and Dietrich (1991) indicate an abundance of basal carbon dates between 4,000 and 7,500 years old, which corresponds with a period of cold and moist conditions that followed a several thousand year period of warm and dry conditions (Worona and Whitlock, 1995). This observation indicates that climatic variation may influence rates of erosion and sedimentation. The influence of climate and human factors, such as timber harvesting, on erosion is currently being investigated in the Coast Range. Recent studies have found that the coincidence of forest removal and high intensity rainfall events can significantly increase the number of shallow landslides (Montgomery et al., 2000). The results of these and other studies are important for future land management decisions.

**Brief Climatic History of Little Lake, Oregon Coast Range (Worona and Whitlock, 1995)**

Rainfall = 150 cm/yr (75-80% occurs Oct-Mar)

Unglaciated during the Fraser glaciation (ice 320 km north in Wash.)

Yr. B.P. Characteristics

42,000-25,000	Cooler, wetter than today (at least 3°C cooler) consistent all along the Oregon coast.
25,000-13,000	Colder, drier, Oregon Coast Ranges supported small if any glaciers. (7-14°C cooler, 50% of today's rainfall)
16,000-13,500	Small warming trend, increased moisture
11,000-10,000	Colder, brief reversal
10,160-9,000	Warm, dry conditions; intensified summer droughts and widespread fires; increased solar radiation from increased tilt of the earth.
6,000-3,000	Cool, moist climate much like today
3,000-2,000	Reduced moisture (somewhat) and cooling 2,000-> Somewhat drier, fires?

## References

- Atwater, B.F., Evidence for great Holocene earthquakes along the outer coast of Washington state, *Science*, 236, 942-944, 1987.
- Baldwin, E.M., Glaciation in the central Coast Range of Oregon, *Oregon Geology*, 55, 87-89, 1993.
- Beschta, R.L., Long-term patterns of sediment production following road construction and logging in the Oregon Coast Range, *Water Resources Res.*, 14, 1,011-1,016, 1978.
- Brown, G.W., and J.T. Krygier, Clear-cut logging and sediment production in the Oregon Coast Range, *Water Resources Res.*, 7 (5), 1189-1198, 1971.
- DeMets, C., R.G. Gordon, D.F. Argus, and S. Stein, Current plate motions, *Geophys. J. Int.*, 101, 425-478, 1990.
- Heimsath, A. M., W.E. Dietrich, K. Nishiizumi, and R.C. Finkel, Stochastic processes of soil production and transport: Erosion rates, topographic variation and cosmogenic nuclides in the Oregon Coast Range. *Earth Surface Processes and Landforms*, 26, 531-552, 2001
- Kelsey, H.M., and J.G. Bockheim, Coastal landscape evolution as a function of eustasy and surface uplift rate, Cascadia margin, southern Oregon, *Geol. Soc. Am. Bull.*, 106, 840-854, 1994.
- Kelsey, H.M., D.C. Engebretson, C.E. Mitchell, and R.L. Ticknor, Topographic form of the Coast Ranges of the Cascadia margin in relation to coastal uplift rates and plate subduction, *Journal of Geophysical Research*, 99, 12,245-12,255, 1994.
- Long, C.J., Whitlock, C., Bartlein, P.J., and Millsbaugh, S.H., 1998, A 9000-year fire history from the Oregon Coast Range, based on a high-resolution charcoal study: *Canadian Journal of Forest Research*, v. 28, p. 774-787.
- Mitchell, C.E., P. Vincent, R.J. Weldon, and M. Richards, Present-day vertical deformation of the Cascadia margin, Pacific Northwest, United States, *J. Geophys. Res.*, 99, 12,257-12,277, 1994.
- Montgomery, D.R., K.M. Schmidt, H.M. Greenberg, and W.E. Dietrich, Forest clearing and regional landsliding, *Geology*, 28, 311-314, 2000
- Personius, S.F., Late Quaternary stream incision and uplift in the forearc of the Cascadia subduction zone, western Oregon, *Journal of Geophysical Research*, B, *Solid Earth and Planets*, 100, 20,193-20,210, 1995.
- Reneau, S.L., and W.E. Dietrich, Erosion rates in the southern Oregon Coast Ranges; evidence for an equilibrium between hillslope erosion and sediment yield, *Earth Surface Processes and Landforms*, 16, 307-322, 1991.
- Reneau, S.L., W.E. Dietrich, M. Rubin, D.J. Donahue, and A.J. T. Jull, Analysis of hillslope erosion rates using dated colluvial deposits, *Journal of Geology*, 97, 45-63, 1989.
- Roering, J.J., J.W. Kirchner, and W.E. Dietrich, Evidence for non-linear, diffusive sediment transport on hillslopes and implications for landscape morphology, *Water Resources Res.*, 35 (3), 853-870, 1999.
- Roering, J.J., and Gerber, M., 2005, Fire and the evolution of steep, soil-mantled landscapes: *Geology*, v. 33, p. 349-352.
- Roering, J.J., Kirchner, J.W., and Dietrich, W.E., 2005, Characterizing structural and lithologic controls on deep-seated landsliding: Implications for topographic relief and landscape evolution in the Oregon Coast Range, USA: *Geological Society of America Bulletin*, v. 117, p. 654-668.
- Trehu, A., T. Asudeh, T. Brocher, J. Luetgert, W. Mooney, J. Nableck, and Y Nakamura. Crustal architecture of the Cascadia forearc, *Science*, 266, 237-243, 1994
- Verdonck, D., Three-dimensional model of vertical deformation at the southern Cascadia subduction zone, western United States, *Geology*, 23, 261-264, 1995.
- Worona, M.A., and C. Whitlock, Late Quaternary vegetation and climate history near Little Lake, central Coast Range, Oregon, *Geological Society of America Bulletin*, 107, 867-876, 1995.

## **Oligocene Intrusions of the Central Oregon Coast Range: Petrology, geochemistry, and geochronology** (Oxford, OSU M.S. Thesis, 2009)

*These intrusions play a critical geomorphic role in shaping the evolution of the Oregon Coast Range as they tend to form linear ridges of high relief and provide resistant bedrock that retards bedrock river incision.*

The Early Oligocene Oregon Coast Range Intrusions (OCRI) consist of gabbroic rocks and lesser alkalic intrusive bodies that were emplaced in marine sedimentary units and volcanic sequences within a Tertiary Cascadia forearc basin. The alkalic intrusions include nepheline syenite, camptonite, and alkaline basalt. The gabbros occur as dikes and differentiated sills. Presently, erosional remnants of the intrusions underlie much of the high topography along the axis of the central Oregon Coast Range. The intrusive suite is most likely associated with Tertiary oblique rifting of the North America continental margin. Dextral shear and extension along the continental margin may have been a consequence of northeast-directed oblique Farallon plate convergence. The OCRI are part of a long-lived (42-30 Ma) magmatic forearc province that includes the Yachats Basalt and Cascade Head Basalt. The timing of Cascadia forearc magmatism correlates with a significant decrease in convergence rates between the Farallon and North American plates from 42 to 28 Ma. The OCRI are also contemporaneous with magmatism that occurred over a broad area of the Pacific Northwest (e.g. Western Cascades, John Day Formation).

New radiometric age data acquired from the Ar-Ar incremental heating experiments indicate that OCRI magmatism occurred between ~36 to 32 Ma; a longer interval than previously thought. The alkaline OCRI are closely associated with the late Eocene OIB-like Yachats Basalt and Cascade Head Basalt forearc volcanic centers in both space and time. In addition, trace element geochemical data suggest similar parental magma sources for the alkaline OCRI and the forearc volcanic centers.

The alkaline OCRI parental magmas were generated from small degrees of partial melting of an enriched OIB-like mantle source. There are two possible mantle sources for the alkaline OCRI: 1) An enriched lithospheric Siletzia mantle source that was previously metasomatized by deep-sourced alkaline melts or 2) upwelling asthenospheric mantle from beneath the subducting slab which would require a slab window. If the alkaline OCRI were derived from the lithospheric Siletzia mantle, then the mantle wedge would have been significantly thicker and possibly hotter during the Tertiary. Presently, the crustal rocks of Siletzia rest directly on the subducting Juan de Fuca plate. The tholeiitic OCRI gabbros are a separate, more widespread, and voluminous pulse of forearc magmatism that was contemporaneous with alkaline OCRI and Cascade Head Basalt magmatism. The Ar-Ar geochronology and previous K-Ar age data reveal that the gabbroic OCRI magmatism was short-lived. The Marys Peak sill and nearby dikes were emplaced between approximately 32 and 33 Ma. The major element geochemistry of the gabbros indicates that their magmatic evolution was driven by crystal fractionation processes at crustal levels. In contrast with the alkaline OCRI, the gabbros are characterized by tholeiitic compositions with lower degrees of incompatible element enrichment. Their trace element chemistry also displays an arc-like signature which indicates the involvement of a subduction-modified mantle source component in their petrogenesis.

The formation of the OCRI gabbroic magmas involved upwelling and decompressional melting within the mantle wedge. Oligocene forearc extension may have become more widespread for a short duration (~2 m.y.) which aided the ascension of relatively dense, iron-rich gabbroic OCRI magmas. During this period, the mantle wedge beneath the forearc experienced larger degrees of decompressional partial melting allowing for the generation of voluminous tholeiitic magmas. Since the gabbros are in close proximity to the Western Cascades arc, their petrogenesis was also linked to the Cascades subduction system, as indicated by their trace element geochemistry. Overall, the OCRI represent the final episode of widespread forearc magmatism and record significant changes in tectonic interactions between the Farallon and North America plates.

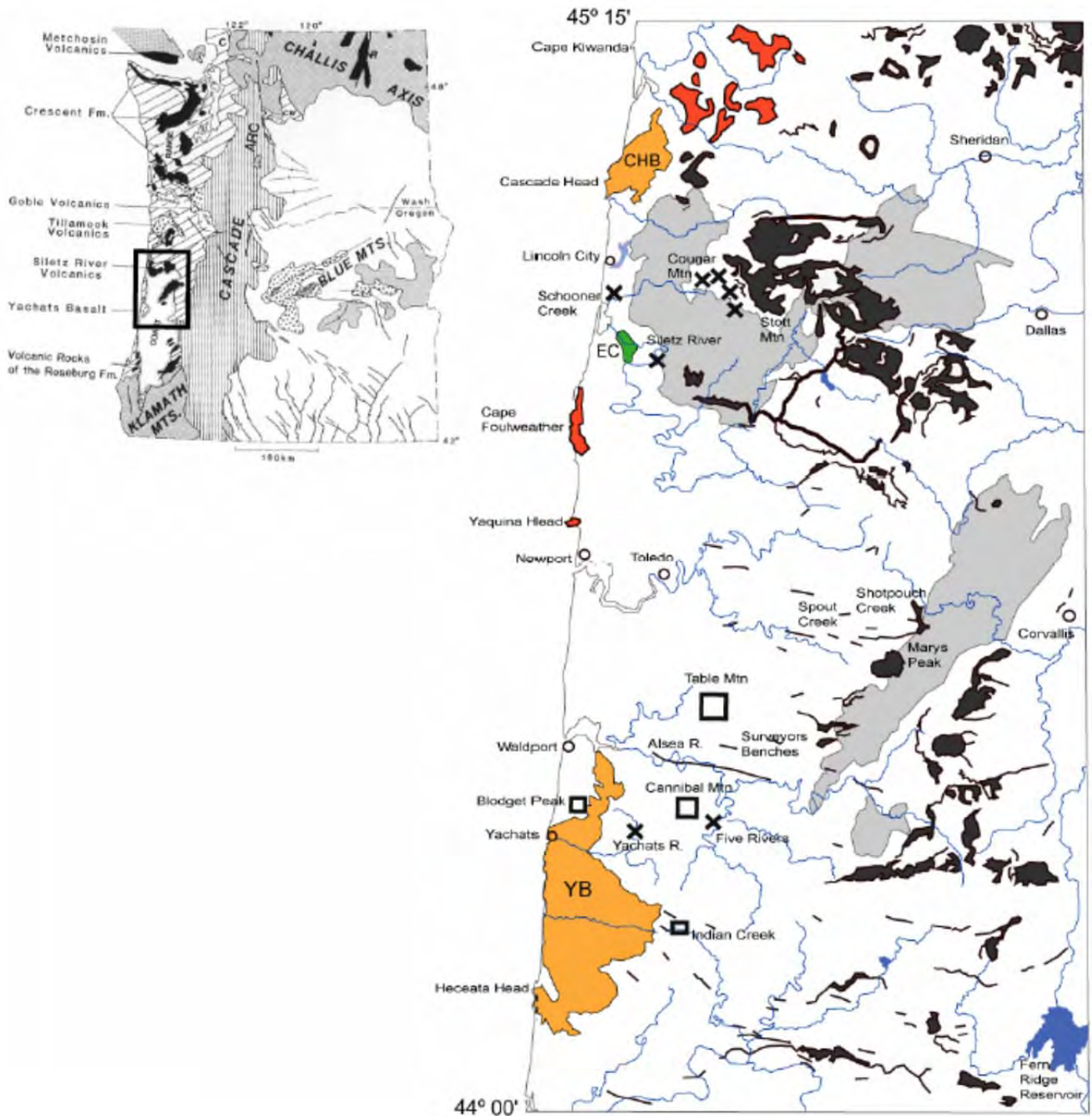
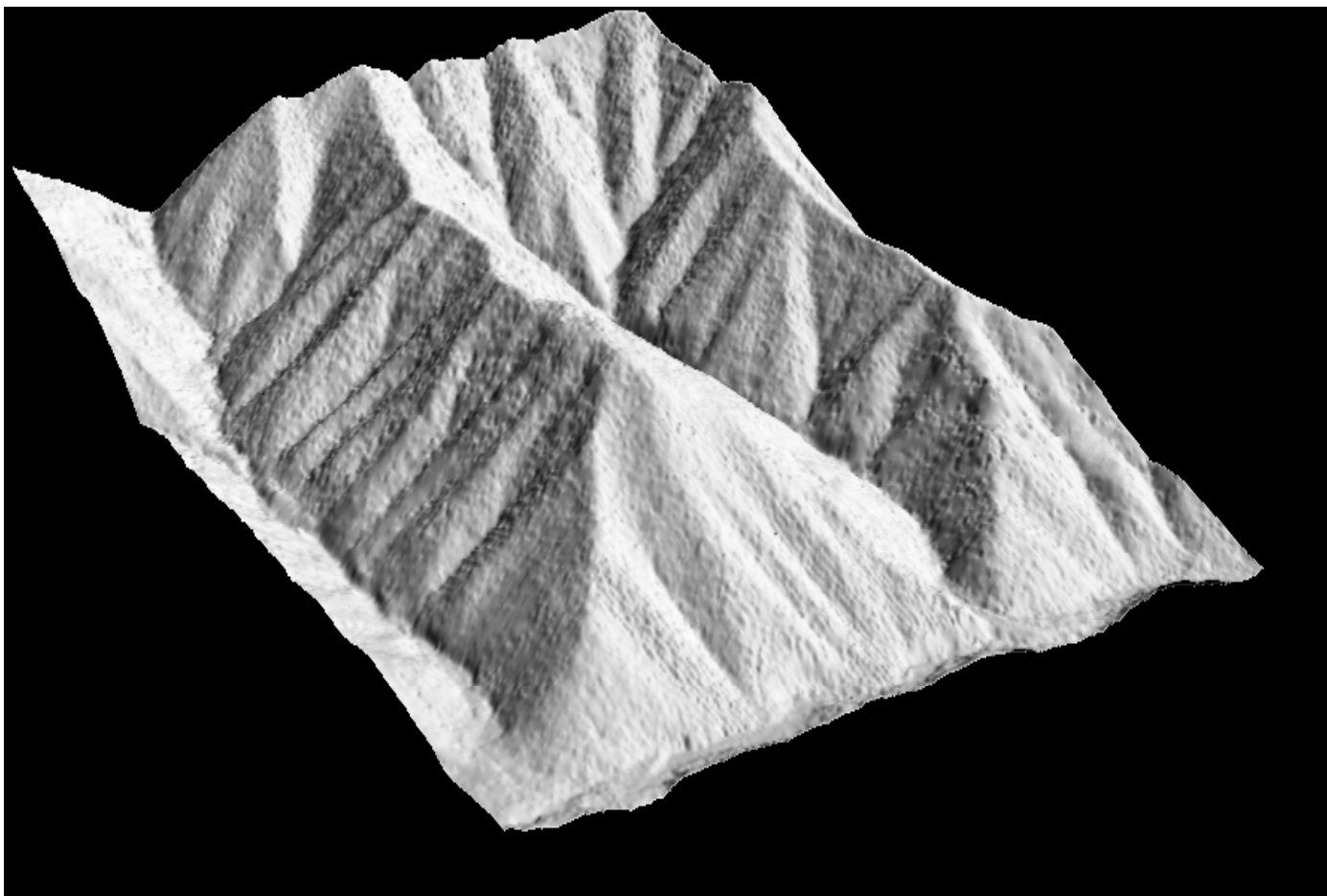
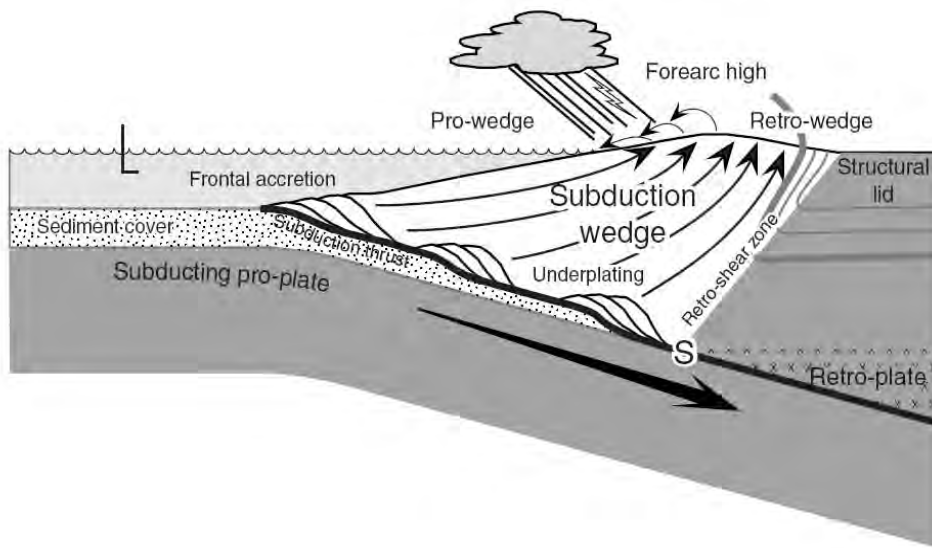
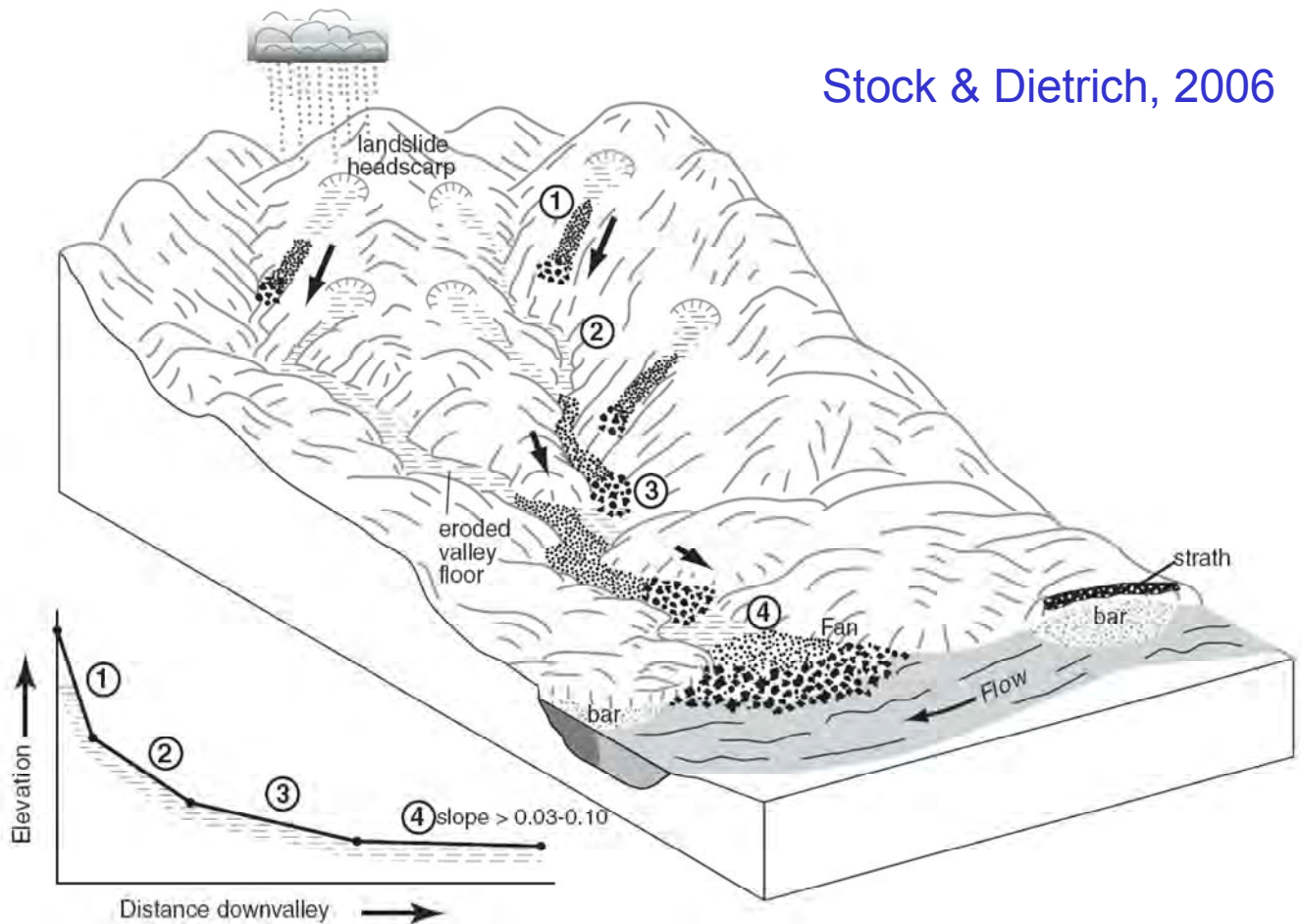
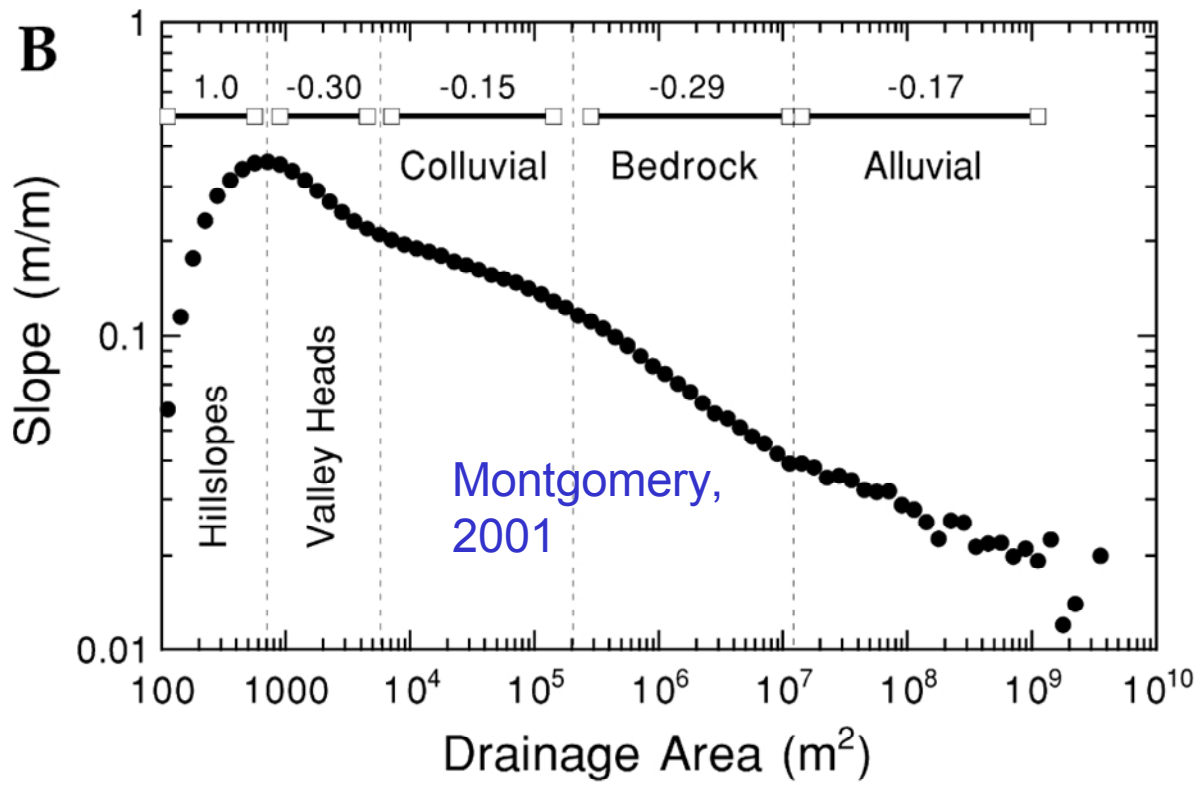
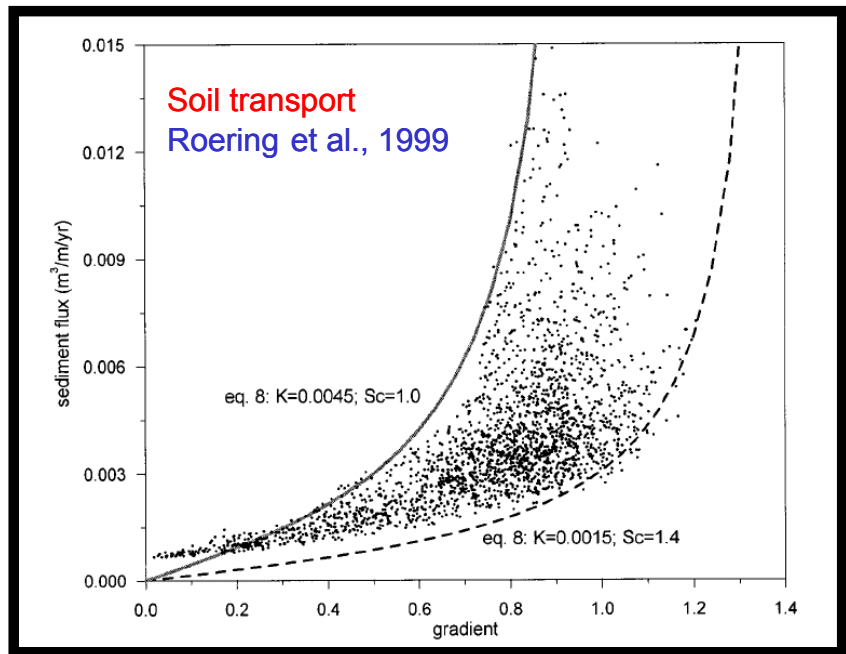
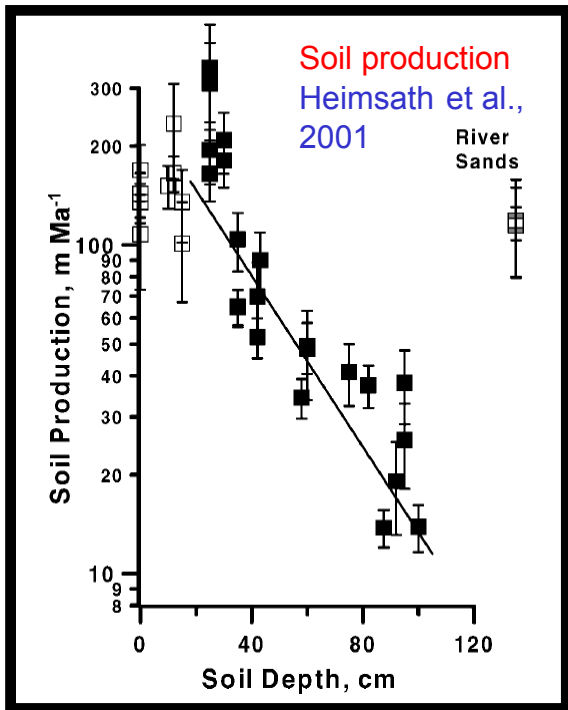
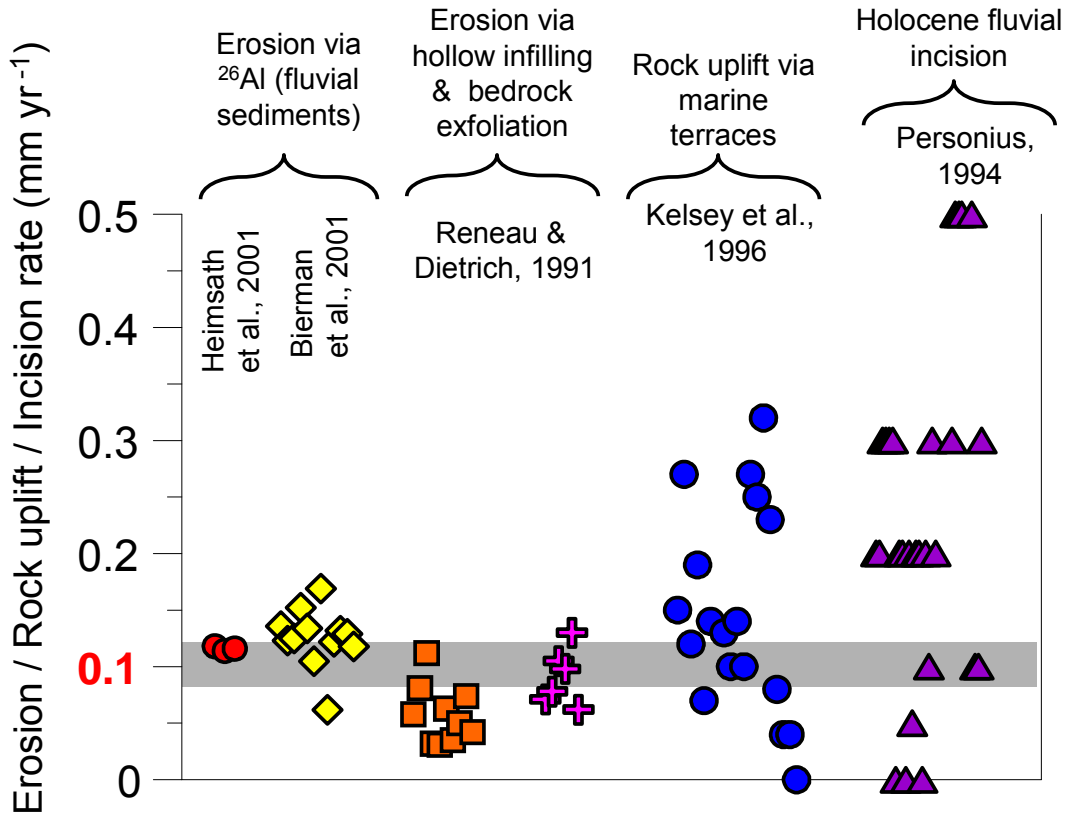


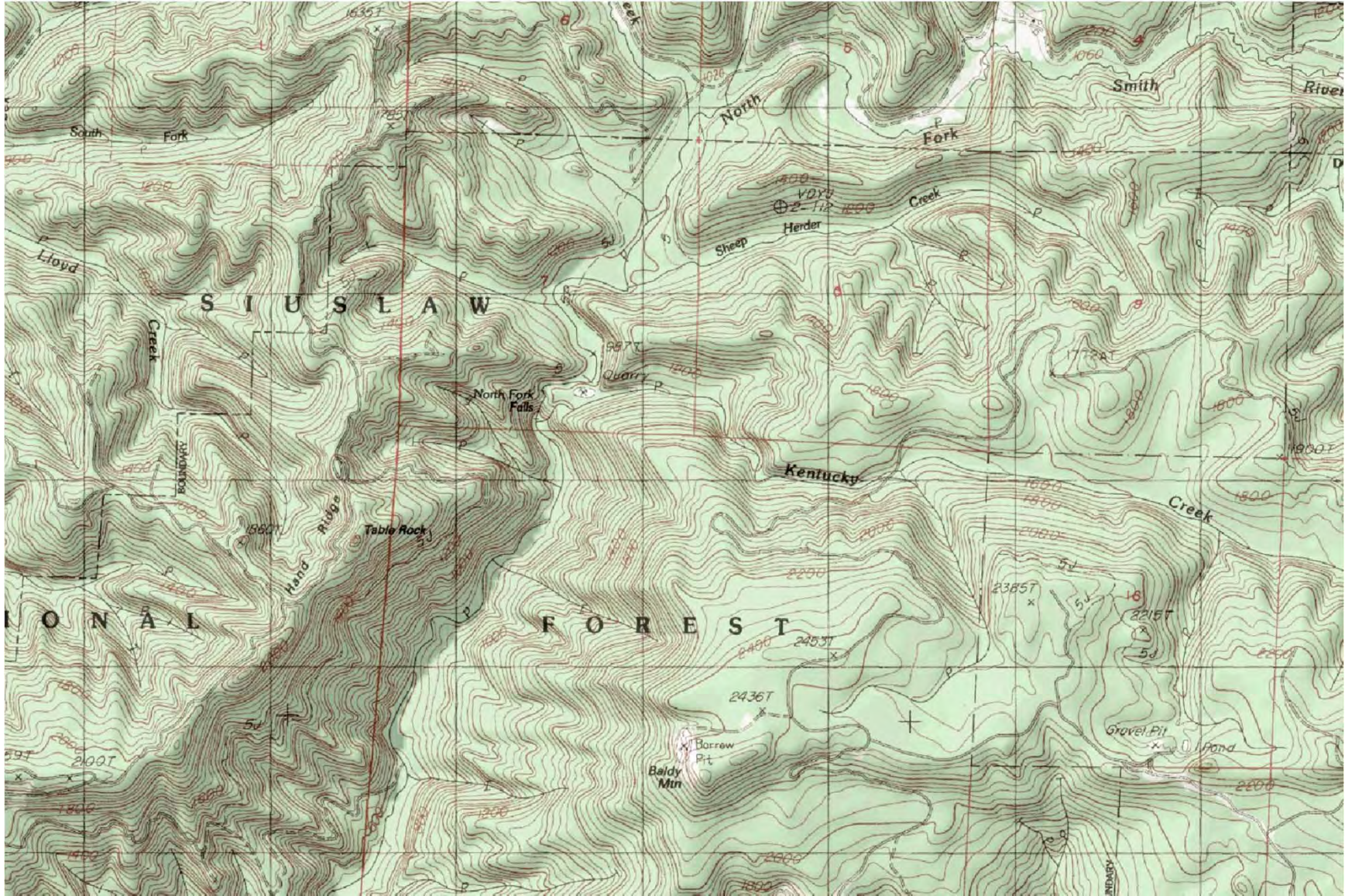
Figure 1: Left: Geologic and tectonic map of the Pacific Northwest from Wells et al. (1984). Major Tertiary Cascadia forearc volcanic centers and Coast Range basement rocks are labeled. Exposures of contemporaneous John Day backarc volcanic deposits are located in the Blue Mountains. The box encloses the area of study. Right: Distribution of igneous rocks within the area of study. Boxes, sampled nepheline syenite intrusions; "X's", sampled camptonite and alkaline basalt intrusions; black bodies, gabbroic intrusions; red bodies, Miocene Columbia River Basalts; light gray areas, exposures of Siletz River Volcanic basement rocks; CHB, Cascade Head Basalt; YB, Yachats Basalt; EC, extrusive camptonite. Figure modified from Snavley and Wagner (1961). Additional information added from Snavley et al. (1976) a, b; Snavley et al. (1968); and Davis et al. (1995).

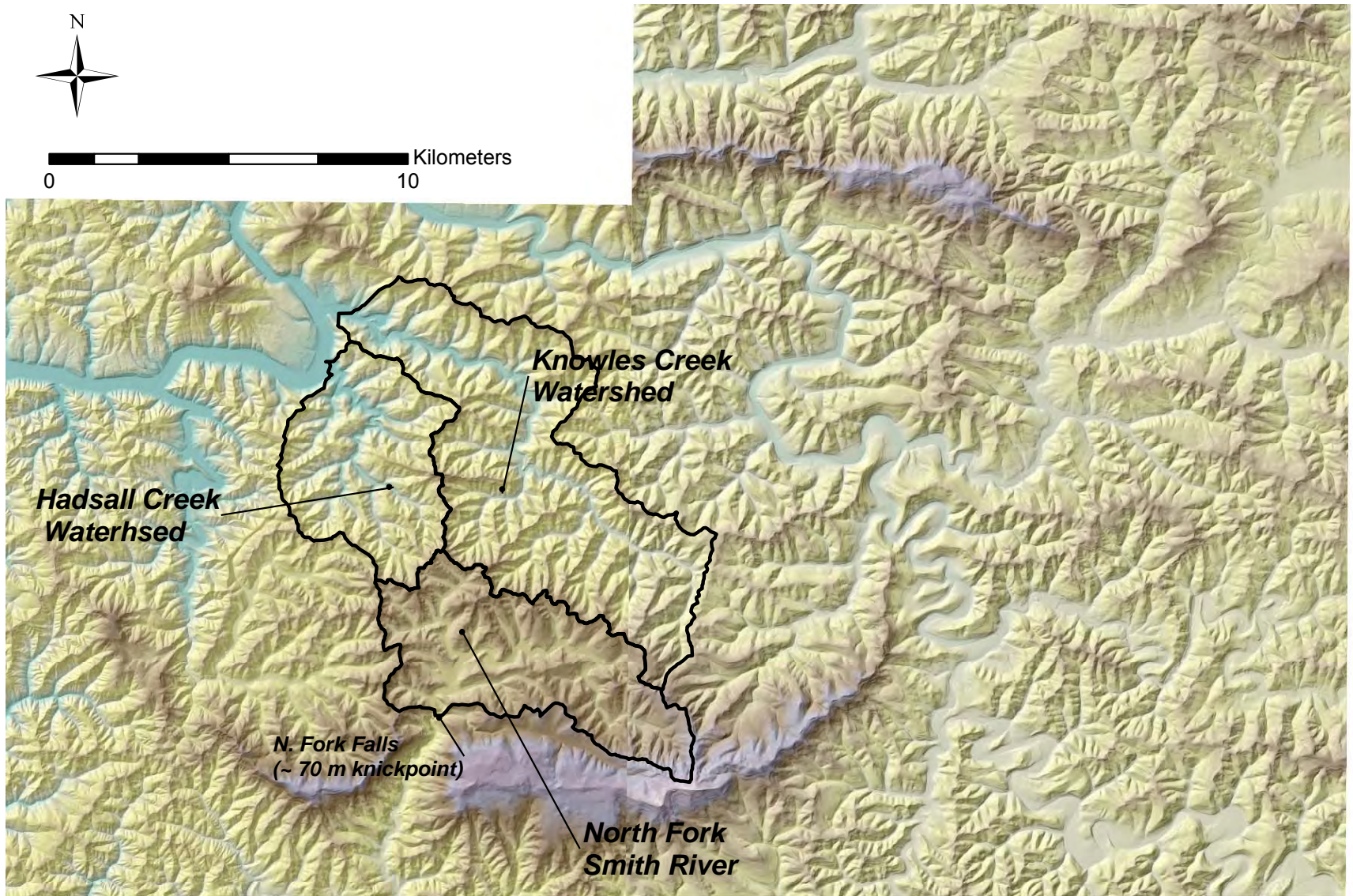


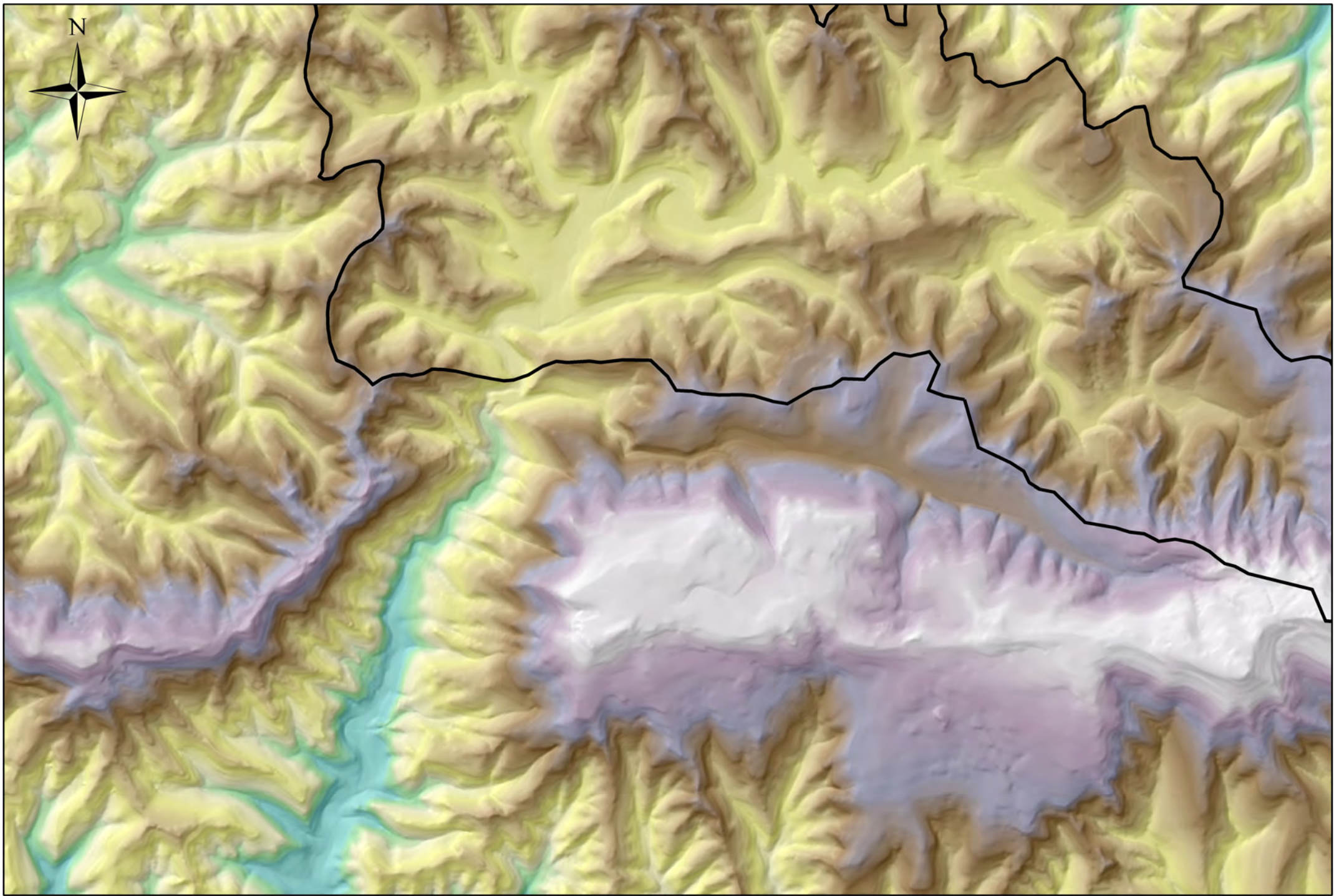












0

3

14

Kilometers

Persistence of waterfalls in fractured rock

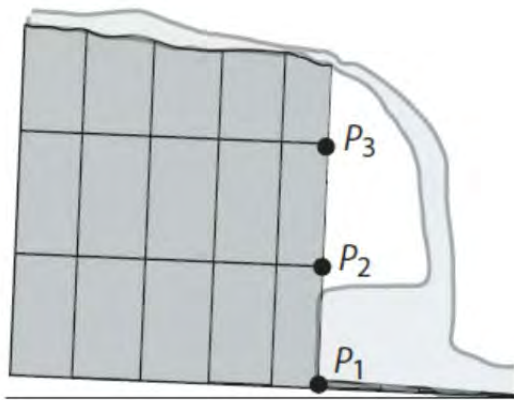


Figure 2. Schematic cartoon showing fractured basalt and three potential points for rotational failure. Two perpendicular joint sets are shown in the schematic, and the third is parallel to the page.

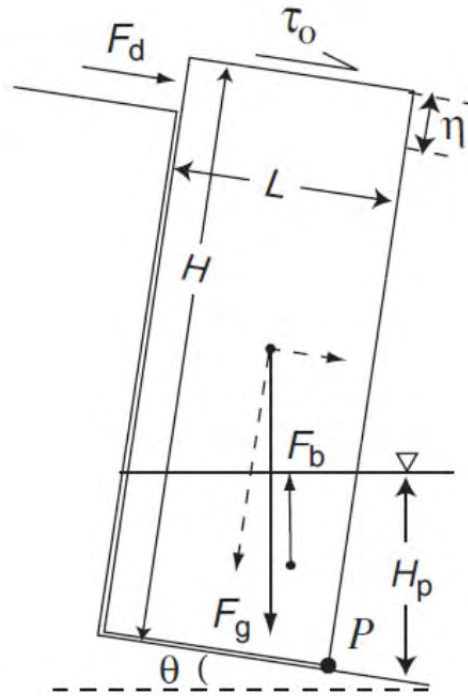
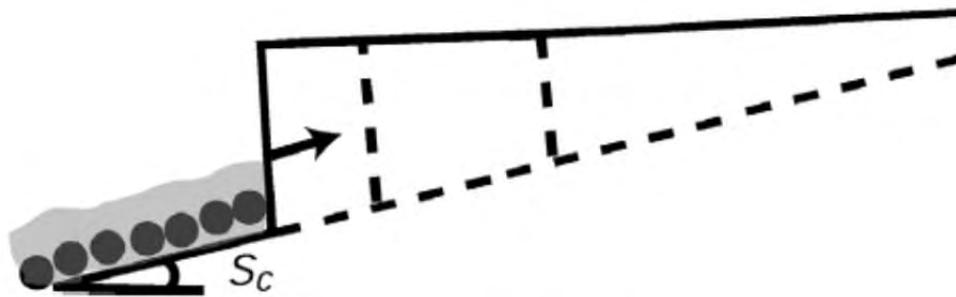


Figure 3. Schematic showing the forces on a rectangular column of rock. See text and notation list for details.

Michael P. Lamb<sup>†</sup> and William E. Dietrich

*GSA Bulletin*; July/August 2009; v. 121; no. 7/8; p. 1123–1134;



**Figure 2.** Schematic of upslope headwall propagation due to seepage erosion, illustrating the necessary condition of debris removal. If the discharge is not sufficient to transport collapsed debris at a given slope, the bed will aggrade until the slope surpasses the critical slope necessary for transport. If this critical slope  $S_c$  is greater than the regional topographic slope, then the headwall will diminish in height as it propagates upslope, eventually leading to the demise of the canyon.

**Citation:** Lamb, M. P., A. D. Howard, J. Johnson, K. X. Whipple, W. E. Dietrich, and J. T. Perron (2006), Can springs cut canyons into rock?, *J. Geophys. Res.*, *111*, E07002, doi:10.1029/2005JE002663.

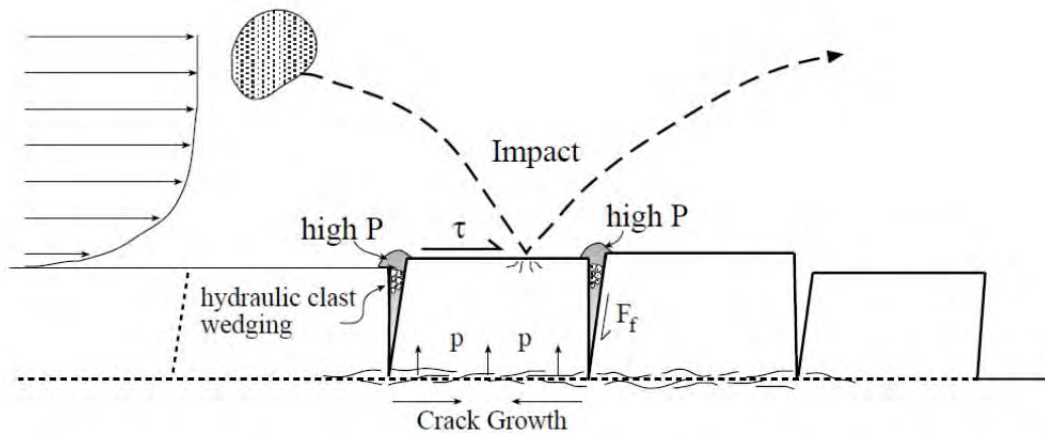


Figure 4. Schematic illustration of the processes and forces contributing to erosion by plucking. Impacts by large saltating grains produce some direct abrasion damage but contribute most importantly to the generation of stresses that drive the crack propagation necessary to loosen joint blocks. Hydraulic clast wedging works to further open cracks. Surface drag forces and differential pressures across the block act to lift loosened blocks. Where the downstream neighbor of a block has previously been removed, both rotation and sliding become possible, and extraction is greatly facilitated.

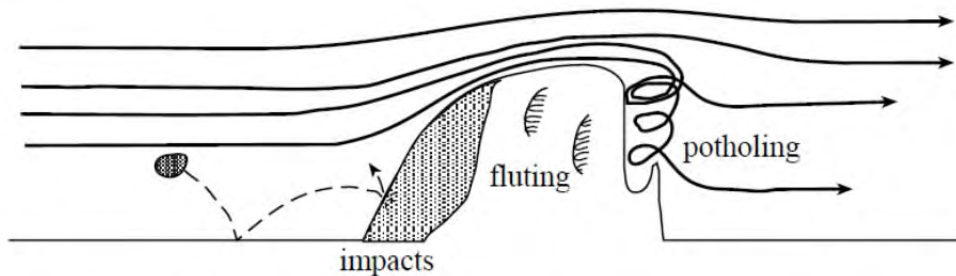


Figure 5. Schematic illustration of the processes contributing to erosion by abrasion. Bedload and the coarsest suspended-load grains are strongly decoupled from the fluid flow and impact the upstream faces of protuberances and obstructions (shaded region). In this zone, surfaces are observed to be smooth and polished, but little abrasion damage appears to occur (see data in Hancock et al., 1998). Fine-scaled flutes and ripples adorn the flanks of massive protuberances where flow separation induces tight, stream-wise vortices (see Figs. 2A and 6A). Large, often coalescing potholes characterize the lee side of obstructions, protuberances, and knickpoints (see Figs. 2B and 6B). The complete obliteration of massive, very hard rocks in these potholed zones testifies to the awesome erosive power of the intense vortices shed in the lee of obstructions (see Fig. 2B).

# Friends of the Pleistocene 2022

## **From Gulley to Gravel to Grit to Grapes**

### **Evolution of the Umpqua River Valley and Oregon Coast Range**

Logan Wetherell, Dr. Jim O'Connor, Dr. Ray Wells, Dr. Eric Kirby,

Dr. Scott Burns, Dr. Josh Roering, Greg Orton, Dr. Lisa Ely

**Camp: 577 Mode Road, Umpqua OR 97486**

**Evolution of the Umpqua Valley and Oregon Coast Range; Supplemental Trip Notes**

Pacific Northwest Cell, Friends of the Pleistocene

Sept. 22-25, 2022

Prepared by Logan Wetherell

**This is not a reviewed guide and is not approved for publication, distribution, or citation**

**The Umpqua River** is one of only two watersheds in western Oregon that has its origins in the High Cascades and meanders west through the Oregon Coast Range (OCR) to the Pacific Ocean. The Calapooya Mountains separate the Umpqua watershed from the Willamette watershed in the north, and the rugged Klamath Mountains from the Rouge River in the south. The North Umpqua River begins in the Cascades at Mt. Thielsen and Diamond Lake while the South Umpqua begins approximately 30 km west of Crater Lake and are continually fed through the summer months by snowmelt.

The North and South Umpqua Rivers flow approximately 150 km before merging at River Forks Park 10 km west of Roseburg. The Umpqua River then meanders through broad farmland until reaching Tyee Mountain in Umpqua where the resistant turbidites of the Tyee Fm cause the Umpqua River to narrow into the canyon. The river follows an incised serpentine course through OCR until reaching weak mudstone of the Elkton Fm at the town of Elkton, where broader floodplains and agriculture appears again. Continuing west, the Umpqua enters another canyon near Scottsburg as the river reenters into the resistant Tyee Fm. The steep-walled canyon continues as the Umpqua reaches tidal waters with broad floodplains abutted by steep ridges appearing as the river enters Winchester Bay and empties into the Pacific Ocean.

The Umpqua River watershed was inhabited by several bands, including the Upper Umpqua, Cow Creek, Yoncalla (Kalapuya), and coastal Quich. In the early 19<sup>th</sup> century, the Upper Umpqua tribes ceded much of its land to the U.S. Government in the 1854 Treaty with the Umpqua and Kalapuya moving to a reservation in Lincoln County as part of the Confederated Tribes of Siletz.

#### **Agenda:**

**Day 1:** Eastern margin of the Oregon Coast Range (OCR) – Umpqua Valley geology and Pleistocene terraces

**Day 2:** Central OCR geomorphology – Controls on river valley width, landslides, sediment transport

**Day 3:** Umpqua River delta and dunes – Post-Pleistocene sea-level rise, coastal terraces, 80k+ yr ghost forests

Camp: 43.342148°, -123.485003°

Day 1

1: Wetherell Vineyards Terraces: 43.342990°, -123.474470°

2: Umpqua Valley Overlook: 43.307349°, -123.530130°

3: Umpqua River and Tye Fm Contact: 43.374201°, -123.514310°

4: Henry Estate Terrace: 43.373775°, -123.479667°

Day 2

5: Umpqua River @ Tye Access Road: 43.431018°, -123.566714°

6: Umpqua River @ Elkton Fm Contact: 43.635621°, -123.568168°

7: Scottsburg Landslide: 43.668839°, -123.803340°

8: Mill Crk and Loon Lake: (43.647679°, -123.872125°), (43.598390°, -123.845726°), (43.532186°, -123.825487°)

Day 3

9: Dean Creek Elk Viewing Area: 43.695288°, -124.037371°

10: Tokatee-Kloutchman Beach/80k+ yr Pleistocene forests: 44.208310°, -124.114780°

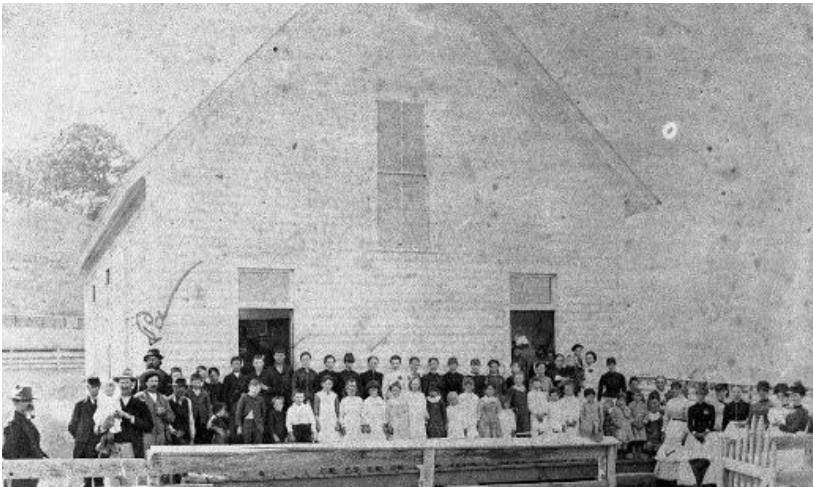
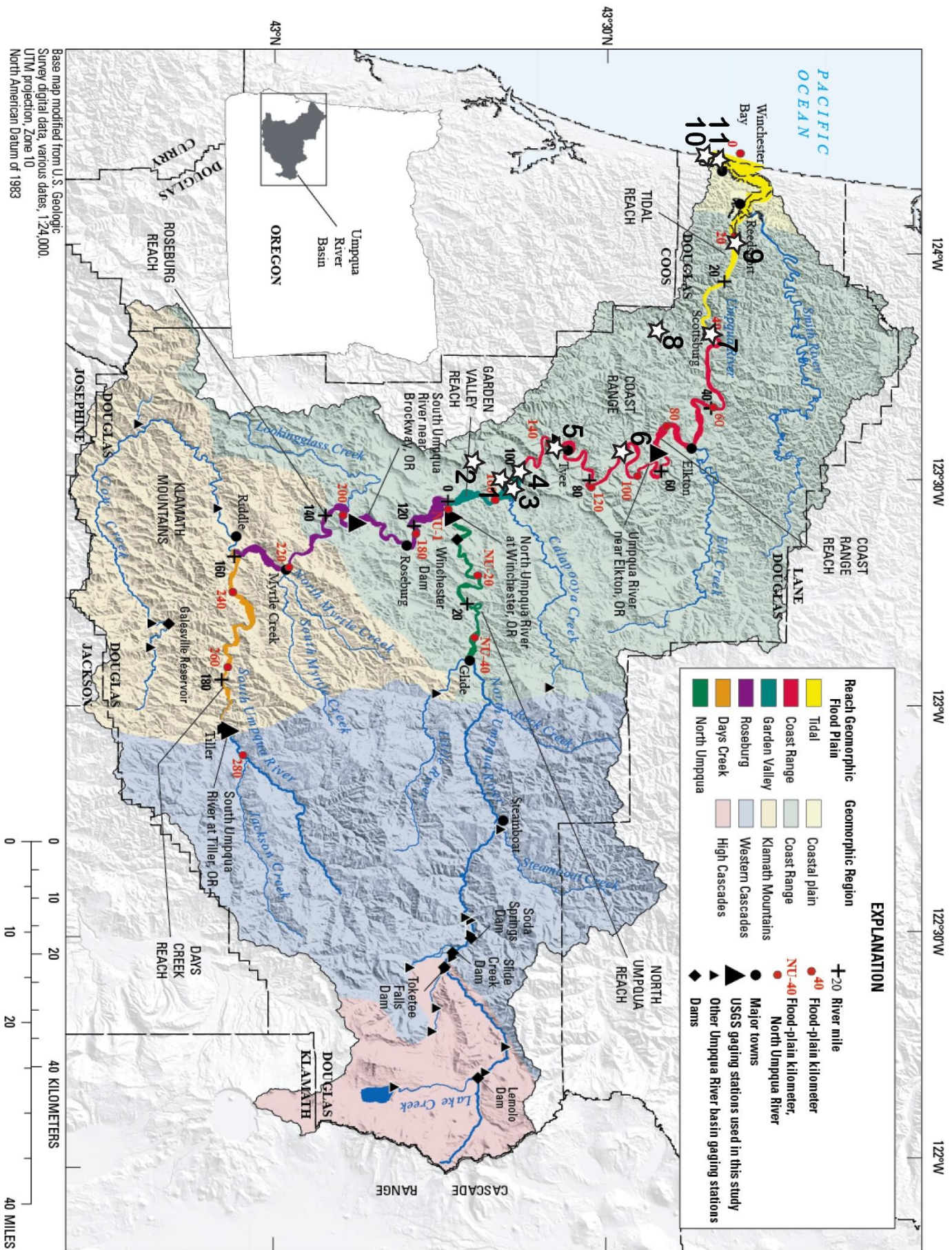


**Figure 2. Above.** Coles Valley School, 1886. The old school was located on the northwestern corner of what is now Wetherell Vineyards at the junction of Iverson Rd and Melqua Rd (follow mowed path to northwest below current barn, historic sandstone foundation blocks composed of Tenmile Fm (Umpqua Grp). **Right.** Adam Doerner and wife Elizabeth, with young Adolph and Lucia, 1885. Adam sold prune and pear brandy and became the first winery in the Umpqua Valley after planting grapes in 1888. Adolph and later his son Ray Doerner would own and operate the original Melrose Vineyards until closing in 1965 and were one of the few wineries in Oregon to survive Prohibition by selling "grape juice" to locals to make their own wine.





Base map modified from U.S. Geologic Survey digital data, various dates, 1:24,000. UTM projection, Zone 10 North American Datum of 1983

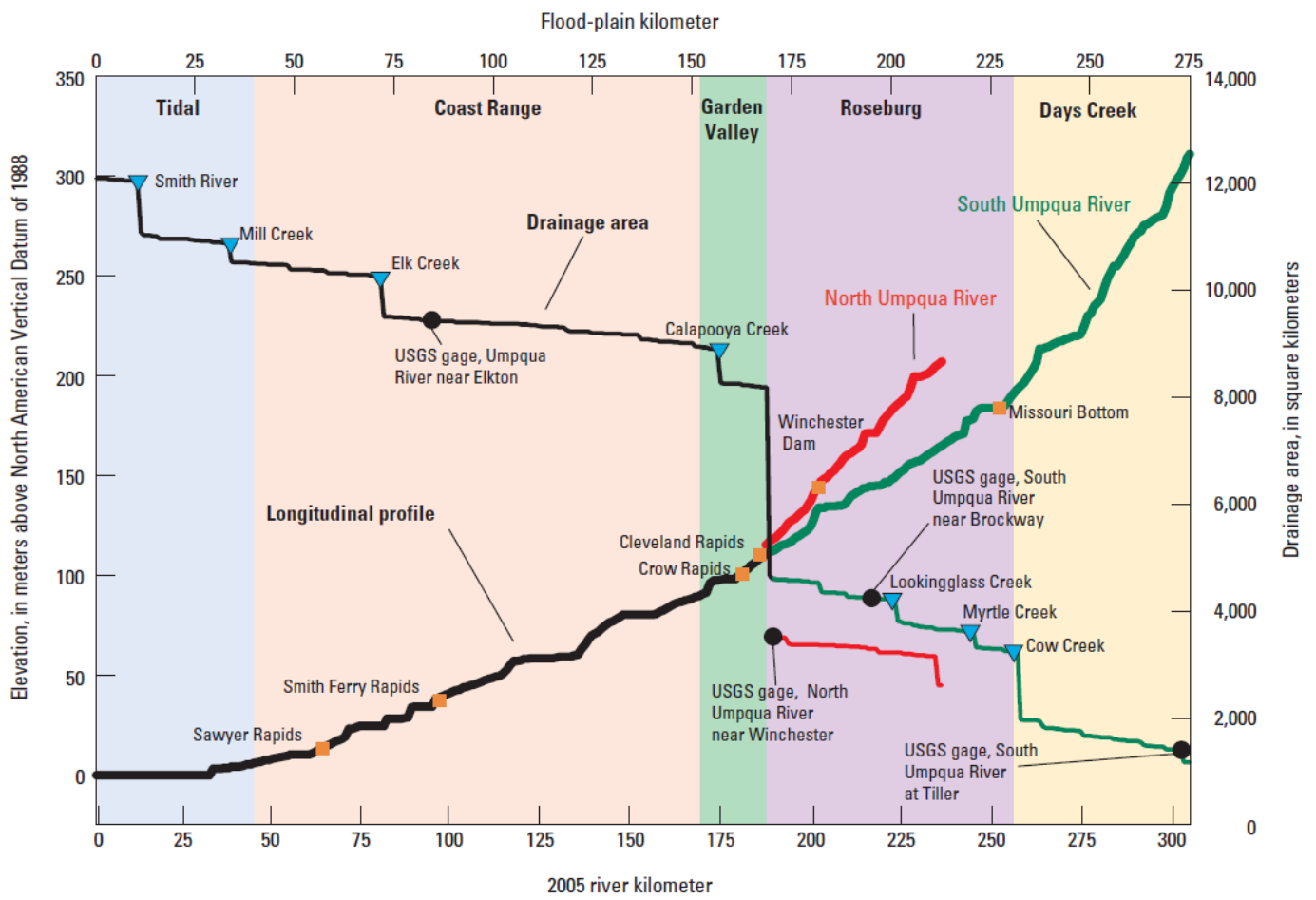


**Figure 3.** The Umpqua River, Oregon, drainage basin and study area. Reaches analyzed are defined by valley geomorphology and tributary junctions. Colored reach extents indicate the geomorphic flood plain. Topography based on U.S. Geological Survey 10-m digital elevation (Wallick et al., 2011).

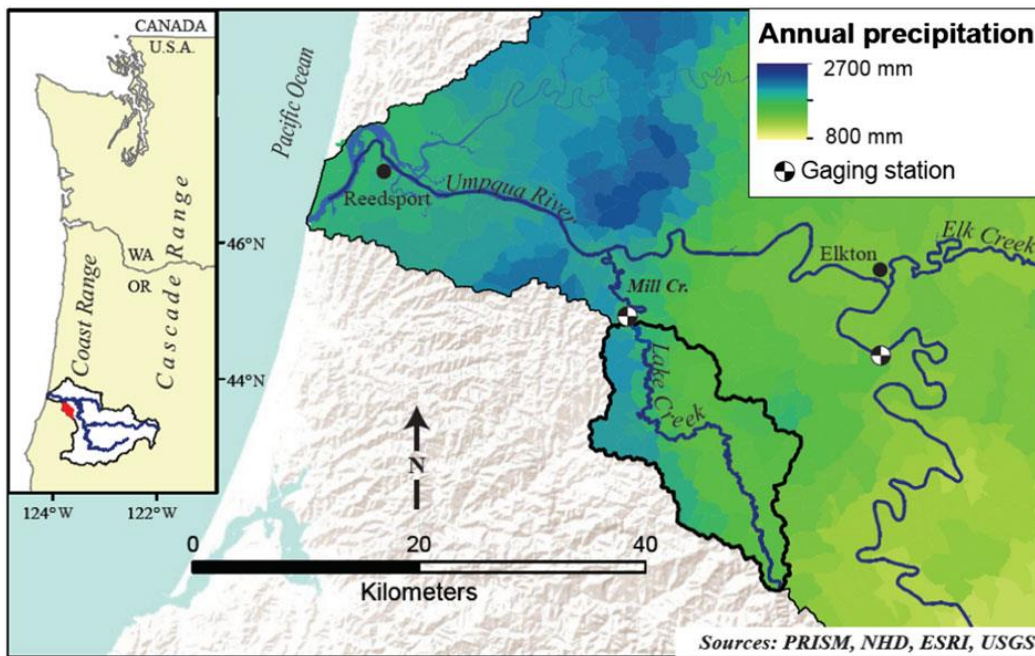


**Figure 4.** Annual precipitation in the lower Umpqua River watershed in central OCR (Richardson et al., 2018). Note drastic increase in precipitation in the central Coast Range compared to the Umpqua Valley near camp.

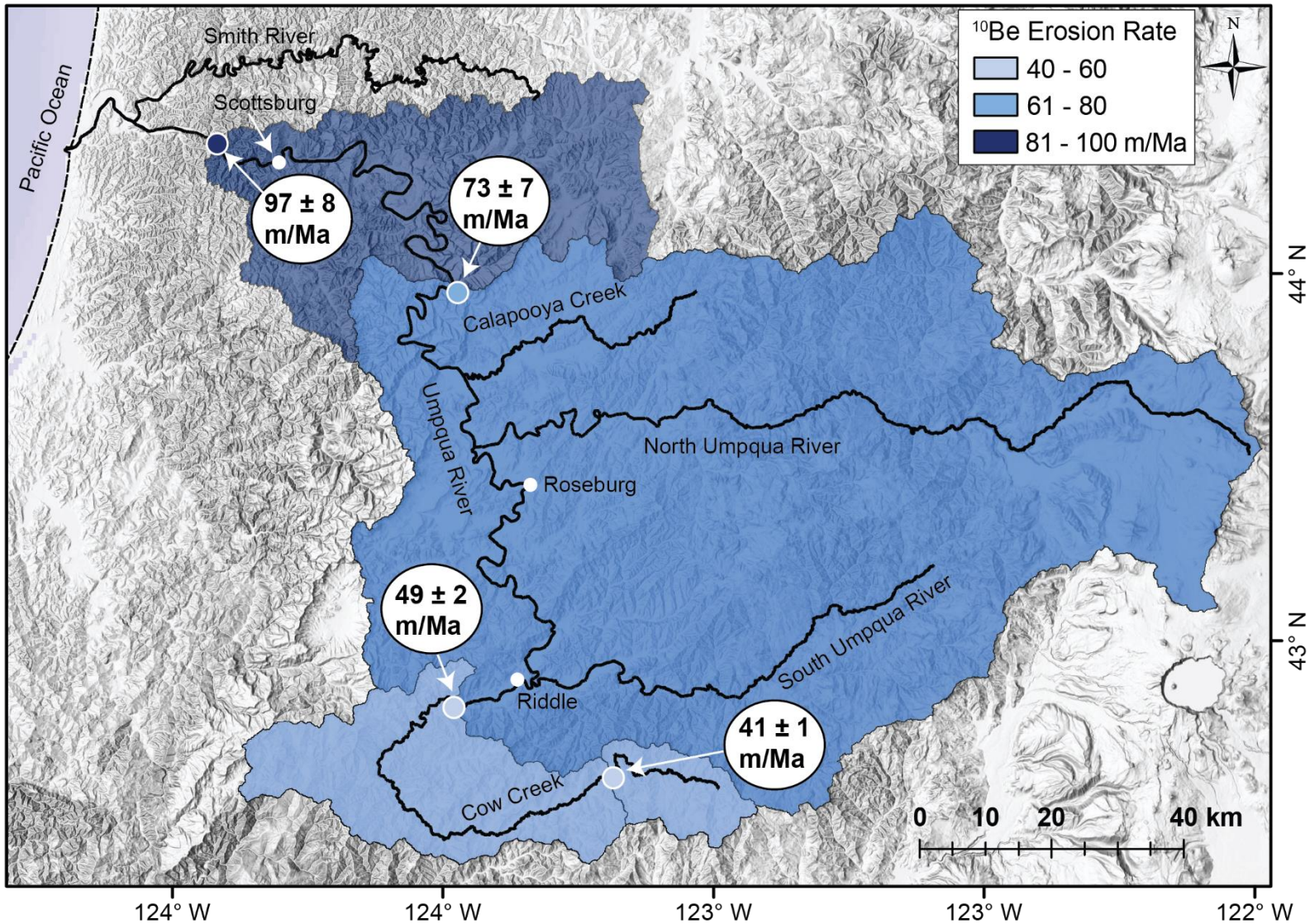


**Figure 13.** Erosion rates from subcatchment positions within the Umpqua River watershed suggest that  $^{10}\text{Be}$  concentrations become progressively more dilute downstream. Unpublished data from W. Hefner, E. Kirby, P. Bierman, L. Ghazi, and J. Pett-Ridge.

## 6: Umpqua River @ Elkton Fm

(Logan, Ray)

**Goals:** Understand the significance of bedrock lithology on topography

**Questions to ask:**

- (1) What is the Elkton Fm and why does it form broad terraces and wider floodplains?
- (2) How do the variations in topographic relief, hillslope morphology, and channel steepness govern the pace and pattern of erosion?
- (3) How often and how high does the water reach during major flood events?

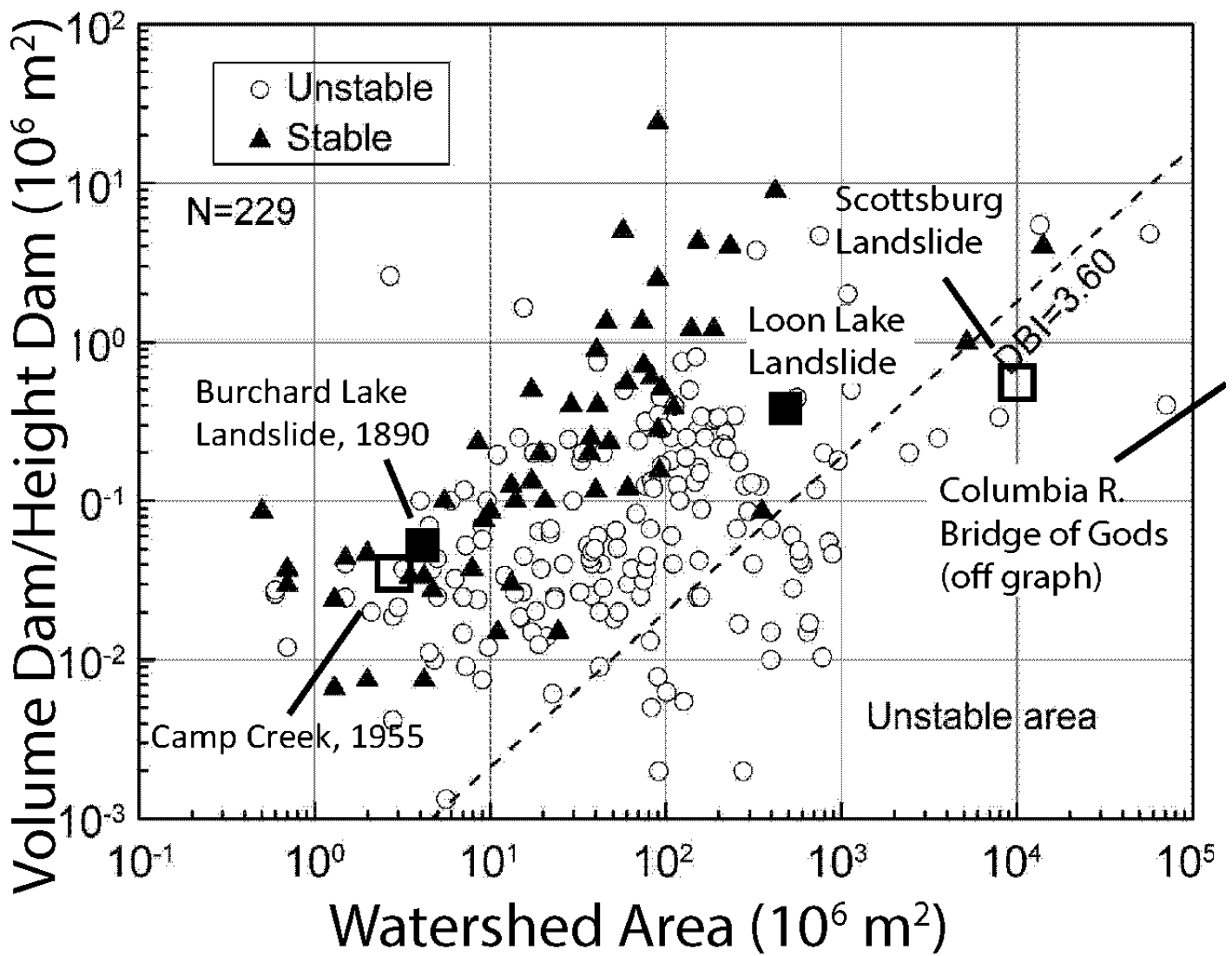
Goals: Observe the transition from Coast Range Reach to Tidal Reach in river morphology. Determine if Scottsburg Landslide could form a landslide dam that would impound the lower Umpqua River.

Questions:

- (1) How does the stream profile and floodplains change after the communities of Wells Creek/Scottsburg?
- (2) Could the large landslide impound the Umpqua River? For what length of time?
- (3) What could be the cause (i.e. coseismic? Precip?) of the landslide? Why did it occur at this location?



**Figure 14.** Scottsburg segment of the Umpqua River and hypothetical landslide-dam terrace created from a 20-m high landslide blocking the Umpqua River. The dip of the turbidites in the Tye Fm dictate the location and direction of translational deep-seated landslides with the easterly dip forming the dip-slip slope planes of the Scottsburg landslide and Burchard Lake (B.L., winter 1890) landslide complexes.



**Figures 15. Top:** Global database of stable and unstable landslide-dammed lakes and calculated dimensionless blockage index modified from Zheng et al., 2021, with regional landslide dams in the nearby Tye Fm and Columbia R. Bridge of the Gods dam added. **Bottom:** Approx. 5-7 m high splash dam constructed on lower Mill Creek, ~15 km below Loon Lake in early 1900's and up-stream log drive on Mill Creek, early 1900's. Much of the modern road winding up Mill Creek would be buried by wood and debris during these log drives.

Goals: Discuss formation and longevity of these remote landslide-dammed lakes along with sedimentation patterns preserved in upper watersheds of the central OCR.

Questions:

- (1) How prevalent are landslide-dammed lakes in the Oregon Coast Range?
- (2) Are the coastal landslide-dammed lakes coseismic? Atmospheric river?
- (3) How stable are the lakes? Could lithology or woody debris play a role in their longevity and stability?
- (4) How do sedimentation rates of the Umpqua River compare to smaller low-order watersheds?

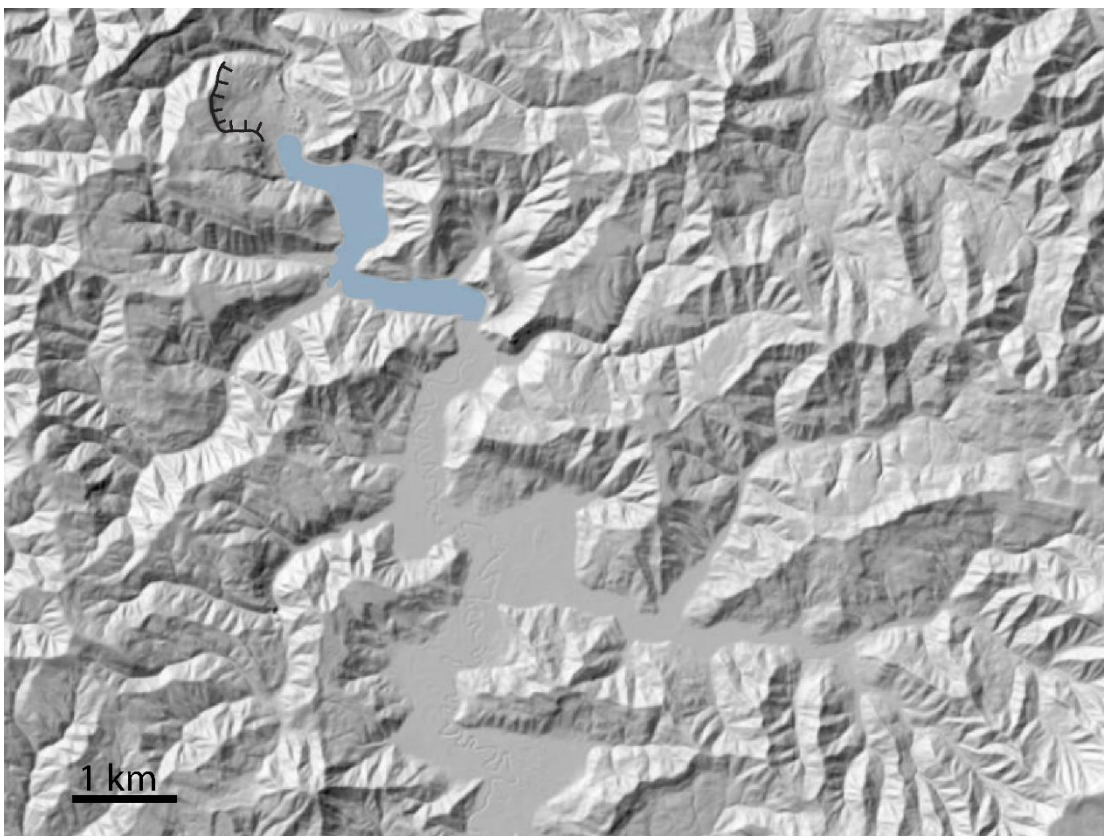
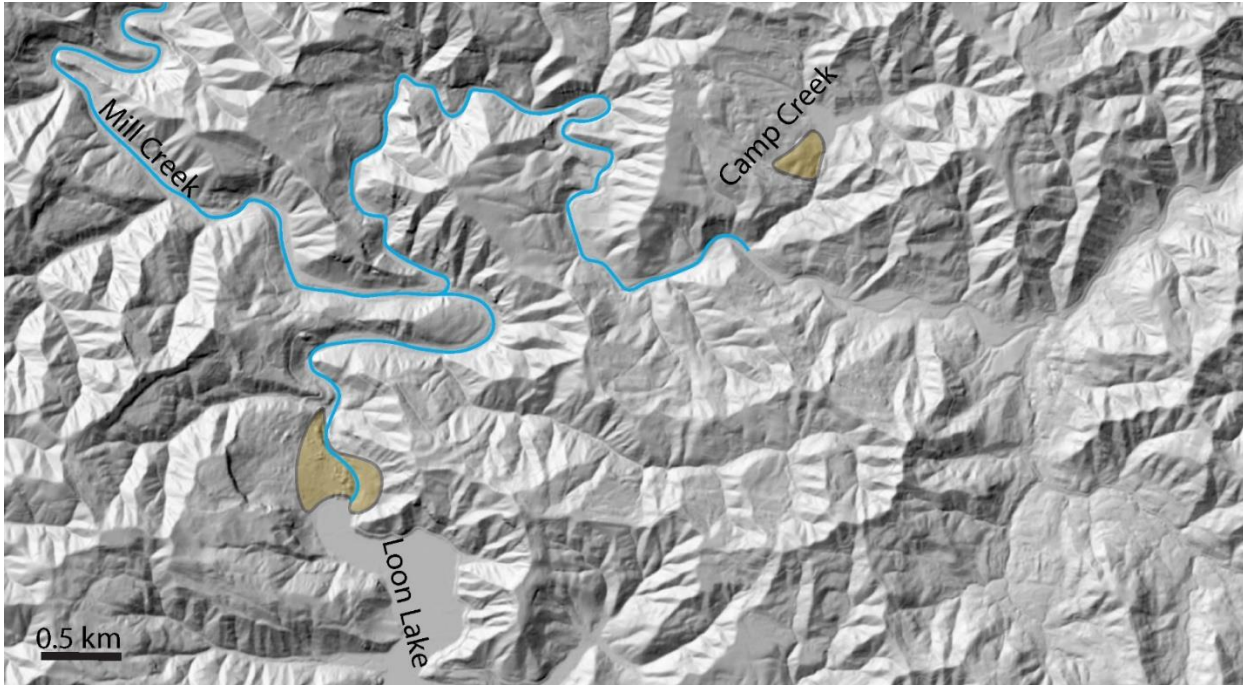


**Figure 16A.** Lidar of Mill Creek and Camp Creek watersheds. Camp Creek formed a temporary landslide-dammed lake in 1955-56, with the Loon Lake landslide dam dated using radiocarbon from submerged trees in the bottom of the lake to 1,400 ybp. **B.** Lidar of Loon Lake and upstream delta. The lake is only a small remnant of its original size and would've been a deep channel prior to the landslide-damming event.

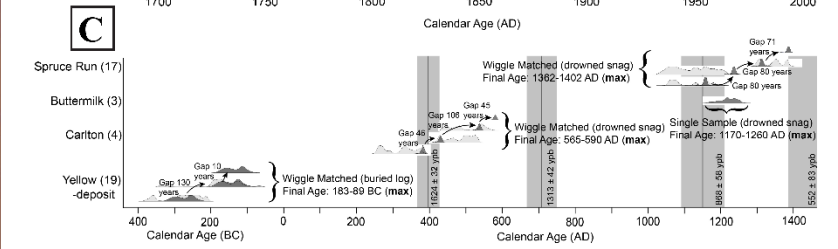
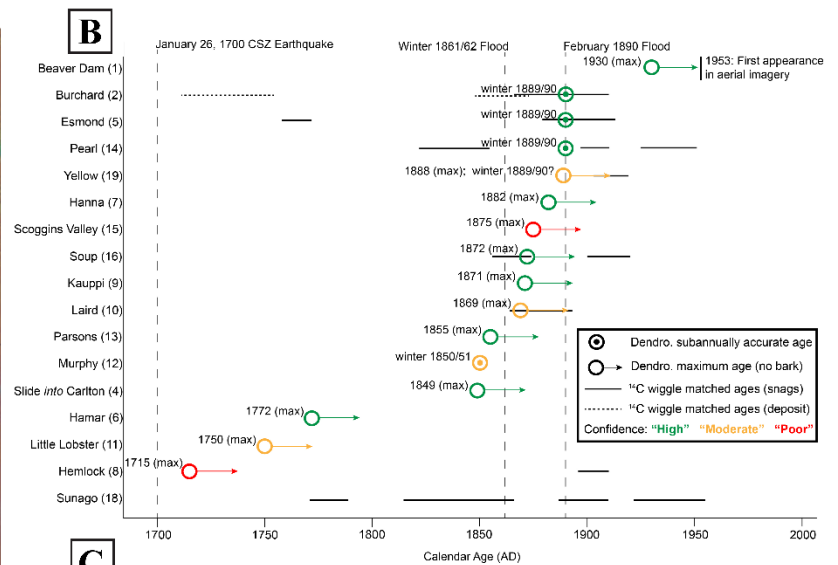
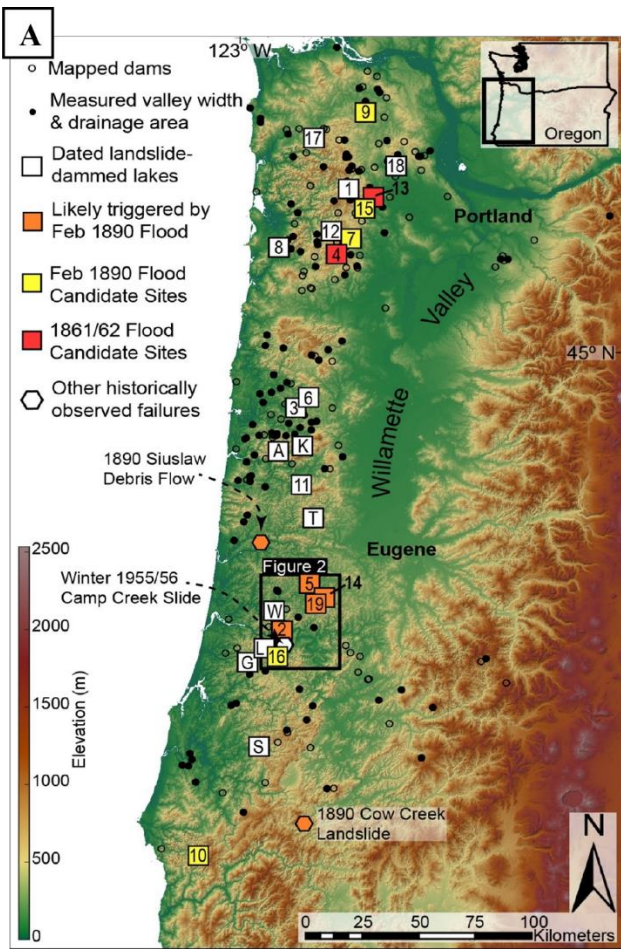


**Figure 17A.** Location of landslide-dammed lakes in western Oregon dated using dendrochronology while searching for coseismic landslides. **B.** Compiled dendrochronology dates of younger landslide-dammed lakes and **C.** Older landslide-dammed lake ages outside dendrochronology range dated using wiggle-matching of spaced tree rings and radiocarbon sampling (Struble et al., 2020).

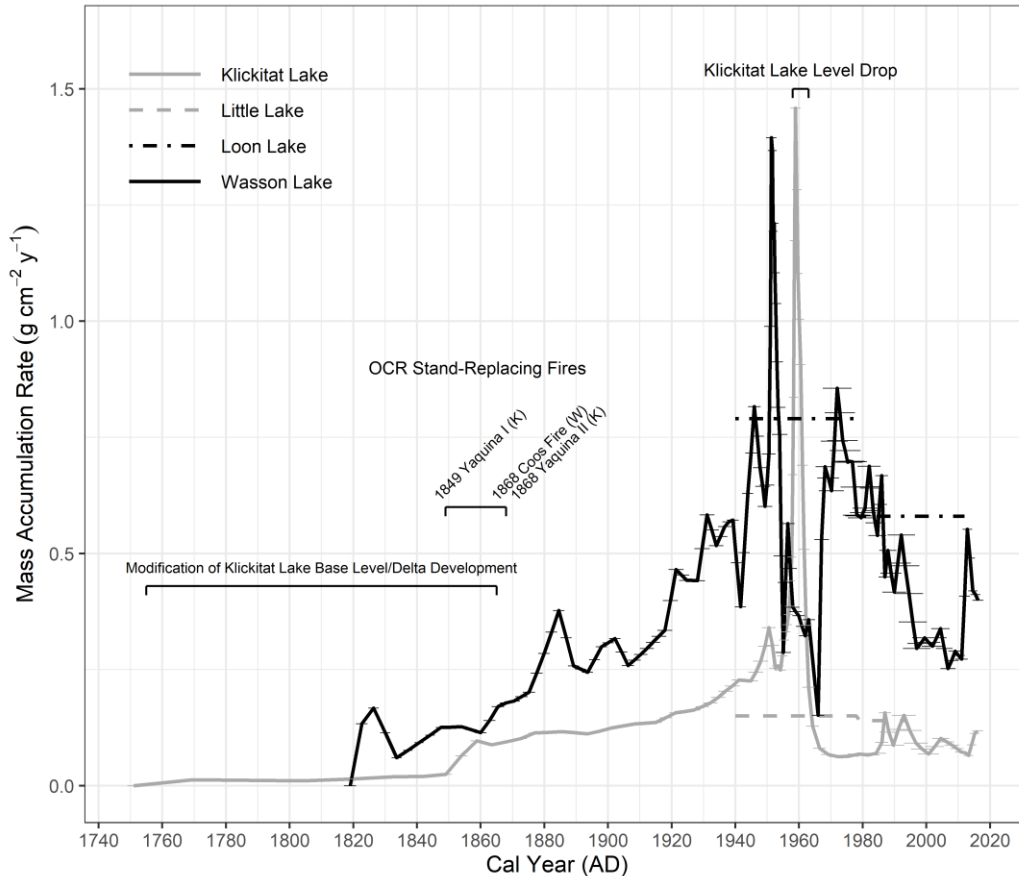


**Figure 18.** Mass accumulation rates of sediment in landslide-dammed lakes of the Tye Fm in the central OCR. Klickitat Lake and Wasson Lake are substantially smaller than Little Lake and Loon Lake, however a N-S pattern is present with northerly lakes having lower sedimentation rates than landslide-dammed lakes in the southern Tye Fm. Interestingly, in the small Klickitat Lake and Wasson Lake watersheds major flood events do not contribute to high sedimentation rates with the 1964 floods well constrained using Cs-137 (Wetherell et al., 2021).

9: Dean Creek Elk Viewing Area

(Jim, Lisa)

Goals: Enjoy the elk herds and the tidal floodplains.

Questions:

- (1) What did this site look like during the Pleistocene?
- (2) How often does this terrace flood? (hint: you're between ~4-10 ft elevation)
- (3) Is it free from tsunamis after a local earthquake? Distal earthquakes?
- (4) How does the local topography along with soils here effect agriculture?
- (5) How many elk do you count?

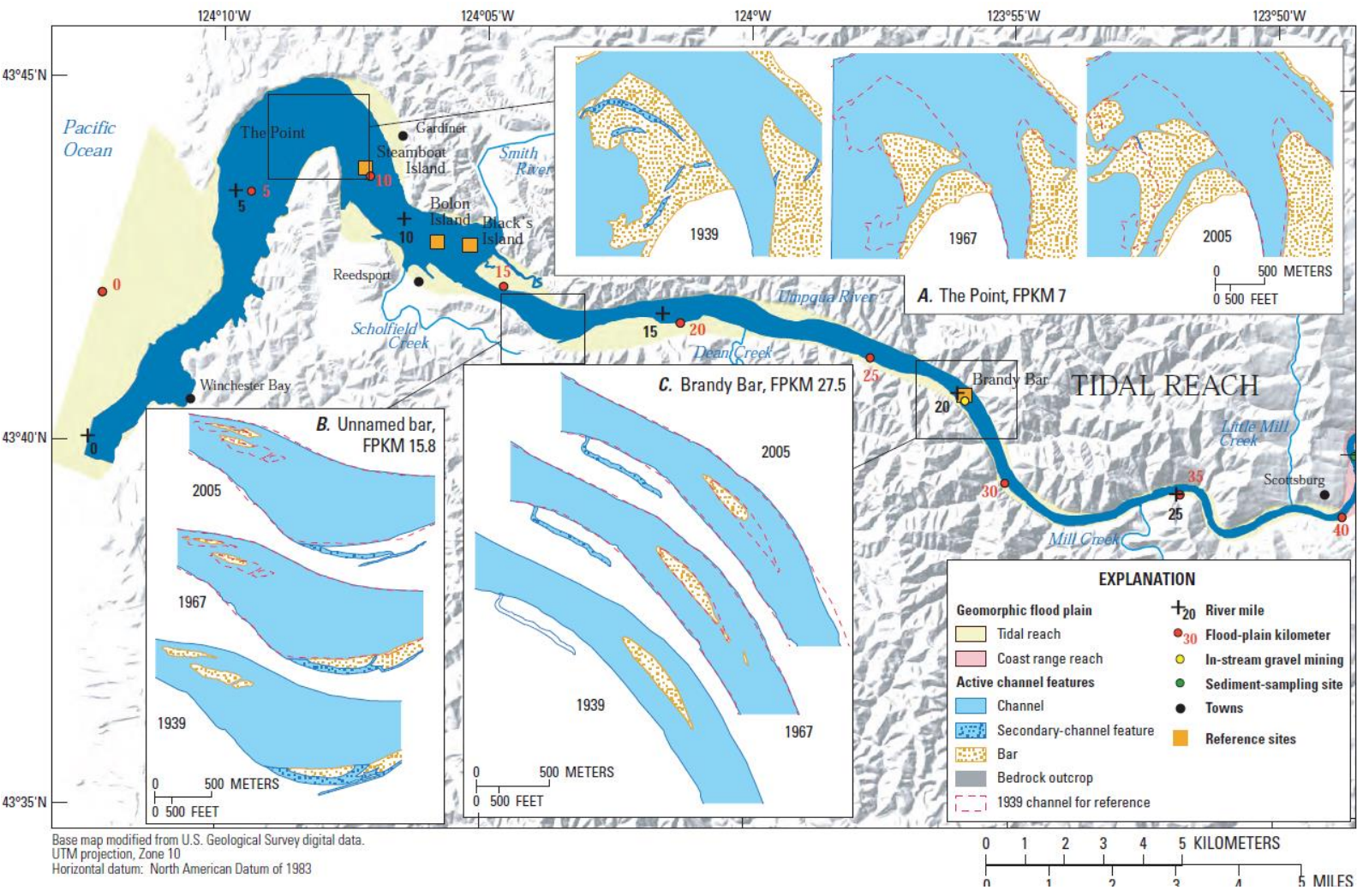
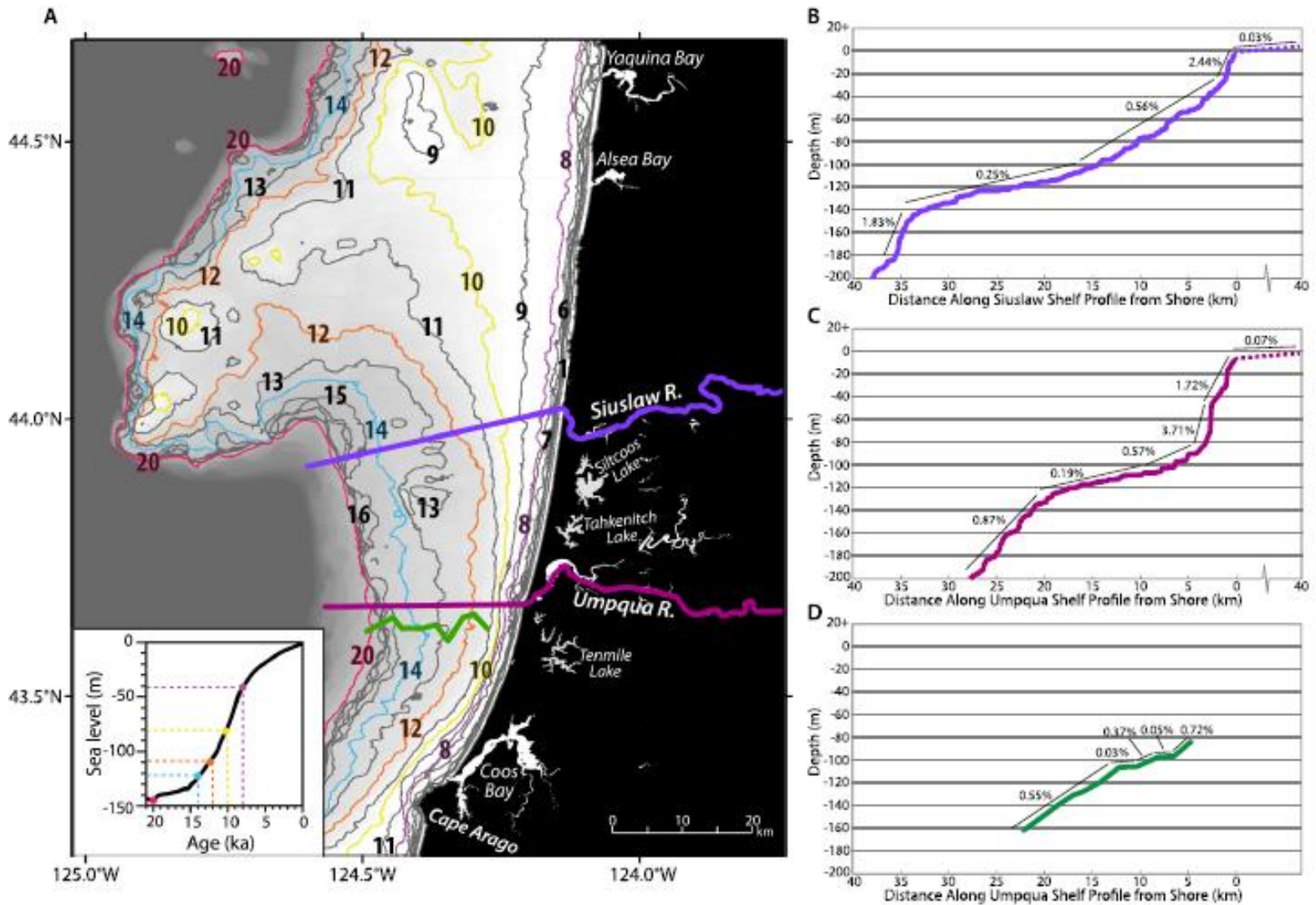


Figure 19. Tidal reach of the Umpqua River extending from the Scottsburg landslide stop to the Pacific Ocean (Wallick et al., 2011).

Goals: Observed 80k+ yr buried ghost “forest” and anastomosing debris flow channels

Questions:

- (1) What type of paleo-environment are we observing in the terrace?
- (2) How do we preserve trees in the upright growth position in an old beach terrace?
- (3) What does the preservation of a 80k+ yr forest suggest about uplift/subsidence at this site?
- (4) How far can you follow the woody horizons at your feet (hint: it’s farther than you think if you have a few hrs)



**Fig. 20A.** Paleoshorelines since the last glacial maximum with profile locations for B–D plotted. Paleoshorelines are based on a glacio-isostatic adjusted sea level curve for the region (Clark et al., 2014). Labels are the age of the shorelines in thousands of years ago. **B–D.** Percent-slope along profiles of the (B) Siuslaw shelf and (C) Umpqua shelf from the modern shoreline to 200 mbsl. D) Slope of mapped paleovalley thalweg of the Umpqua River channel. Depths are plotted at distances along Umpqua shelf profile for comparison of cross-shelf gradient differences (Klotsko et al., 2021).

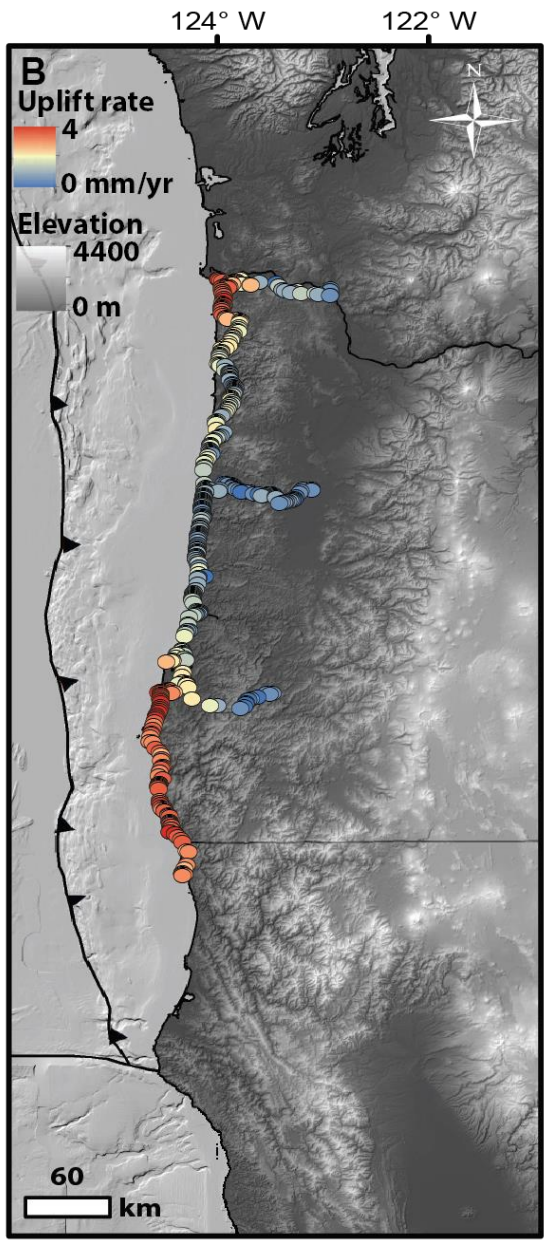
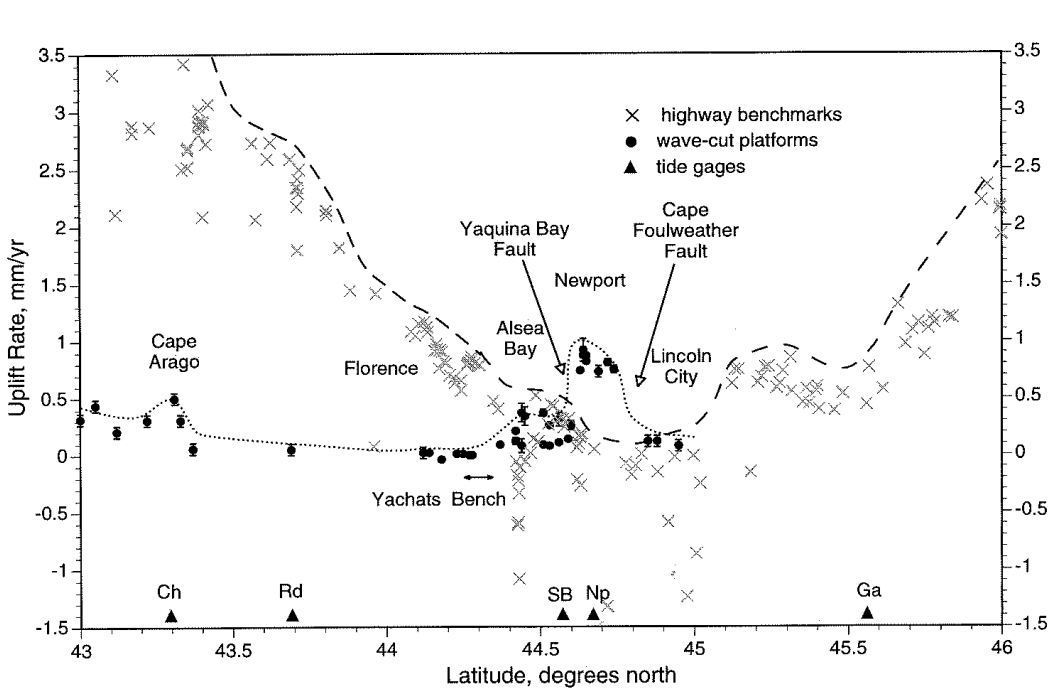


**Figure 21A.** Along-coast variation in average uplift rates since 125k assigned from wave-cut platforms and dated elevations compared to uplift rates for 1941-1987 (X symbol is derived from releveling of highway benchmarks, Mitchell et al., 1994). Dotted line tracks the variation in average platform uplift rates, dashed lines delineates the upper limit for benchmark uplift rates, triangles show locations of the tide gauges that provide independent check on historic uplift rates from releveling. Some benchmarks yield uplift rates significantly below upper limit due to subsidence. Vertical bars represent range of platform uplift rates determined for the shoreline angle of the 80, 105, and 125k platforms (Kelsey et al., 1996). **B.** Forearc topography (30-m USGS DEM) and geodetic uplift rates from Burgette et al. (2009) shown as colored circles.

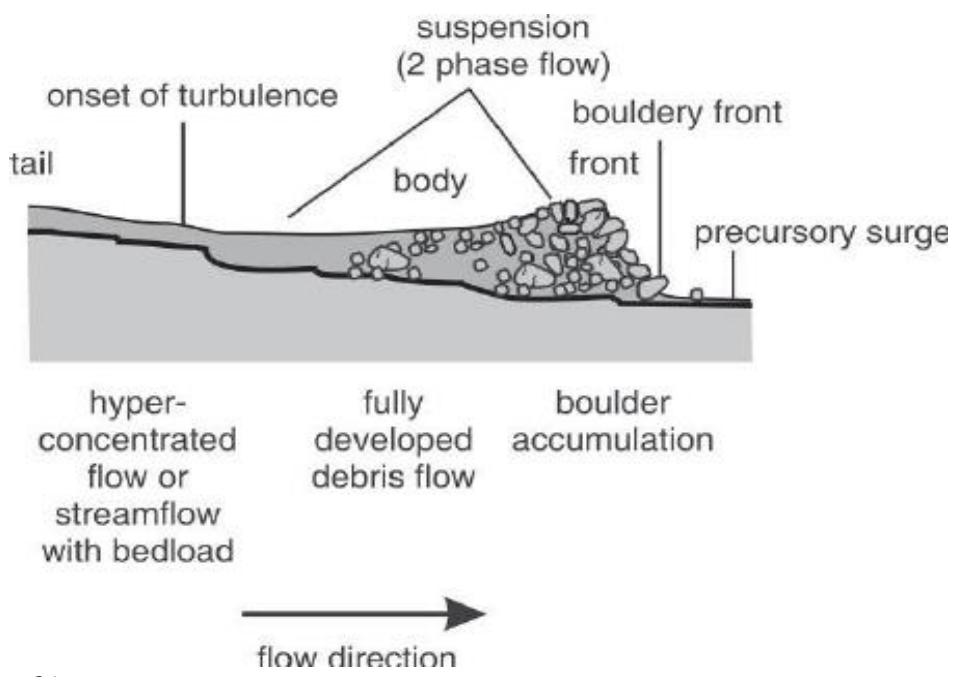


**Figure 22.** Debris flow surge schematic from Pierson, 1986. The material in the 80k-yr terrace and wave-cut face ranges from debris-rich sands to imbricated boulders, suggesting bombardment of the Pleistocene wave-cut platform concurrent with lowering sea levels by anastomosing debris flows coming out of the channels immediately to the east. Several trees are preserved in growth position within the debris flows having been buried upright with roots still in place in the underlying debris flow.